AUM SRI SAI RAM

Dedicated with love and gratitude at
the Lotus Feet
Of SAI

Measurement of Volatile Organic Compounds and Total OH Reactivity in the Atmosphere

Dissertation
zur Erlangung des Grades
„Doktor der Naturwissenschaften“
am Fachbereich Chemie
Johannes Gutenberg-Universität
in Mainz

Vinayak Sinha
geboren in Chingola, Sambia

Mainz, 2007

Measurement of Volatile Organic Compounds and Total OH Reactivity in the Atmosphere

Abstract

Volatile organic compounds play a critical role in ozone formation and drive the chemistry of the atmosphere, together with OH radicals. The simplest volatile organic compound methane is a climatologically important greenhouse gas, and plays a key role in regulating water vapour in the stratosphere and hydroxyl radicals in the troposphere. The OH radical is the most important atmospheric oxidant and knowledge of the atmospheric OH sink, together with the OH source and ambient OH concentrations is essential for understanding the oxidative capacity of the atmosphere.

Oceanic emission and / or uptake of methanol, acetone, acetaldehyde, isoprene and dimethyl sulphide (DMS) was characterized as a function of photosynthetically active radiation (PAR) and a suite of biological parameters, in a mesocosm experiment conducted in the Norwegian fjord. High frequency (ca. 1 $minute^{-1}$) methane measurements were performed using a gas chromatograph - flame ionization detector (GC-FID) in the boreal forests of Finland and the tropical forests of Suriname. A new on-line method (Comparative Reactivity Method - CRM) was developed to directly measure the total OH reactivity (sink) of ambient air.

It was observed that under conditions of high biological activity and a PAR of ~ 450 μmol photons m^{-2} s^{-1}, the ocean acted as a net source of acetone. However, if either of these criteria was not fulfilled

then the ocean acted as a net sink of acetone. This new insight into the biogeochemical cycling of acetone at the ocean-air interface has helped to resolve discrepancies from earlier works such as Jacob et al. (2002) who reported the ocean to be a net acetone source (27 Tg yr^{-1}) and Marandino et al. (2005) who reported the ocean to be a net sink of acetone (- 48 Tg yr^{-1}). The ocean acted as net source of isoprene, DMS and acetaldehyde but net sink of methanol. Based on these findings, it is recommended that compound specific PAR and biological dependency be used for estimating the influence of the global ocean on atmospheric VOC budgets. Methane was observed to accumulate within the nocturnal boundary layer, clearly indicating emissions from the forest ecosystems. There was a remarkable similarity in the time series of the boreal and tropical forest ecosystem. The average of the median mixing ratios during a typical diel cycle were 1.83 μmol mol^{-1} and 1.74 μmol mol^{-1} for the boreal forest ecosystem and tropical forest ecosystem respectively. A flux value of (3.62 ± 0.87) x 10^{11} molecules cm^{-2} s^{-1} (or 45.5 ± 11 Tg CH4 yr^{-1} for global boreal forest area) was derived, which highlights the importance of the boreal forest ecosystem for the global budget of methane (~ 600 Tg yr^{-1}).

The newly developed CRM technique has a dynamic range of ~ 4 s^{-1} to 300 s^{-1} and accuracy of ± 25 %. The system has been tested and calibrated with several single and mixed hydrocarbon standards showing excellent linearity and accountability with the reactivity of the standards. Field tests at an urban and forest site illustrate the promise of the new method.

The results from this study have improved current understanding about VOC emissions and uptake from ocean and forest ecosystems. Moreover, a new technique for directly measuring the total OH reactivity of ambient air has been developed and validated, which will be a valuable addition to the existing suite of atmospheric measurement techniques.

Bestimmung von flüchtigen organischen Verbindungen und der OH Reaktivität in atmosphärischen Luftproben

Flüchtige organische Verbindungen spielen eine wichtige Rolle in der Bildung von Ozon. Zusammen mit OH Radikalen treiben sie zahlreiche chemische Reaktion in der Atmosphäre an.

Der einfachste flüchtige Kohlenwasserstoff, Methan, ist ein wichtiges Treibhausgas und reguliert die Konzentration von Wasserdampf in der Stratosphäre und Hydroxidionen in der Troposphäre. Das Hydroxil-Radikal ist das wichtigste Oxidationsmittel der Atmosphäre. Um die Oxidationsprozesse in der Atmosphäre zu verstehen müssen die Quellen, die Senken und die Konzentration der Hydroxil-Radikale in der Luft quantifiziert werden.

Diese Arbeit umfasst drei Teile. Im ersten Teil werde Ergebnisse bezüglich der Emission und Absorption von flüchtigen organischen Verbindungen durch Phytoplankton präsentiert. In verschiedenen Mesokosmenkosmen in einem norwegischen Fjord wurde die Emission und Absorption von Methanol, Aceton, Acetaldehyde, Isopren und Dimethylsulfid (DMS) gemessen und die Abhängigkeit von der photosynthetisch aktiven Strahlung (PAR) studiert.

Der zweite Teil präsentiert Messungen der Methankonzentration in einem borealen Nadelwald in Finnland und in einem tropischen Urwald in Surinam und eine Abschätzung des Ökosystemflusses dieses wichtigen Treibhausgases. Die Messungen wurden mit einer hohen Frequenz (ca. 1 Messung/Minute) mittels eines Gaschromatographen mit Flammenionisationsdetektor durchgeführt.

Im dritten Teil wird eine neue online Methode zur Messung der OH Reaktivität (OH-Senke) in Luft entwickelt, die auf einem Vergleich der OH-Reaktivität von Luft mit der OH-Reaktivität einer bekannten Substanz beruht (Comparative Reactivity Method - CRM).

Es konnte gezeigt werden, dass wenn die Anzahl der Planktonzellen (Biologische Aktivität) hoch ist und PAR über einem Grenzwert von ~ 450 μmol Photonen m^{-2} s^{-1} liegt der Ozean eine Actetonquelle ist. Wenn eine der beiden Bedingungen nicht erfüllt ist, ist der Ozean hingegen eine Senke für Aceton. Dies ist ein wichtiger Beitrag zum Verständnis des biogeochemischen Acetonzyklus. Bisher widersprüchliche Ergebnisse z.B. von as Jacob et al. (2002) deren Ergebnisse nahe legen, dass der Ocean eine Quelle von Aceton ist (27 Tg yr^{-1}) und von Marandino et al. (2005) deren Ergebnisse den Ocean als Senke zeigen (- 48 Tg yr^{-1}) können im Lichte dieser neuen Ergebnisse erklärt werden. Isopren, DMS und Acetaldehyd wurden emittiert, Methanol absorbiert. Für alle flüchtigen organischen Verbindungen konnte eine starke Abhängigkeit der Emission von der photosynthetisch aktiven Strahlung festgestellt werden. Daher wird empfohlen das die stoffspezifische Abhängigkeit von PAR und Indikatoren biologischer Aktivität zukünftig in die Berechnung der globalen Emissionen flüchtiger organischer Verbindungen durch die Ozeane mit einbezogen wird.

Methan reicherte sich in der nächtlichen Grenzschicht an, was eine Emission durch das Ökosystem “Wald” nahe legt. Die Zeitreihen im borealen und tropischen Wald zeigen verblüffende Ähnlichkeit. Die Konzentration von Methan lag bei 1.83 μmol mol^{-1} im borealen

und 1.74 μmol mol^{-1} im tropischen Wald-Ökosystem. Der globale Ökosystemfluss wird auf (3.62 ± 0.87) x 10^{11} Moleküle cm^{-2} s^{-1} (oder 45.5 ± 11 Tg CH4 yr^{-1} für den borealen Nadelwald) geschätzt. Das Unterstreicht die Bedeutung des borealen Nadelwalds als Ökosystem für das globale Methanbudget (~ 600 Tg yr^{-1}).

Die neu entwickelte CRM- Methode kann die OH-Senke in einem dynamischen Arbeitsbereich von ~ 4 s^{-1} bis zu 300 s^{-1} mit einer Richtigkeit und Genauigkeit von ± 25 % messen. Die Methode wurde mit mehreren Einkomponentenstandards und einem 19-Komponenten Mix getestet und kalibriert und zeigt eine exzellente Linearität und Richtigkeit innerhalb des dynamischen Arbeitsbereiches. Testmessungen an urbaner Luft in Mainz und im tropischen Urwald (Brownsberg, Surinam) zeigen wie viel versprechend diese neue Methode ist.

Die Ergebnisse dieser Dissertation haben den bisherigen Wissenstand bezüglich der Emission und Absorption flüchtiger Organischer Verbindungen aus den Ozeanen und aus Wald Ökosystemen erweitert. Darüber hinaus wurde eine neue Methode zur Messung der OH-Reaktivität in Luftproben entwickelt und getestet. Diese neue Messmethode wird den Kanon der bestehenden Messmethoden an einer entscheidenden Stelle erweitern und ergänzen.

Contents

1. Introduction

1.1 Structure of the atmosphere

The atmosphere envelops the Earth as a protective envelope of gas and its existence is vital for many forms of life including human beings. It is composed primarily of the gases N_2 (~ 78%) and O_2 (~ 21%), with the remainder made up of water vapour, argon and other trace species, whose abundances are controlled over geological time scales by the biosphere, uptake and release from crustal material, and degassing of the interior.

The Earth's atmosphere is characterized by variations of temperature and pressure with altitude. In fact, the variation of the average temperature profile with altitude is the criterion that is used to distinguish the layers of the atmosphere. Figure 1.1 shows the different layers of the atmosphere. The troposphere is the lowest layer and extends from the Earth's surface to an average altitude of 10-15 km depending on the latitude and season. The troposphere is characterized by decreasing temperature with increasing altitude and rapid vertical mixing, compared to the other layers. In the stratosphere, short wavelength solar radiation is absorbed by ozone leading to adiabatic heating and temperature increase with increasing altitude. In this way, the atmosphere shields the Earth's surface from most of the harmful UV-rays of the Sun. Above the stratosphere is the mesosphere, where the temperature decreases with increasing altitude. The thermosphere is present above the mesosphere and is distinguished by a very low gas density. The absorption of far-UV

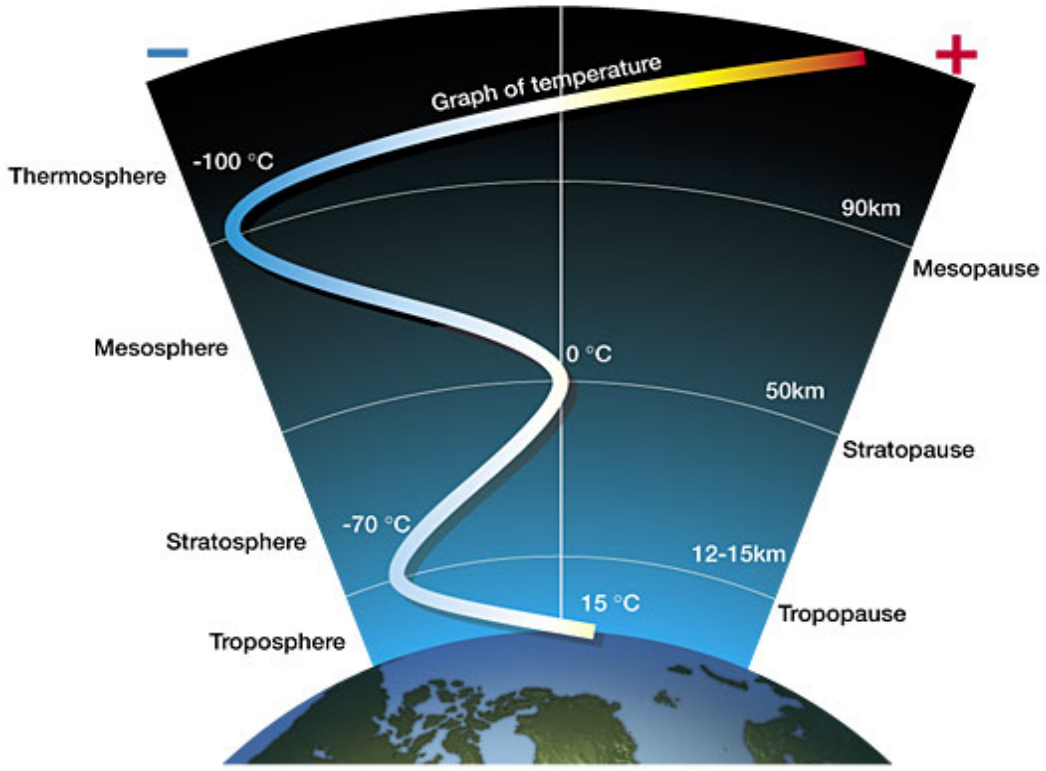

Figure 1.1: The layers of the atmosphere.

wavelength radiation by gaseous oxygen and nitrogen molecules can heat it up to temperatures of 2000 K, depending on solar activity (Brasseur et al, 1999; Warneke, 2000). While oxygen and nitrogen comprise almost 99% of the total atmospheric volume, it is the trace gases in the atmosphere, which are present in minute mixing ratios of parts per billion and parts per trillion, that drive the fascinating chemistry and physics of the atmosphere. In the next section, we describe the importance of the atmospheric trace gases present as volatile organic compounds.

1.2 Importance of atmospheric volatile organic compounds (VOCs)

The term volatile organic compounds (VOCs), is used for denoting the entire set of vapour phase organics excluding CO and CO_2. Little was known about organic compounds in the earth's atmosphere before 1950, beyond that methane and formaldehyde were present (Glueckauf, 1951). Thereafter, problems of haze and smog spurred air-pollution research and now it is well established that VOCs play a key role in the chemistry of the atmosphere. Figure 1.2 shows a schematic of the typical sources, sinks and fate of VOCs in the atmosphere. Volatile organic compounds enter the atmosphere

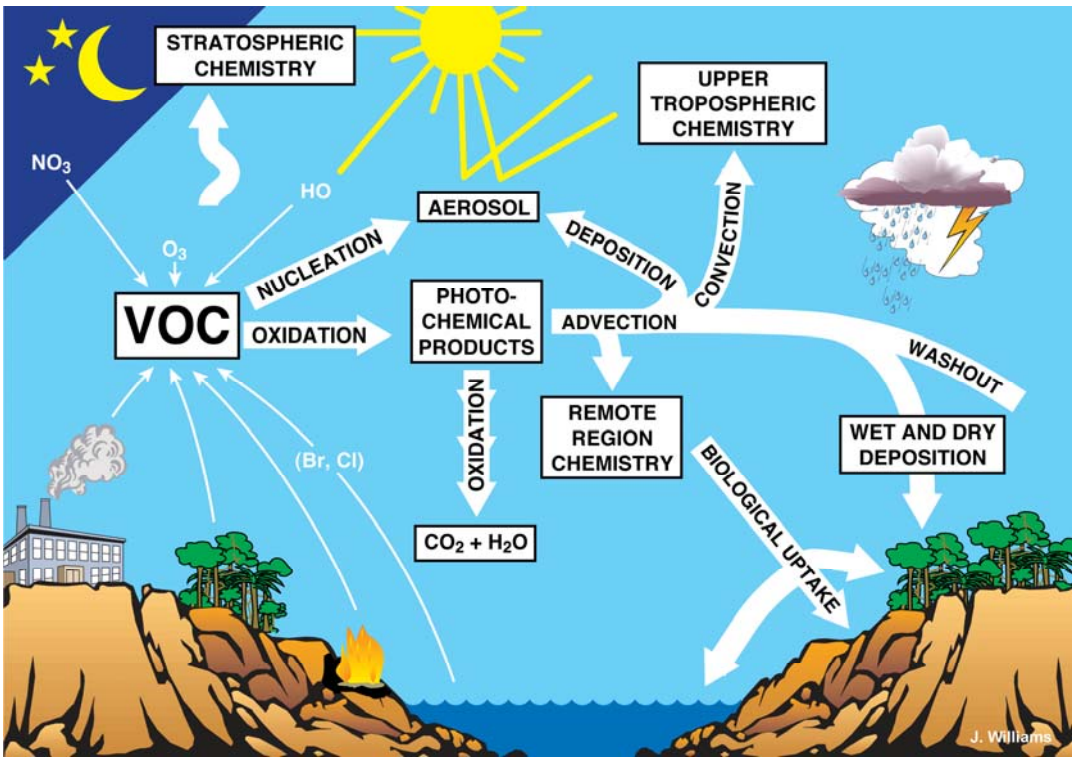

Figure 1.2: Schematic showing origin and fate of volatile organic compounds in the atmosphere.

through processes associated with life, such as the growth, maintenance, and decay of plants, animals, and microbes. Combustion of living and dead organisms, such as biomass burning or fossil-fuel consumption, also releases organic compounds into the atmosphere. Ultimately if an emitted VOC continues to remain in the gas phase, it is oxidized to CO_2 and water. VOCs are emitted to the atmosphere from a variety of anthropogenic and biogenic sources. From a global perspective, biogenic volatile organic compounds are mostly emitted in the Tropics, whereas anthropogenic compounds are predominantly emitted in the temperate zones of the northern hemisphere between 40° and 50° latitude. Methane (CH_4) is the simplest volatile organic compound. Atmospheric methane mixing ratios have nearly tripled since pre-industrial times (Prather et al. 2001; IPCC 2001), and it is estimated that approximately 600 Tg CH_4 (1 Tg = 10^{12} g) is emitted annually. An estimated 1150 Tg (C) of biogenic VOCs are emitted each year to the atmosphere from vegetation or via microbial production (Guenther et al., 1995). Emission rates of the biogenic VOCs are highly variable, being strongly dependent on temperature and light intensity, as well as stress induced by injuries, parasites or atmospheric pollutants such as O_3 (Kesselmeier and Staudt, 1999).

In 1952, Haagen-Smit showed that volatile organic compounds and nitrogen oxides (NO_x) combine photochemically to produce ozone, which is a pulmonary irritant and phyto-toxic (Haagen-Smit, 1952). VOCs can have an impact on health and the environment either directly or indirectly after undergoing a complex series of

atmospheric reaction cycles resulting in secondary pollutants such as O_3 and aerosol (Williams 2004a and references therein). The simplest VOC, methane, has significant implications for climate warming and atmospheric chemistry, as it plays a key role in regulating stratospheric water vapour and tropospheric hydroxyl radicals (Khalil, 2000; Lelieveld et al. 1998). In the next section we describe the importance of hydroxyl radicals (the main atmospheric oxidant) which react with VOCs, to drive the photochemistry and composition of the atmosphere, influencing the radiative budget and ultimately impacting the Earth's climate.

1.3 Importance of OH Chemistry and Reactivity

The hydroxyl radical (OH) does not react with any of the major constituents of the atmosphere, such as N_2, O_2, CO_2, or H_2O, yet it is the most important reactive species in the troposphere. Every year, approximately 1.3 billion tonnes of natural and anthropogenic gases are emitted into the troposphere (Goldstein and Galbally, 2007). Photochemical reactions, initiated by the hydroxyl radical (OH), oxidize many of these emitted primary atmospheric pollutants such as carbon monoxide (CO), sulphur dioxide (SO_2), nitrogen oxides (NO_x = NO and NO_2) and VOCs (Volatile Organic Compounds) into forms, which are more readily removed from the atmosphere by deposition or formation of aerosol. Ultimately, if a compound remains in the gas phase it will be oxidised to CO_2 and water by the OH radical, which is

therefore vital for maintaining the self cleansing capacity of the atmosphere (Levy 1971; Heard and Pilling, 2003; Lelieveld et al., 2004). If OH simply reacted with other species and was not regenerated in some manner, its concentration would be far too low, inspite of its reactivity, to be an important player in tropospheric chemistry. In reality, while reacting with atmospheric trace gases, OH is generated in catalytic cycles, leading to sustained concentrations on the order of 10^6 molecules cm^{-3} during daylight hours.

The main reaction that produces OH in the atmosphere, is the photolysis of O_3 with solar UV ($\lambda \leq 320$ nm) followed by reaction of the excited oxygen atoms (O^1D) with water vapour,

$$O_3 + h\nu \rightarrow O_2 + O(^1D) \quad (1.1)$$

$$O(^1D) + H_2O \rightarrow 2OH \quad (1.2)$$

Figure 1.3 depicts a summary of the main photochemical processes involving the hydroxyl radical (OH), including all the main OH sources and OH sinks.

Since the OH radical is the main oxidant of the atmosphere, the lifetime of most volatile organic compounds is determined primarily by the rate at which they react with OH radicals. The rate at which a volatile organic compound reacts with OH radicals in the atmosphere is also referred to as its OH reactivity and is mathematically expressed as:

$$\text{OH reaction rate of a VOC, } R_{VOC} = k_{VOC+OH}\,[\text{VOC}] \quad (1.3)$$

where k_{VOC+OH} is the rate coefficient for the reaction of VOC with OH in cm^3 $molecule^{-1}$ s^{-1}, and [VOC] is the concentration of the volatile organic compound in molecule cm^{-3}, so that R_{voc} has the units of s^{-1}.

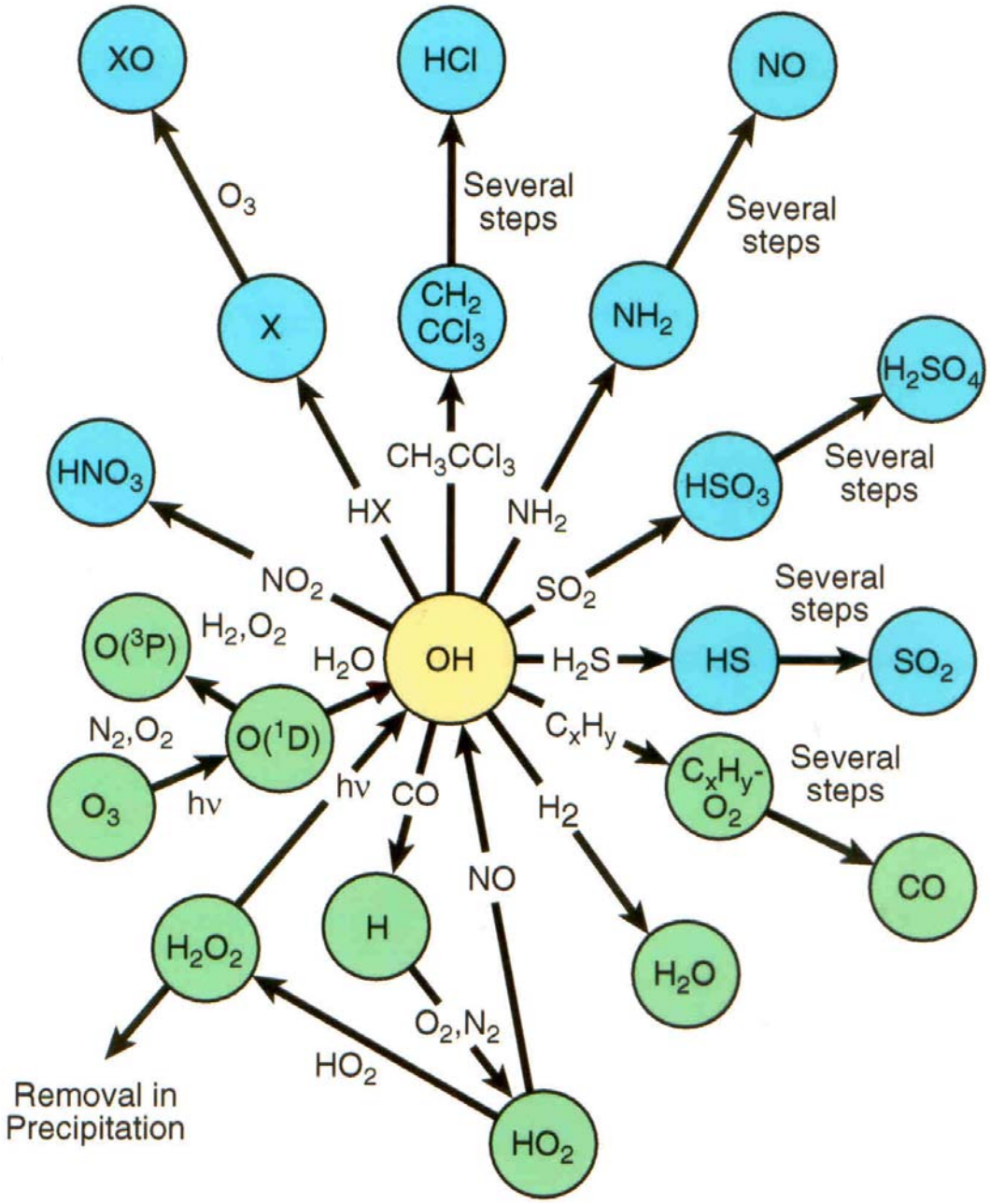

Figure 1.3: Schematic showing the main atmospheric photochemical processes involving the hydroxyl radical (OH).

Total OH reactivity (or OH sink) is a very valuable tool for assessing how well we understand the atmosphere's OH chemistry, and therefore its oxidation capacity. For example, OH production rates can also be estimated by simultaneous measurements of total

OH reactivity and OH concentrations, assuming the steady state of OH using,

$$\frac{d\,OH}{d\,t} = P_{OH} - k[OH] = 0 \tag{1.4}$$

where P_{OH} and k represent the OH production rate and the measured first-order decay rate of OH radicals, respectively. One can also determine the lifetime of the OH radical using the OH reactivity, because the lifetime of OH radicals is simply the inverse of the total OH reactivity.

1.4 Summary

From the discussion so far, it is clear that volatile organic compounds and OH radicals are among the main drivers of tropospheric chemistry. Thus in order to understand the chemistry and composition of the troposphere, it is imperative that we understand the factors that influence VOC emissions and uptake from different ecosystems. This is also important to ascertain their contribution to the global VOC budget. Finally, in order to understand the oxidative capacity of the atmosphere, which is driven mainly by the hydroxyl radicals, in addition to knowledge of the OH sources and ambient OH radical concentrations, knowledge of the OH reactivity (OH sink) is an indispensable tool.

1.5 Research objectives and thesis outline

The objectives of this research project have been three fold –

1) To understand how light and marine biology affects the oceanic emission and / or uptake of the volatile organic compounds: methanol, acetone, acetaldehyde, isoprene and dimethyl sulphide (DMS). This is of great relevance in understanding the global budgets of these VOCs because the contribution of the ocean to the global budgets of these VOCs is not well understood. The motivation for this study, experimental approach, discussion of the new findings and conclusions are presented in Chapter 2 of this thesis.

2) To examine emissions of methane from forest ecosystems and get a first order estimate of the emissions using in-situ field data. This work assumes added significance in the wake of recent work by Keppler et al. (2006) who reported a significant new source of methane emissions by terrestrial plants under aerobic conditions. The complete details regarding the experimental procedure, measurement results and findings are presented in Chapter 3 of this thesis.

3) To develop a new online technique capable of measuring the OH reactivity of ambient air and deploy it in the field after validation and testing for interferences. The concept, design, interference testing and validation, including first measurements from the tropical rainforest are presented in Chapter 4 of the thesis.

Finally in Chapter 5, a summary of the new findings is presented along with the conclusions and outlook.

2. Air-sea fluxes of methanol, acetone, acetaldehyde, isoprene and DMS from a Norwegian fjord following a phytoplankton bloom in a mesocosm experiment

The ocean's influence on volatile organic compounds (VOCs) in the atmosphere is poorly understood. This work characterises the oceanic emission and / or uptake of methanol, acetone, acetaldehyde, isoprene and dimethyl sulphide (DMS) as a function of photosynthetically active radiation (PAR) and a suite of biological parameters. The measurements were taken following a phytoplankton bloom, in May / June 2005 with a proton transfer reaction mass spectrometer (PTR-MS), from mesocosm enclosures anchored in the Raunefjord, Southern Norway. The net flux of methanol was always into the ocean, and was stronger at night. Isoprene and acetaldehyde were emitted from the ocean, correlating with light ($r_{avcorr,\ isoprene}$ = 0.49 ; $r_{avcorr,\ acetaldehyde}$ = 0.70) and phytoplankton abundance. DMS was also emitted to the air but did not correlate significantly with light ($r_{avcorr,\ dms}$ = 0.01). Under conditions of high biological activity and a PAR of ~ 450 μmol photons m^{-2} s^{-1}, acetone was emitted from the ocean, otherwise it was uptaken. The inter - VOC correlations were highest between the day time emission fluxes of acetone and

acetaldehyde (r_{av} = 0.96), acetaldehyde and isoprene (r_{av} = 0.88) and acetone and isoprene (r_{av} = 0.85). The mean fluxes for methanol, acetone, acetaldehyde, isoprene and DMS were - 0.26 ng m^{-2} s^{-1}, 0.21 ng m^{-2} s^{-1}, 0.23 ng m^{-2} s^{-1}, 0.12 ng m^{-2} s^{-1} and 0.3 ng m^{-2} s^{-1} respectively. This work shows that compound specific PAR and biological dependency should be used for estimating the influence of the global ocean on atmospheric VOC budgets.

2.1 Introduction

As the ocean covers some 70% of the Earth's surface area, its potential effect on atmospheric trace gases is enormous. Remarkably, the net primary production of the ocean (48.5 PgC yr^{-1}, P= peta =10^{15}) is comparable to that of the terrestrial environment (56.4 PgC yr^{-1})(Field et al. 1998), despite the total amount of biomass in the surface ocean being 100 times less than on land. Ocean biology influences the concentrations of dissolved gases directly (through photosynthesis and emission), and indirectly (through photochemistry of by-products). Such processes lead to an uptake from, or an emission to, the overlying atmosphere for a suite of organic gases (e.g. CO_2, DMS, isoprene, acetone). These gases are known to significantly impact the atmosphere, influencing ozone photochemistry and aerosol physics (Williams 2004a and references therein) even at trace concentrations. Dimethyl sulphide and isoprene have both been established as emissions from the surface ocean to the atmosphere and the distribution of these sources has been investigated by several groups (Bonsang et al. 1992; Kettle and Andreae 2000; Palmer and Shaw 2005). Many hundreds of atmospherically important species have been characterised and inventoried from terrestrial sources (Olivier et al. 1994; Guenther et al. 1995), but in comparison, very little work has been done on assessing the emission of volatile organic compounds from the ocean.

It was discovered quite recently that the surface ocean can play an important role in the budgets of organic trace gases, particularly oxygenated species such as acetone (propanone), methanol, and

acetaldehyde (ethanal) (Singh et al. 2003). These species have been shown to be ubiquitous in the atmosphere (Singh et al. 2001) and to influence radical budgets in the upper troposphere (McKeen et al. 1997; Tie et al. 2003; Colomb et al. 2006 (in press)). Furthermore, the surface ocean has been shown to be a massive reservoir for oxygenated organic species, both indirectly from aircraft measurements (Singh et al. 2000) and directly from ship borne measurements (Williams et al. 2004b).

There have been several global budget estimates for the oxygenated species methanol (Singh et al. 2000; Galbally and Kirstine 2002; Heikes et al. 2002), and acetone (Singh et al. 1994; Singh et al. 2000; de Laat et al. 2001; Jacob et al. 2002; Singh et al. 2004). The large range of these budget estimates (75-490 Tg yr^{-1} methanol ; 37-148 Tg yr^{-1} acetone) indicates their currently uncertain nature, and in all these budgets the role of the ocean is the most uncertain factor. In the case of methanol, there is general consensus that methanol is uptaken from the atmosphere to the ocean. The latest budget estimates by Singh et al. (2004) and Jacob et al. (2005) estimate a 10-15 Tg yr^{-1} sink accounting for approximately 20 % of the global budget. It is not yet clear as to what is responsible for maintaining an under saturation of methanol in surface waters, although certain methylotrophic bacteria are known to consume methanol (Kiene 1993). In the case of acetone, there is remarkably poor agreement concerning the effect of the ocean on the global acetone budget. Using an inverse modelling approach, Jacob et al. (2002) deduced an oceanic source of 27 Tg yr^{-1} (some 33% of a total

budget of 95 Tg yr^{-1}); Singh et al. (2004) estimated a small net sink (in a total budget of 95 Tg yr^{-1}); whereas Marandino et al. (2005) extrapolate an oceanic sink of 48 Tg yr^{-1} (in a total budget of 101 Tg yr^{-1}), from flux measurements made over the Pacific Ocean. Clearly, further measurements are required in parallel with biological parameters to elucidate these seemingly contrary findings. Moreover, significant median mixing ratios of the reactive species acetaldehyde (204 ± 40 pptv) have been reported by Singh et al. (2003), even after the application of a pollution filter on the dataset. Despite its potential atmospheric importance, no global budget estimate of acetaldehyde has been made to date.

In this study we characterise the effect of the ocean on ambient atmospheric mixing ratios of methanol, acetone, acetaldehyde, isoprene and DMS as a function of light and a suite of biological parameters. The measurements were made under semi-controlled conditions from custom-built mesocosms deployed in the Raunefjord, Southern Norway (see Figure 2.1). Mesocosm studies provide a useful interface between laboratory culture studies and open ocean surveys. While laboratory studies cannot generate the community dynamics of natural ecosystems, open ocean studies are complicated by horizontal and vertical mixing in both the air and water phases. Mesocosms therefore offer an excellent opportunity to study natural plankton communities under controlled conditions.

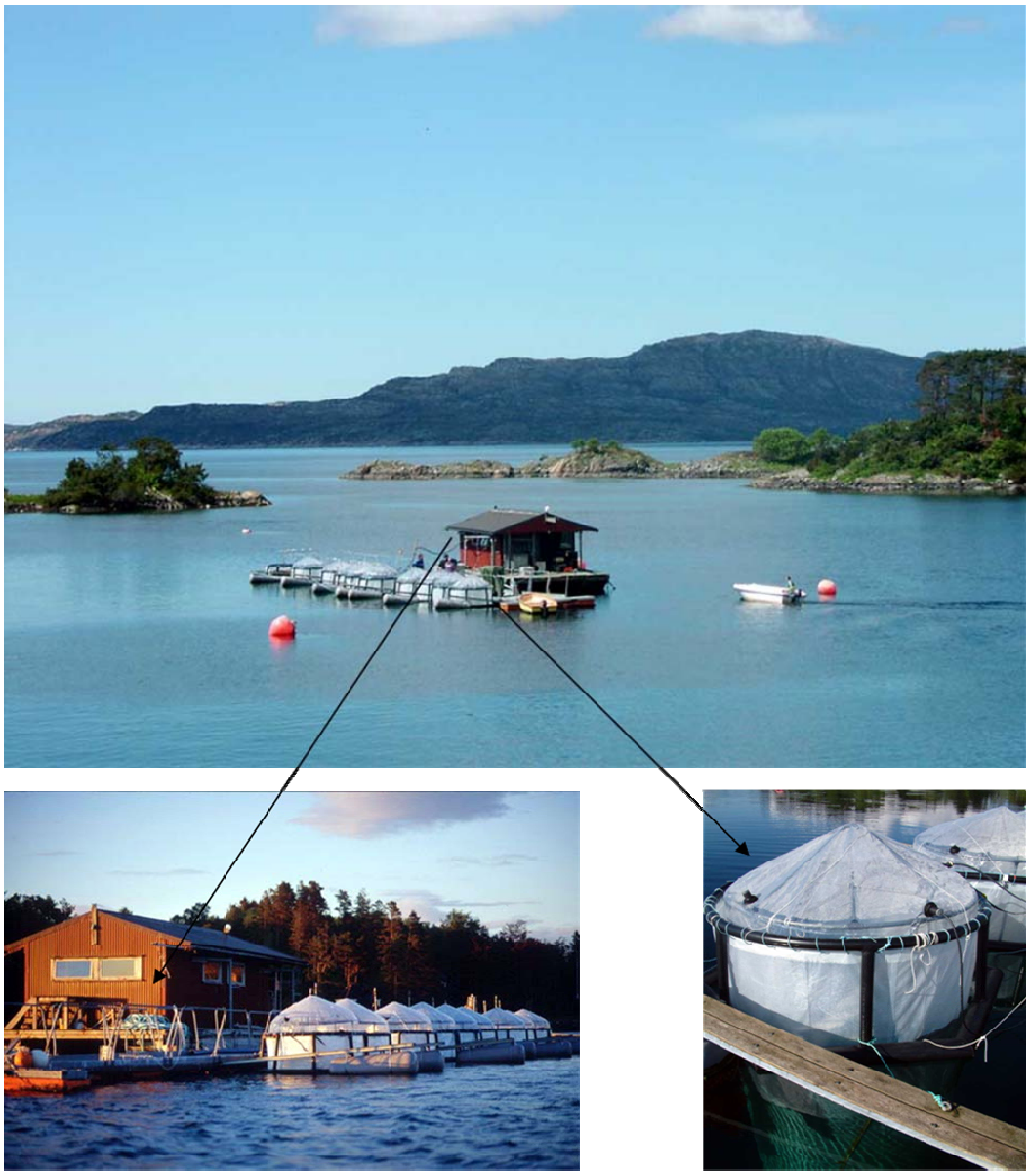

Figure 2.1: View of the University of Bergen raft facility with attached mesocosms, located in a fjord 20 km south of Bergen. The enlarged views show the mesocosms and the raft in detail.

2.2 Experimental

2.2.1 The Mesocosms

A total of nine polyethylene enclosures (hereafter referred to as mesocosms) were deployed in a fjord at the University of Bergen Marine Biological Station, 20 km south of Bergen, Norway. The construction and operation of such mesocosms has been described in detail elsewhere (Williams and Egge 1998; Engel et al. 2005), hence only a brief description is given here. The polyethylene enclosures (~20 m^3 water volume; 9.5 m water depth; ~4.3 m^3 headspace volume) were filled with unfiltered, nutrient-poor, post-bloom fjord water, which was pumped from 12 m depth adjacent to a raft anchored in the centre of the fjord. The enclosures were covered by gas-tight tents made of ETFE foil (Foiltec, Germany), which allowed for 95% light transmission of photosynthetically active radiation (PAR). In order to stratify the water column and avoid re-introduction of sedimented material into the surface sea layer, 0.6 m^3 of freshwater was added and mixed into the upper 5 m of the mesocosms. Throughout the study, the upper 5m layer was gently mixed by means of an aquarium pump. A bloom of the coccolithophore *Emiliania huxleyi* was induced by adding nitrate and phosphate in the ratio of 25:1 yielding initial concentrations of approximately 15 µmol L^{-1} NO_3^- and 0.6 µmol L^{-1} PO_4^3. The development of the bloom is seen in the profile of Chlorophyll a and the trace gas measurements presented herein were conducted in the aftermath of the bloom (see Figure 2.2).

The air flow into several mesocosms was dosed with additional

CO_2 in order to also study the effects of elevated CO_2 on marine biology (see PeECE study website at http://peece.ifm-geomar.de). In this work, we present measurements only from the duplicate mesocosms which were flushed with ambient air, since these most closely represent the ambient atmosphere of today and are not subject to additional biological responses associated with altering dissolved CO_2. Based on the rate of the ambient air inflow and the volume of the mesocosm headspace (~ 4.3 m^3), the total headspace-air replacement time was 191 minutes and 170 minutes for mesocosms 7 and 8 respectively. The inflow and outflow air from both mesocosms was sampled for a suite of volatile organic compounds.

Irradiance was continuously measured every 10 minutes throughout the study by using a Li-Cor cosine sensor (LI-192SA), mounted on top of the floating mesocosm laboratory.

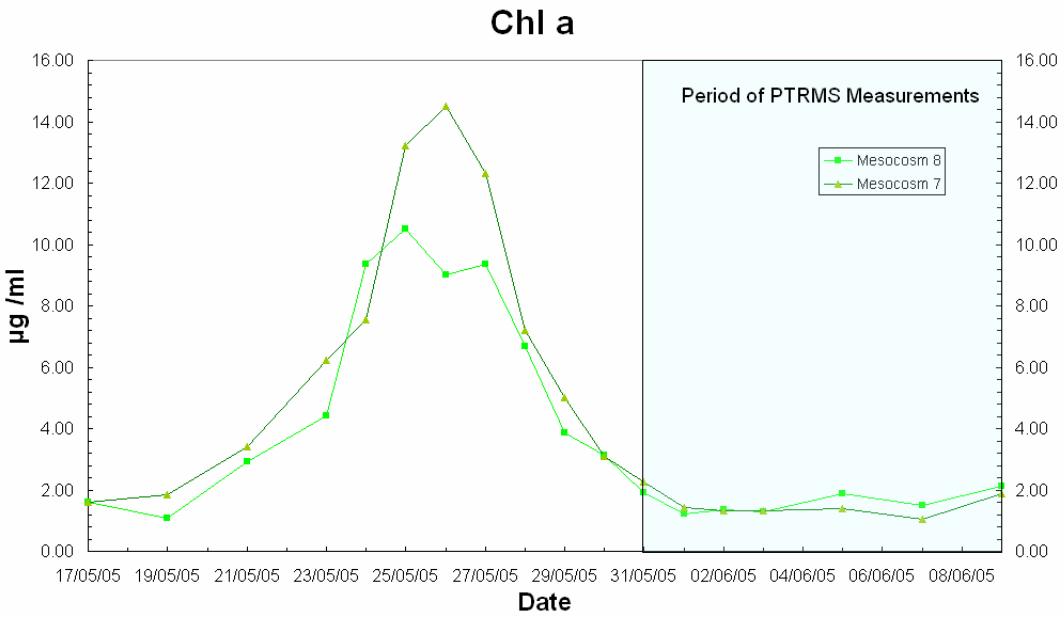

Figure 2.2: Time series of Chlorophyll a in mesocosms 7 and 8.

2.2.2 PTR-MS

A proton transfer reaction mass spectrometer (PTR-MS) was employed to measure masses 33, 59, 45, 63 and 69, which have been attributed to methanol, acetone, acetaldehyde, DMS and isoprene respectively. These identifications are in keeping with previous studies although minor contributions from other species, such as propanal to mass 59 cannot be ruled out (Lindinger et al. 1998a; Williams et al. 2001). The instrument was positioned on a floating raft to which the mesocosms were attached, in a fjord that opened to the sea some 5 km away (see Figure 1). Ambient air and air from the headspace of each mesocosm was drawn rapidly (~ 4.3 L min^{-1}) and continuously through 0.64 cm diameter and 25 m long Teflon lines shrouded from sunlight. The inlet residence time was less than 12 seconds. A fraction of this flow was sampled online by the PTR-MS. The entire inlet system of the PTR-MS including switching valves comprised of Teflon. Within the instrument, organic species with a proton affinity greater than water are chemically ionised by proton transfer with H_3O^+ ions and the products are detected using a quadrupole mass spectrometer (Lindinger et al. 1998a). Further details of the operation of the PTR-MS used here are given elsewhere (Salisbury et al. 2003).

Sequential measurements of ambient air and air from the duplicate mesocosms 7 and 8 were made for 10 minutes each, in the order — mesocosm 7, ambient air and mesocosm 8. Calibrations were performed during the campaign using a commercial gas standard (Apel-Reimer Environmental Inc.). The total uncertainties of the

measurements are estimated to be 21.3 %, 15 %, 19%, 17% and 14 % for methanol, acetone, acetaldehyde, isoprene and DMS respectively. This includes a 5 % accuracy error inherent in the gas standard and a 2 σ precision error for all the compounds. Detection limit was defined as the 2 σ error in the instrument signal, while measuring methanol at an average mixing ratio of 1 nmol mol^{-1} and each of the other compounds at an average mixing ratio of 0.5 nmol mol^{-1}. The individually calculated precision errors and detection limits were as follows, methanol (16.3 %; 0.24 nmol mol^{-1}), acetone (10 %; 0.07 nmol mol^{-1}), acetaldehyde (14 %; 0.06 nmol mol^{-1}), isoprene (12 %; 0.06 nmol mol^{-1}) and DMS (9 %; 0.05 nmol mol^{-1}).

2.2.3 Biological parameters methods

Chlorophyll a (Chl a) was determined in 250 to 500 ml samples filtered on glass fibre filters (GF/F, Whatman). For pigment extraction, filters were homogenised in plastic vials together with 1 ml acetone (100%) and a mixture of glass beads (2 and 4 mm) by shaking (5 min) in a cooled Vibrogen cell mill (Buehler, Germany). Afterwards the extracts were centrifuged (5000 rpm, 10 min, cooled at -10°C). This procedure corresponds, with minor modifications, to the method of Derenbach (1969).

The content of Chlorophyll-a was then determined by means of HPLC (High Performance Liquid Chromatography), using the method of Barlow et al. (1997).

Phytoplankton cell counts were performed with a FACSCalibur flow-cytometer (Becton Dickinson) equipped with an air-cooled laser

providing 15 mW at 488 nm and with a standard filter set-up. The algal counts were obtained from fresh samples at high flow rate (100 µl min^{-1}). The trigger was set on red fluorescence and the samples were run on the cytometer for 300s. Discrimination of the algal groups was based on dot plots of side-scatter signal (SSC) and pigment autofluorescence (chlorophyll and phycoerythrin).

Samples for enumeration of bacteria were fixed with glutaraldehyde (0.5% final concentration), frozen in liquid nitrogen and stored at -70^{o}C (Marie et al., 1999a). The samples were stained with SYBR Green I (Molecular Probes Inc., Eugene, OR) and analysed according to Marie et al. (1999b). The discrimination of bacteria groups was based on groups observed in scatter plots of SSC signal versus green DNA-dye (SYBR Green) fluorescence. Fluorescence beads (Molecular Probes) with a diameter of 0.95µm were added to each sample analysed as an internal reference. Data files were analyzed using EcoFlow (version 1.0.5, available from the authors).

2.3 Results

2.3.1 General trends – gas phase species

Figure 2.3 shows a time series for measurements of methanol, acetone, acetaldehyde, isoprene and DMS measured as masses 33, 59, 45, 69, and 63 respectively. In each case the inflowing ambient air mixing ratio is plotted with the measurements from within mesocosms 7 and 8. Measurements of the inflowing ambient air,

including average, median and standard deviation are summarized in Table 2.1. Variability in the ambient air was highest for methanol followed by acetaldehyde, acetone, isoprene and DMS (see σ values in Table 2.1). For all species, good agreement can be seen between the two duplicate mesocosms. Where the mixing ratios of a particular species in the mesocosm air were significantly lower than ambient air, we infer that an uptake occurred into the seawater. Conversely when mesocosm air mixing ratios were higher than the inflowing ambient air, an emission from seawater into the air was deduced.

Diel cycles were seen in the mesocosms for acetone, acetaldehyde and isoprene, which exhibited maxima and minima typically from 12 pm - 4 pm and 12 am - 8 am respectively. In contrast, methanol showed no clear diel cycle in the mesocosms, the variation and absolute values of the mesocosm data being generally suppressed with respect to the ambient air. DMS mixing ratios in the mesocosm air were observed to be generally higher in the evening rather than daytime. We investigate the light and biology dependence of these emissions and uptakes in section 2.3.2.

2.3.2 Fluxes of organic species in relation to light (PAR) and biological parameters

At the outset, it should be noted that the emission and uptake fluxes reported here represent the net fluxes from seawater to air and vice versa, inside the mesocosm. Hence the fluxes may be the resultant of separate, strong sinks and sources within the mesocosm system.

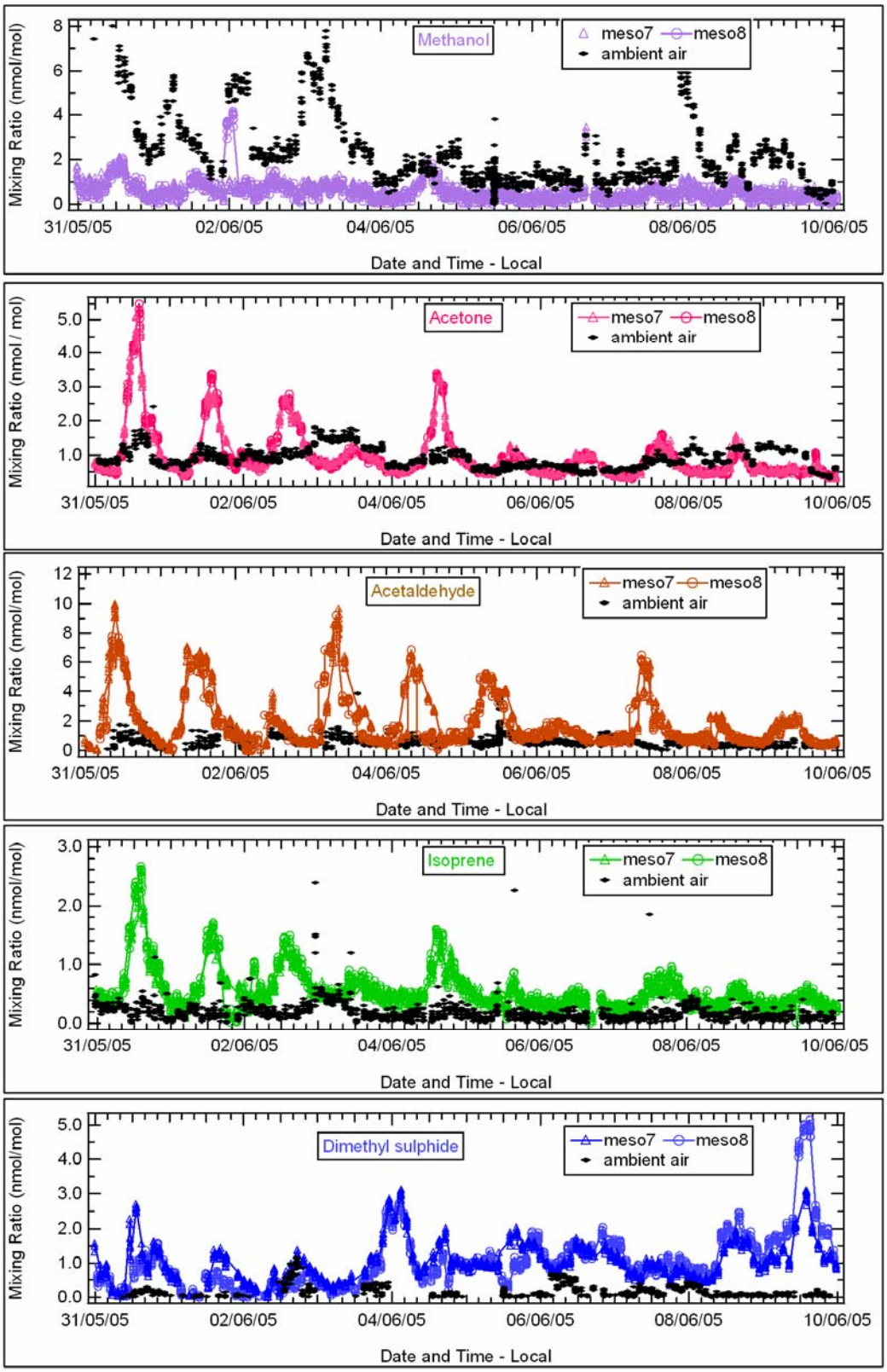

Figure 2.3: Time series of methanol, acetone, acetaldehyde, isoprene and DMS from inside and outside the duplicate mesocosms 7 and 8.

Table 2.1: Average, Median, Standard Deviations, Minima and Maxima for Measurements of the Ambient Marine Air flushed into the Mesocosms.

	Units (nmol mol^{-1})					
	Average	Median	Minimum	Maximum	σ	n
Methanol	2.26	1.86	B.D.L	7.99	1.56	1171
Acetone	0.87	0.80	0.28	2.40	0.29	1228
Acetaldehyde	0.60	0.55	B.D.L	3.96	0.45	1099
Isoprene	0.18	0.18	B.D.L	2.38	0.17	1123
DMS	0.17	0.40	B.D.L	1.15	0.18	651

B.D.L = Below Detection Limit

Fluxes of the various VOCs were calculated according to equation 2.1,

$$F_{voc} = \frac{Q}{A}(m_{in,voc} - m_{out,voc})\frac{M_{voc}}{V_m} \qquad (2.1)$$

where F_{voc} is flux of the VOC in μg m^{-2} s^{-1}, $m_{in,voc}$ and $m_{out,voc}$ are the VOC mixing ratios (nmol mol^{-1}) in the inflowing ambient marine air and mesocosm air respectively, Q is the flow rate of the ambient air into the mesocosm in m^3 s^{-1}, A is the surface area of the seawater enclosed by the mesocosm in m², M_{voc} is the molecular weight of the VOC in kg $kmol^{-1}$ and V_m is the molar gas volume in m^3 $kmol^{-1}$ (= 23.233 at 1013.25 hPa and 283 K).

Figure 2.4 depicts the time series of the VOC fluxes and PAR in the duplicate mesocosms 7 and 8 while Table 2.2 gives a summary of the averages, medians and standard deviations of the VOC fluxes in the duplicate mesocosms.

Figure 2.5 shows daily plankton cell counts of the coccolithophore *Emiliania huxleyi*, the cyanobacterium *Synechococcus sp*., other nano and picophytoplankton and free-living heterotrophic bacteria. The trace gas measurements covered two

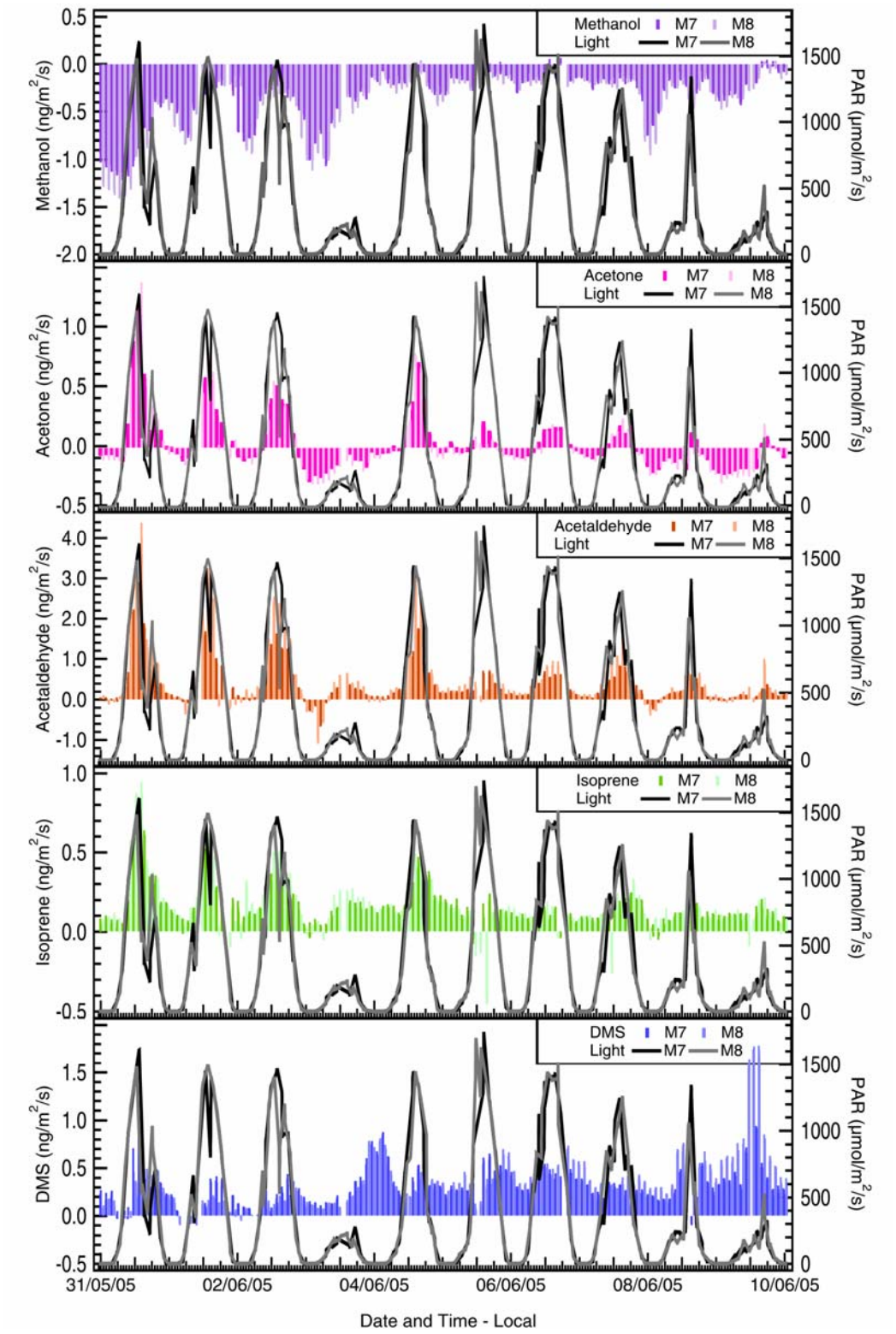

Figure 2.4: Flux profiles of methanol, acetone, acetaldehyde, isoprene, DMS and photosynthetically active radiation (PAR) as a function of time in the duplicate mesocosms 7 and 8.

Table 2.2: Comparison of Fluxes in the Duplicate Mesocosms 7 and 8.

	Units (ng m^{-2} s^{-1})					
	Average (7)	Average (8)	Median (7)	Median (8)	σ(7)	σ(8)
Methanol (U)	0.33	0.39	0.26	0.27	0.29	0.30
Acetone (U)	0.08	0.10	0.05	0.07	0.06	0.08
Acetone (E)	0.21	0.26	0.19	0.34	0.23	0.29
Acetaldehyde (E)	0.34	0.49	0.19	0.26	0.49	0.70
Isoprene (E)	0.14	0.14	0.12	0.12	0.12	0.17
DMS (E)	0.30	0.35	0.30	0.27	0.17	0.29

U = Uptake from atmosphere to seawater; E = Emission from seawater to atmosphere

subsequent phases of the phytoplankton bloom, from 31st May -5th June - the final phase of bloom decline, and from 6th June - 10th June - a post-bloom phase of low phytoplankton standing stocks characterized by an increase in cyanobacterial cell numbers.

The photosynthetically active radiation (PAR) generally ranged from 0 to 1500 µmol photons m^{-2} s^{-1} on most days (Fig. 2.4). Due to overcast conditions significantly lower daily maxima of ca. 400 µmol photons m^{-2} s^{-1} occurred on the 4th and 10th of June.

From the Figures 2.4, 2.5 and Table 2.2 we note that there is good consistency in the magnitude and direction of the fluxes as well as the biological parameters in the two mesocosms. The fluxes of the individual organic compounds are examined in detail in the subsequent sections.

Methanol:

Throughout the experiment, the net flux of methanol was always into the seawater from the mesocosm air above it. Thus methanol was uptaken both during the day and at night. The average of the Pearson

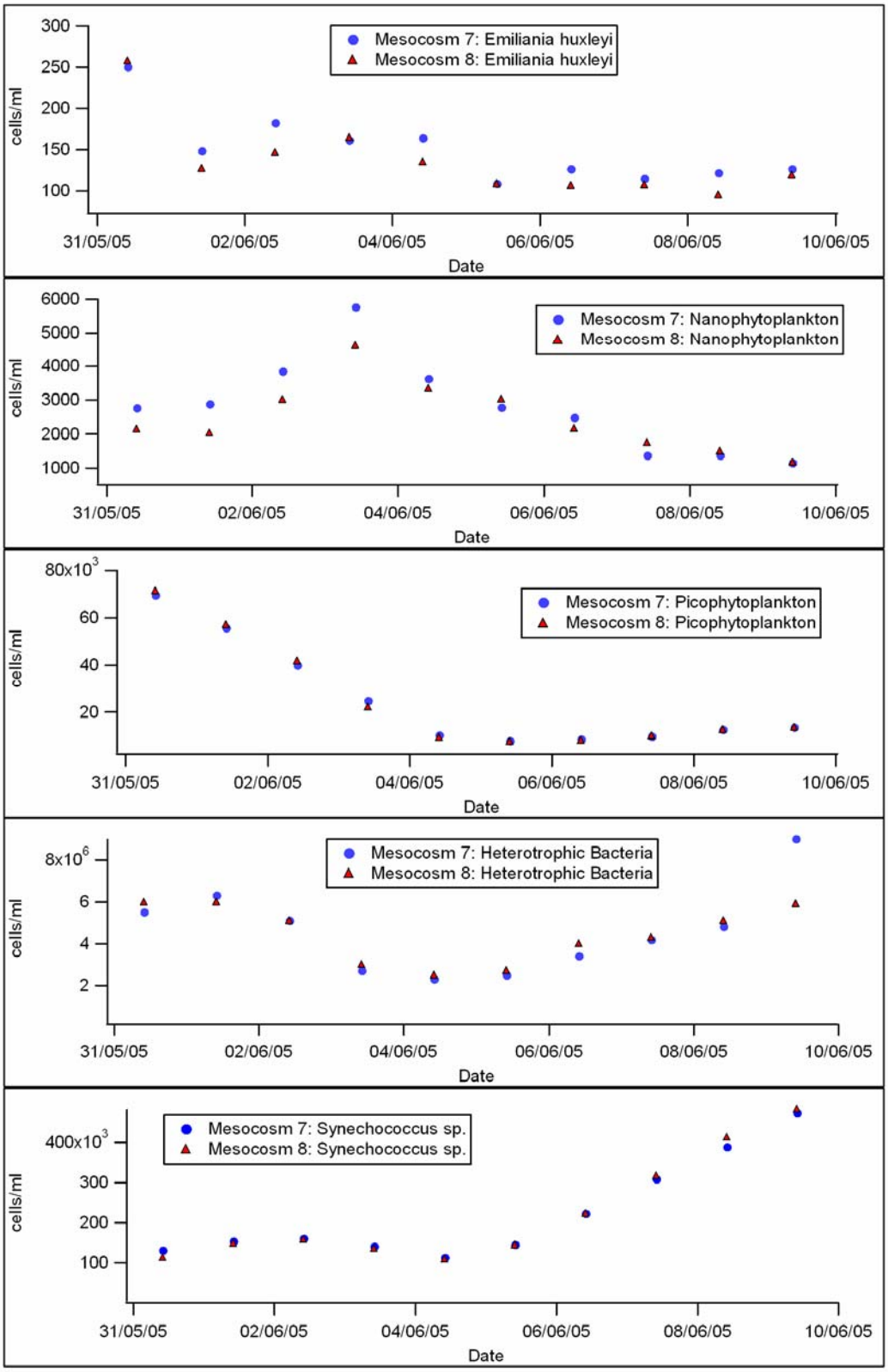

Figure 2.5: Daily variation of selected phytoplankton and bacteria over the measurement period for the duplicate mesocosms 7 and 8.

linear correlation coefficients in the duplicate mesocosms (hereafter referred to as r_{avcorr}), calculated for the methanol uptake fluxes and the photosynthetically active radiation (PAR) was 0.18. The period from 31st May - 5th June (phase of bloom decline) had stronger methanol uptake compared to 6th June - 10th June (post-bloom phase with low phytoplankton abundance). Methanol uptake was generally higher during night-time, indicating that it was not driven by photosynthetic activity. The mean flux in both mesocosms calculated using median values was -0.26 ng m^{-2} s^{-1}, the negative value indicating the direction from air to seawater.

Acetone:

During the daylight sections of the experiment, acetone was emitted from the seawater to the air above it, if PAR exceeded 450 µmol photons m^{-2} s^{-1}, while at night it was always uptaken from the air to the seawater. The acetone flux shows good correlation with PAR ($r_{avcorr,\ acetone}$ = 0.70). Furthermore, the emission fluxes were higher in the phase of bloom decline with still relatively high phytoplankton abundances (31st May - 5th June) compared to the low biomass post-bloom phase (6th June - 10th June). The average of the median uptake fluxes and emission fluxes (uptake from air to sea water and emission from sea water to air) in both mesocosms was -0.06 ng m^{-2} s^{-1} and 0.27 ng m^{-2} s^{-1} respectively. Overall for the entire measurement period, the flux was an emission of 0.21 ng m^{-2} s^{-1}.

Acetaldehyde and Isoprene:

Acetaldehyde and isoprene were emitted from the seawater to the overlying air throughout the measurement period, with almost no

evidence of seawater uptake. The fluxes of acetaldehyde and isoprene show strong correlation with each other (r_{avcorr} = 0.86). The flux of acetaldehyde shows greater correlation with PAR ($r_{avcorr,\ acetaldehyde}$ = 0.70) compared to isoprene flux and PAR ($r_{avcorr,\ isoprene}$ = 0.49). There was a decrease in the flux of both acetaldehyde and isoprene during the second phase of the measurement period, from 6th June - 10th June. Mean emission flux strengths calculated from median values in the duplicate mesocosms were 0.23 ng m^{-2} s^{-1} and 0.12 ng m^{-2} s^{-1} for acetaldehyde and isoprene respectively.

Dimethyl sulphide (DMS):

In both mesocosms, DMS was always emitted from the seawater to the air above it. DMS fluxes showed negligible correlation with PAR ($r_{avcorr\ dms}$ = 0.01). Emission occurred at similar rates irrespective of light intensity, as seen on June 4th, which was particularly overcast. Remarkably, among all the measured organic species' fluxes, only the DMS flux did not decrease in the second phase i.e. from 6th June - 10th June. The mean DMS emission flux calculated using median values from both mesocosms was 0.3 ng m^{-2} s^{-1}.

2.4 Discussion

This is the first time that air-sea fluxes of organics have been analyzed and quantified during a mesocosm experiment. From the point of view of trace gas exchange, the mesocosm is a transparent tent, set over an area of ocean surface (circa 3 m^2) and extending from 1.5 m over the surface to 9.5 below. The tent contains a pocket of gas

which is ventilated with ambient air at a constant flow (residence time of the air is 191 minutes for mesocosm 7 and 170 minutes for mesocosm 8). The mesocosm experiment differs markedly from the static chamber flux experiments often conducted in soil and plant science. Most importantly, the uppermost 5m of seawater in the mesocosm is kept well mixed (see Figure 2.6) by use of an aquarium pump (constant flow) and it is from this volume that chlorophyll and DOC measurements are made. In the "real" world many physical parameters may affect the sea-air flux of a given species, for example, the wind speed (as was shown by Carpenter et al. 2004) and mixing down from the ocean uppermost mixed layer. Thus, in the open ocean mixing, dispersal and advection of the water mass complicate the interpretation of the data. On the other hand, the mesocosm system has low, almost constant air flow, subdued wave activity and possible wall effects from the enclosures, which might cause deviance from conditions in the natural environment. However, the beauty of the mesocosm experiment is that the wind speed and the downward mixing are kept as constant as possible by means of a constant air flow and the effective mixing of the 0-5m seawater layer, thus allowing other potentially controlling parameters to be investigated. Particularly suited for investigation in the mesocosm system is the significance of: a) ocean biology producing or consuming organic trace species in the seawater, b) that organic chemicals in the seawater (either directly or indirectly produced by the biology) may be photochemically degraded abiologically to organic gases that subsequently escape to the air. A considerable advantage of the

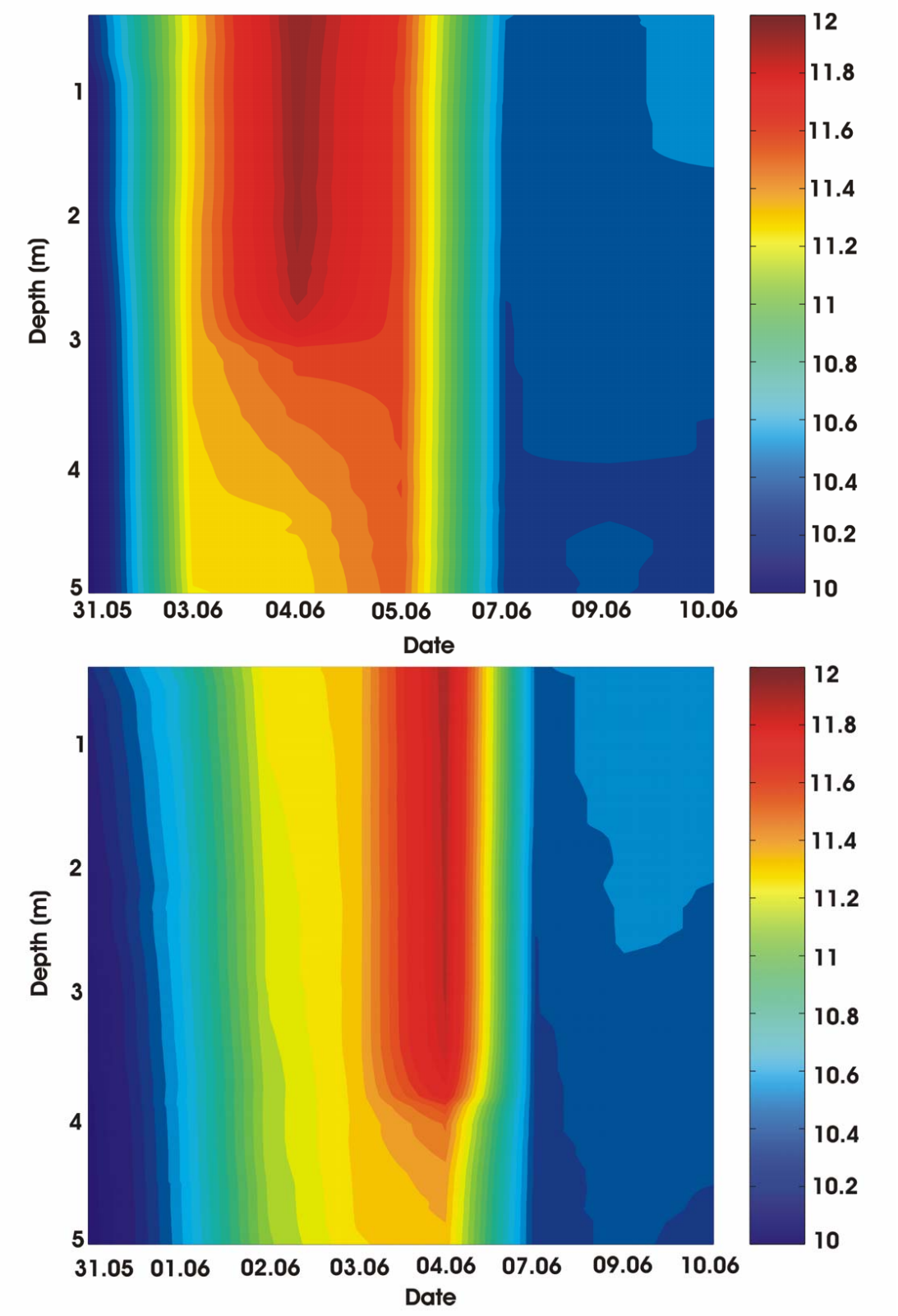

Figure 2.6: Daily (11 a.m.) depth profiles of temperature in the waters (upper 5 m) of mesocosm 7 (above) and mesocosm 8 (below).

mesocosm experiment over laboratory studies of single plankton species is that the plankton ecosystem is investigated as a whole, and possible interactions between plankton species (community dynamics) can occur. Furthermore within the mesocosm experiment the biology can be monitored, as opposed to "real world" aircraft studies (e.g. Singh et al 2003) or coastal studies (e.g. Carpenter et al. 2004).

While previous oceanic flux studies of these compounds have been based on either air-sea flux models (Liss and Mervilat 1986) or inverse modelling (Jacob et al. 2002; de Laat et al. 2001), in this study we infer fluxes from the difference in direct measurements of the air, before and after controlled interaction with the underlying seawater. Thus, assumptions and uncertainties pertaining to the model based studies are absent in this approach.

Before discussing the correlation of the VOC fluxes with light and ocean biology we would like to examine the potential effects of parameters such as friction velocity, the changing temperature in the mesocosm waters (by possible 'green house' heating effect) and possible persistent surface microlayer formation. In the mesocosm system, the influence of any dynamic parameter (e.g. friction velocity) on the VOC fluxes is constant because the air flow through the system is not changing and the water in the first 5m is constantly mixed. Thus the observed variation in the VOC fluxes cannot be accounted for, in terms of such dynamic parameters. The daily depth profile of mesocosm water temperature is shown in Figure 2.6 (the measurements were taken at 11 am everyday when PAR is almost at

its maximum value for the day, see Figure 2.4). Note that the temperature in the water of the mesocosms did not differ significantly for the 'sunny' days compared to the overcast days on the 3rd, 8th and 9th June. This is because the wind buffeting and wave action on the sides of the mesocosm tents coupled with the constant ambient air flushing rate of 30 L/min ensures good mixing within the mesocosm system and prevents the accumulation of thermal energy quite efficiently. For the maximum change in the mesocosm water temperature of 2 °K observed between different days at 11 a.m. (see Figure 2.6), the change in the Henry's law partitioning between the aqueous and gas phase for the OVOCs is shown in Table 2.3. These results clearly show that the maximum temperature effect would cause only a 13 % relative concentration change for methanol, 12 % relative concentration change for acetone and 12.4 % relative concentration change for acetaldehyde concentrations in the gas phase based on the change in the Henry's law partitioning. The relative change in the mixing ratios, between a diel minima and maxima is however much greater, varying between 500 % - 1500 % depending on the VOC and the biological phase (see Figure 2.3). Moreover a diel variation time series generated purely by the temperature effect should show no significant difference between the two biological phases. The issue of a persistent surface microlayer is an important one. Such a surface microlayer owing to its surfactant nature, would offer resistance to gas exchange between the bulk water layer and the atmosphere and also be more enriched in Dissolved Organic Matter (DOM) compared to the bulk water, due to inefficient transport and

Table 2.3: Change in Henry's law partitioning due to change in temperature of the mesocosm waters.

Compound	**Henry's law constant** (Cwater/Cair)	**Temperature** (K)
Methanol	13003	283
Methanol	11519	285
Acetone	1430	283
Acetone	1279	285
Acetaldehyde	969	283
Acetaldehyde	862	285

inhibited mixing. In the experimental set up, water in the first 5m was continuously circulated by means of an aquarium pump and the outlet of the pump was set near the surface in order to inhibit microlayer formation. The fact that species produced in the bulk water such as isoprene, mirror PAR (see Figure 2.4) without any significant time phase shift, support the theory that the combined effects of the waves buffeting the mesocosm tents and the internal mixing within the upper 5 m water column in the manner described earlier, prevent the occurrence of a persistent surface microlayer.

From the observations presented in section 2.3.2 we now examine the light and biology dependence of our derived fluxes within the context of the available literature. In this study, it is extremely difficult to implicate specific biological parameters for the emission or uptake of a particular trace gas, as the biological parameters were measured only once a day and the measured flux represents a net process due to possibly different sources and sinks. Nevertheless to give some idea about possible correlations between the VOC fluxes and the few biological parameters measured in this study, we have done a linear

regression analysis of the daily averaged VOC flux (row) against the measured biological parameters (column) in both the mesocosms (see Figure 2.7). For acetone, the daily emission flux and daily uptake flux has been treated individually. While interpreting the correlations, it should be borne in mind that at different stages in their life cycle, biological organisms can exhibit different responses and that community dynamics can cause coincidental correlations between individual VOCs and the biological parameters. Furthermore, some of the measured biological parameters are individual species such as *Emiliania huxleyi* and *Synechococuss sp.* while the others like nano plankton (size class), pico plankton (size class) and heterotrophic bacteria are bulk parameters that comprise of more than one species, so appropriate care should be taken while interpreting the significance of the correlations. Moreover, the chlorophyll content and hence photosynthetic activity depends to considerable degree on the cell size of the autotrophic species, so one cell of *Emiliania huxleyi* will be more potent in producing isoprene (a by product of photosynthesis) than one cell of the other smaller autotrophic species.

Day-time emission of acetone from seawater to the air occurred during the period of bloom decline, when phytoplankton biomass was still high, and comparatively low or absent during the post-bloom period of low phytoplankton abundances. Daily averaged acetone emissions seem to correlate positively with the measured daily abundance of *Emiliania huxleyi* ($r = 0.67$) and picophytoplankton ($r = 0.70$) while there seems to be negative correlation with *Synechococcus sp*. ($r = -0.57$) (see Figure 2.7). Light-dependency of acetone

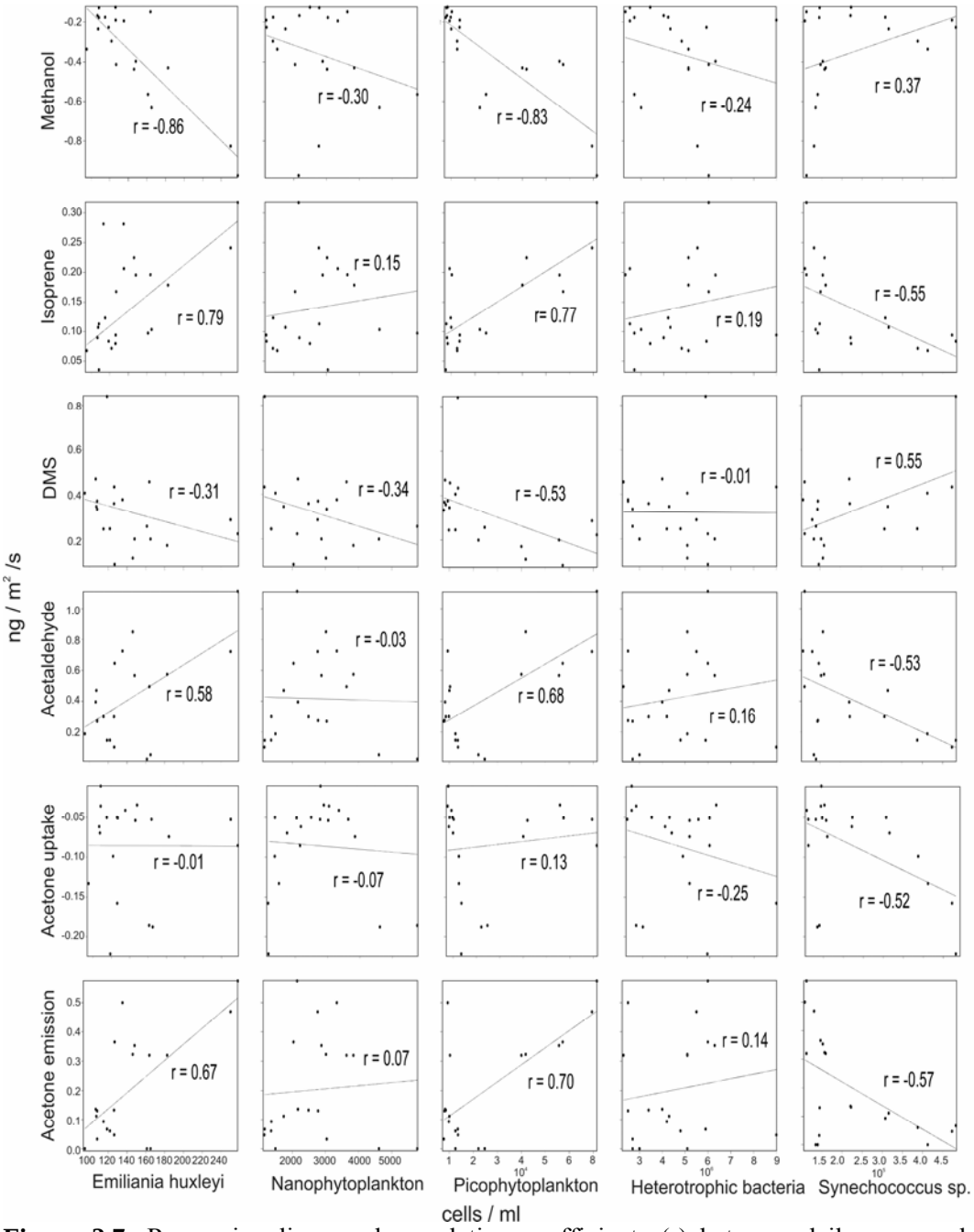

Figure 2.7: Regression lines and correlation coefficients (r) between daily averaged VOC fluxes (individual rows) and daily abundance of the biological parameters (individual columns) using data from both mesocosms.

emission was indicated on June 4th, when maximum light intensities below ~ 350 µmol photons m^2 s^{-1} shifted day-time acetone emission

to acetone uptake. Can we reconcile these results with the study by Marandino et al. (2005), which reported that acetone is always uptaken from the air to the seawater? It is well established that dissolved organic matter produces acetone by solar irradiation (Zhou and Mopper 1997). During both phases of plankton succession covered by our measurements, i.e. from 31st May – 5th June and 6th June – 10th June, the dissolved organic matter (DOM) in the seawater did not show significant variance. Concentrations of dissolved organic carbon (DOC), nitrogen (DON) and phosphorus (DOP) were more or less constant during the measurement period with mean values of DOC = 100 ± 7 μmol L^{-1}; DON = 8 ± 3 μmol L^{-1} and DOP = 0.26 ± 0.04 μmol L^{-1} (Wohlers et al. in preparation). However, since the second phase had considerably less emission of acetone (see Figures 2.4 and 2.5), despite similar PAR and DOM concentrations as during the first phase, the implication is that acetone production in seawater is biologically mediated and light dependent. In the absence or under low activity of the relevant production pathway, acetone consumption in seawater can exceed its production, leading to net acetone uptake by the ocean. This was the situation during the second phase of this study and may have been the cause during the study of Marandino et al. (2005) in the oligotrophic N.W. Pacific.

Net uptake of methanol from air into seawater appears to be attenuated by light, and biological dependence can be inferred from the decrease in the second phase, as plankton abundance and biomass declined. Of course the methanol uptake might have decreased simply because the water was under saturated in the

beginning and became gradually more saturated towards the end of the experiment. If uptake was driven solely by physical undersaturation, the same trend would have been also seen in the acetone profiles (see Fig 2.3 and 2.4). Let us nonetheless consider this hypothesis further. The well mixed mesocosm water volume is ~15 m^3 . In order to saturate this volume of water at 283 °K, and assuming there is absolutely no methanol in the water to start with; one would need 214 mg of methanol(Taking H= 10000 and Cair =1 nmol/mol). Using an uptake flux of 1 ng/m^2/s (a generous value as can be seen from Fig 2.3 and Fig 2.4), during the period 17th till 30th May, we calculate that ~1.2 mg methanol would have been available for dissolution in this 14 day period, indicating that based on this criteria alone, the mesocosm water would still be significantly undersaturated before we commenced our measurements with the PTRMS on the 31st of May. Now, if the mesocosm waters' under saturation was just a function of 'physically driven' under saturation then there should have been a constant decrease in the uptake flux of methanol over time, because the degree of undersaturation would decrease. What we see however is that on the afternoon of 2nd June and 9th June, even for similar mixing ratios of methanol in the ambient air of around 2 nmol/mol, the uptake flux of methanol is in fact more than 1.6 times higher on the 9th of June. Clearly this is inconsistent with the notion of an undersaturation driven solely by physical parameters and suggests a possible biological contribution to the maintenance of undersaturation in the mesocosm water. What we are suggesting here is that surface waters in the mesocosm are in fact close to equilibrium

and that the undersaturation is driven by the biological uptake. A comparison of the deposition velocity found by Carpenter et al. 2004 (0.02-0.33 cm s^{-1}; best estimate = 0.09 cm s^{-1}) to that observed in our mesocosm study (circa 0.05 cm s^{-1}) shows reasonable agreement. We interpret the deposition velocity of methanol found by Carpenter et al. 2004 as not indicating an uptake entirely dominated by aerodynamic resistance (interpreted as the turbulent resistance in the atmosphere) even at the reasonably high wind speeds of 8 m s^{-1}. If this were the case (i.e. surface resistance is unimportant) then deposition velocities would be higher (similar to those of HNO_3 ca. 0.5-1 cm s^{-1}). The comparison of modeled and measured values for methanol wind speed dependencies given by Carpenter et al.2004 do not show a particularly good match, especially at low wind speeds despite being described a good agreement (see Fig 6 in Carpenter et al. 2004), perhaps because the model is not fully describing the processes in play and ocean biology contributes to the uptake. As mentioned in the results section, we also observed reduced uptake during daylight hours in the first phase, which was characterized by higher plankton abundance. Heikes et al. (2002) report that methanol has been observed in the headspace of laboratory phytoplankton cultures. Either the biological uptake of methanol from air to seawater is less during the day, or methanol is produced in seawater by phytoplankton during the day or both processes together result in the reduced uptake of methanol, from air to seawater during the day. The second phase has higher *Synechococcus sp* and free living heterotrophic bacteria but the methanol uptake flux does not increase. This seems to suggest

that the cyanobacteria *Synechococcus sp* and the free living heterotrophic bacteria do not consume methanol significantly under these conditions (| r | < 0.38 for both; Figure 2.7). Surprisingly, methanol uptake shows correlation with *Emiliania huxleyi* and picophytoplankton (| r | = 0.86 and | r | = 0.83 respectively). We would like to stress that for reasons outlined earlier, this does not necessarily imply that *Emiliania huxleyi* and picophytoplankton uptake methanol by night, although based on our dataset it seems to be a possibility.

Acetaldehyde and isoprene are generally emitted from the seawater to the overlying air. The emissions correlate with both photosynthetically active radiation, as well as the measured biological parameters (r = 0.58 for acetaldehyde with *Emiliania huxleyi* , r = 0.79 for isoprene with *Emiliania huxleyi* and r = 0.68 for acetaldehyde with picophytoplankton and r = 0.77 for isoprene with picophytoplankton), with decrease in the second phase of the measurements. It should also be noted that some isoprene and acetaldehyde production occurs under overcast conditions and even at night. Like acetone, acetaldehyde is also produced by the photochemical degradation of dissolved organic matter (DOM) in seawater (Zhou and Mopper 1997), while planktons are known to produce isoprene (Milne et al. 1995). The high degree of correlation between isoprene and acetaldehyde for the entire study (r = 0.86) and the decrease in both isoprene and acetaldehyde emissions in the second phase, coupled with the insignificant variance in the dissolved organic matter (DOM) during both phases, suggest that there might

be some biologically mediated production of acetaldehyde in seawater, from which emission then occurs to the overlying air.

DMS emissions do not seem to depend on light and the emission rate is quite comparable in both phases. It is well established that DMS is produced in seawater both by direct release from phytoplankton and by bacteria and zooplankton mediated grazing (Dacey and Wakeham 1986; Gabric et al. 2001). Further, Nguyen et al. 1998 have reported appreciable DMS production in sea water during the senescence phase of phytoplankton. Thus, DMS emission in the first phase is probably due to direct release from phytoplankton while grazing processes seem to be responsible for the DMS emission during the second phase.

It is also useful to try and look at correlations amongst the

Table 2.4: Pearson Correlation Coefficient (r_{av}) between the VOC fluxes.

	Methanol	Acetone	Acetaldehyde	Isoprene	DMS
Day^{+}					
Methanol	1	-0.19	-0.15	-0.28	0.2
Acetone	-	1	0.96	0.85	0.01
Acetaldehyde	-	-	1	0.88	-0.01
Isoprene	-	-	-	1	0.02
DMS	-	-	-	-	1
Night*					
Methanol	1	0.36	0.44	0.24	0.29
Acetone	-	1	0.64	0.45	0.01
Acetaldehyde	-	-	1	0.58	0.26
Isoprene	-	-	-	1	0.23
DMS	-	-	-	-	1

+ = Day defined as whenever PAR > 100 µmol m^{-2} s^{-1}; * = Night defined as whenever PAR ≤ 100 µmol m^{-2} s^{-1}

emission fluxes of isoprene, acetone, acetaldehyde, DMS and the uptake fluxes of acetone and methanol with each other during day and night repectively to try and gauge if they might have common mechanisms linked to their uptake and/or emissions. The Pearson linear correlation coefficient (r_{av}) for all possible pairs among the measured VOC fluxes is shown in Table 2.4. The strongest correlations seem to be for the day time emission fluxes of acetone and acetaldehyde (r_{av} = 0.96), acetaldehyde and isoprene (r_{av} = 0.88) and acetone and isoprene (r_{av} = 0.85). Since isoprene is widely established as a biogenic emission, these correlation values support our hypothesis that acetone and acetaldehyde emissions have some biological dependence. The other notable feature is that at least for air were probably due to a local source of macro algae, which were growing near the raft but outside conditions during our study, DMS emission does not correlate with any of the other VOC fluxes.

In Table 2.5, we compare the mixing ratios and fluxes measured here with previous studies on methanol, acetone, acetaldehyde, isoprene and DMS in the marine boundary layer. The general level of the ambient air mixing ratios of the oxygenates presented here are consistent with earlier studies, while for isoprene and DMS, they are somewhat higher. Proton transfer reaction mass spectrometry measurements are upper limit estimates because of possibly more than one species contributing to the measured mass. It should be noted that the high mixing ratios of isoprene and DMS in the ambient the mesocosms. Isoprene might additionally have been impacted by trees on the coast and the nearby islands.

Table 2.5: Comparison with earlier works on Marine Emissions and Uptake of VOCs.

Med../Ave*. (nmol mol^{-1})	Sea-Air flux	Oceanic Source ($ng\ m^{-2}\ s^{-1}$)	Oceanic Sink ($Tg\ yr^{-1}$)	Location	Reference ($Tg\ yr^{-1}$)
Methanol					
0.87	-12.5[a]	-	-	Tropical Atlantic	Williams et al.2004b
0.57	-0.6[a]	-	8	Pacific Ocean (0-2km)	Singh et al.2003
0.57	-	-	15	Pacific Ocean (0-2 km)	Singh et al.2004
2.0	-2.81[a]	-	-	New England Coast	Mao et al.2006
0.9	-	30[b]	85	-	Heikes et al.2002
-	-	-	0.3	-	Galbally and Kirstine et al.2002
-	-	-	10	-	Jacob et al.2005
1.86	-0.26[+]	-	2.97	Raunefjord, Norway	This work
Acetone					
0.52	5.71[a]	-	-	Tropical Atlantic	Williams et al.2004b
1.3	-3.22[a]	-	-	New England Coast	Mao et al.2006
0.47	-1.2[a]	-	14	Pacific Ocean (0-2km)	Singh et al.2003
0.36	-2.92[a]	-	48	North Pacific Ocean	Marandino et.al.2005
0.38	-	-	-	Caribbean Sea	Zhou et al.1993
-	-	27	14	-	Jacob et al.2002
0.5	-	-	-	Mace Head	Lewis et al.2005
0.8	-0.06[+](U) 0.27[+](E)	3.13	0.68	Raunefjord, Norway	This work
Acetaldehyde					
0.2	11[a]	125	-	Pacific Ocean (0-2km)	Singh et al.2003
0.44	-	-	-	Mace Head	Lewis et al.2005
0.50	-	-	-	Caribbean Sea	Zhou et al.1993
0.55	0.23[+]	2.62	-	Raunefjord, Norway	This work
Isoprene					
0.04	0.02-0.24[a]	0.26-2.7	-	NW Pacific Ocean	Matsunaga et al.2002
-	0.02[a]	0.22	-	Near shore North Sea	Broadgate et al.1997
-	0.12[a]	1.4	-	NW Pacific Ocean	Bonsang et al.1992

<0.01	0.01-0.08[a]	0.08-0.9	-	Florida Straits	Milne et al.1995
-	-	0.1-0.7	-	North Atlantic	Baker et al.2000
-	-	0.12	-	-	Palmer et al.2005
0.18	0.12[+]	1.4	-	Raunefjord, Norway	This work
Dimethyl sulphide					
0.05	1.79[a]	-	-	Tropical Atlantic	Williams et al.2004b
-	1.44-4.3[a]	-	-	Equatorial Pacific Ocean	Huebert et el.2004
0.03-0.34	-	-	-	Southern Indian Ocean	Sciare et al.2000
-	-	29-104[d]	-	-	Andreae et al.1990
-	-	25-72[d]	-	-	Kettle et al.2000
-	-	50.37[d]	-	-	Nguyen et al.1978
0.4	0.3[+]	3.42[d]	-	Raunefjord, Norway	This work

a = converted from original units to (ng m^{-2} s^{-1}); b = best estimate; + = average of median values in duplicate mesocosms

d = converted from (Tg S yr^{-1}) to (Tg DMS yr^{-1}) ; * = where both median and average are available, median has been used

The relative abundances of the organic trace gases reported in this work and measured using the same instrument, fit with the trend discerned from measurements in previous studies (Zhou and Mopper 1993; Mao et al. 2006 and other references in Table 2.5). The trend is: methanol > acetone > acetaldehyde > isoprene ~ DMS. The reported median values also show that the sum of the oxygenates is approximately six times higher than the sum of isoprene and DMS in the marine boundary layer. Interestingly, when fluxes are compared, the sum of the fluxes of oxygenated VOCs (0.23+ 0.27- 0.26) is almost a factor of two smaller compared to the sum of isoprene and DMS (0.12+ 0.3).

Compared with direct methanol, acetone and acetaldehyde fluxes reported from a terrestrial pine plantation (Karl et al. 2005), the

oceanic fluxes reported here and in previous works (see Table 2.5) are 2-3 orders of magnitude lower.

Before we discuss the results concerning the 'tentative global extrapolation' of the VOC fluxes measured in this study, we wish to highlight the associated uncertainties of the employed approach. As mentioned earlier, the mesocosm is an artificial set up with low and almost constant wind speed, possible wall losses and subdued wave activity, conditions that may represent significant deviance from 'natural' oceanic conditions. For example, methanol uptake flux may be enhanced under the mesocosm conditions while DMS emission flux may be under estimated. Wall losses in the mesocosm cannot be ruled out but if they were the dominant player, one would have seen uptake all the time, i.e. ambient air would be stripped of the compound in the mesocosm by the walls and not the sea. The two most polar compounds we examine are methanol and acetone. While we do observe uptake with methanol, acetone clearly shows emission as well. The wall loss also does not account for the flux changes relating to biology or light. Stratification and mixing of the water column in the mesocosms is designed to simulate open ocean conditions. Stratification prevents re- introduction of sedimented material into the surface sea layer and mixing ensures efficient transport between the bulk and surface waters. However all things considered, it is apparent that in the mesocosm system, physical parameters are not favourable for sea-air gas exchange. Consequently, they are not the dominant factors controlling the VOC fluxes in the mesocosm, rather ocean biology and PAR are the primary driving

forces of the sea-air fluxes in the mesocosms. Thus, the flux derived from the mesocosms gives an idea of how important ocean biology and PAR can be for the marine emissions and / or uptake of the different VOCs. All the oceanic VOC budget estimates, except perhaps DMS, are based on the few measurements conducted in the "open" oceans in "selected" oceanic regions which have been extrapolated to the global oceans (references in Table 2.5), although conditions vary widely and vastly from one part of the global ocean to the other. Given this current uncertainty in VOC fluxes from / to the ocean (as highlighted in Table 2.5 of the manuscript), the fluxes from this study can be used to "tentatively extrapolate" for an "indication of the possible global flux" for comparison with previous budget estimates and to ascertain which species are most significant for atmospheric chemistry.

Although this study took place in coastal waters, chlorophyll a (2.28 – 1.05 μg L^{-1}, nutrient values (PO_4^{3-} = 0.05 μmol L^{-1}; NO_3^- = 1 μmol L^{-1}; SiO_3^- = 0.25 μmol L^{-1} , Riebesell et al. in preparation) and dissolved organic matter (DOM; 97-110 μmol L^{-1}) measured in the mesocosm seawater between 31st May –and 10th June are representative of vast areas of the global oceans. The up-scaling of the fluxes was based on the entire global ocean surface area of 3.61 x 10^{14} m^2, and all results are summarized in Table 2.5.

For methanol we estimate a net oceanic sink of 2.97 Tg yr^{-1}. This is higher than the 0.3 Tg yr^{-1} oceanic sink proposed by Galbally and Kirstine et.al. (2002) and lower than the estimates reported by Singh et al. (2003) , Heikes et al. (2002) and Jacob et al. (2005). Based on

the same measurements but different models, methanol oceanic sinks of 8 Tg yr^{-1} and 15 Tg yr^{-1} were proposed by Singh et al. (2003) and Singh et al. (2004) respectively, showing that different model parameterizations give quite different results.

Except for Jacob et al. (2002), all previous studies have estimated a net oceanic sink for acetone. We estimate an emission flux and uptake flux of 3.13 Tg yr^{-1} and 0.68 Tg yr^{-1} respectively. It should be mentioned that during the period of our field study in Norway, there was 18 hours of daylight and only 6 hours of darkness. As established in this study, acetone emissions are influenced by both a critical PAR threshold and biological activities, parameters that have not been incorporated in up-scaling the measurements obtained in this or previous studies.

Measurements of acetaldehyde are currently viewed with some scepticism due to recently reported potential sampling problems for this species. Apel et al. (2003) reported an artefact for acetaldehyde could occur within inlets, even on inert surfaces. Interferences in stratospherically influenced air have been reported by Northway et al. (2004) and Singh et al. (2004) for PTR-MS and GC systems respectively, suggesting an interfering surface related phenomenon affecting all instruments. Furthermore, acetaldehyde measurements appear to be inconsistent with simultaneously measured species such as PAN and ethane when compared with models (Singh et al. 2004; Lewis et al. 2005). However, by measuring the difference in the acetaldehyde mixing ratios, for the inflowing ambient air and the mesocosm air, we have minimized possible systematic artefacts. As

an additional precaution, all the Teflon inlets used for sampling ambient air and mesocosm air, had the same dimensions and were shrouded from sunlight, using black tubing. The case for acetaldehyde emission not being an artefact is strengthened as it correlates with both isoprene and the independently measured biological trends. Our estimate of a global acetaldehyde oceanic source of 2.62 Tg yr^{-1} is significantly lower than the only other estimate of 125 Tg yr^{-1} reported by Singh et al. (2003). It should be noted that a direct emission of acetaldehyde through biological processes as suggested here is a good explanation why acetaldehyde levels were not consistent with ethane (formerly considered the main precursor) in the marine boundary layer.

Estimated global marine isoprene fluxes extrapolated from in-situ measurements range from 0.1-1.4 Tg yr^{-1} (Bonsang et al. 1992; Broadgate et al. 1997; Matsunaga et al. 2002; Shaw et al. 2003; Broadgate et al. 2004). The latest estimate based on satellite chlorophyll observations totals 0.12 Tg yr^{-1} (Palmer and Shaw. 2005). This is small in comparison with terrestrial emissions of ca. 500 Tg yr^{-1} and the results of this study (1.4 Tg yr^{-1}) are in agreement with this estimate.

Dimethyl sulphide fluxes reported in this study (3.42 Tg yr^{-1}) are significantly lower than those reported in previous open ocean studies (25-104 Tg yr^{-1};Nguyen et al. 1978; Andreae 1990; Kettle and Andreae 2000; Sciare et al. 2000; Huebert et al. 2004). Two factors may contribute to the difference between the flux estimates of this study and previous studies. Firstly, measurements being in the

aftermath of a phytoplankton bloom, characterized by depleting nutrients and generally moribund phytoplankton populations, DMS emissions are expected to be low. Alternatively it could be that the predominant biological species during our measurement period were not prolific DMS emitters.

2.5 Conclusion

From the discussion above it is clear that the air-sea flux of each trace gas depends differently on light and biological activity. Therefore on a global scale, extremely large variations in such fluxes can be expected as a consequence of the range of solar and biological conditions over the oceans. From the extensive ocean studies done on DMS emission fluxes, it is also apparent that seasonality and biological hotspots are very important factors. Thus, specifically parameterized models constrained by measurements from locations that represent the varied geographical areas of the global ocean are needed to form more accurate estimates of the oceanic contribution to the global budgets of different volatile organic compounds. This study has shown that PAR and ocean biology can act as quite important players in the emissions of acetone, acetaldehyde and isoprene from the ocean to the atmosphere. Photochemical and global ocean models that consider ethane to be the main source of acetaldehyde in the marine boundary layer may be able to resolve discrepancies between measured and modeled acetaldehyde concentrations by considering the additional biological source. The strong correlations between the day time emission fluxes of acetone,

acetaldehyde and isoprene may also be useful for modeling the air-sea emission fluxes of these VOCs. Possible methanol uptake at night by phytoplankton species must be investigated in future studies, as this could be a major source of methanol undersaturation in the global oceans. In order to further improve our understanding of the biogeochemical cycling of VOCs at the sea-air interface, we recommend that in future mesocosm experiments, both aqueous and gas phase concentrations should be monitored and the mesocosm air should be actively circulated with a fan to ensure thorough mixing in the gas phase. Further, a more exhaustive suite of biological parameters, measured at a higher frequency than in this study may yield valuable insights for biological production and / or consumption of VOCs in the seawater. Finally, the results have shown that the mesocosm approach is a new and novel technique, particularly suited for clarifying the vast uncertainties that exist in the field of Ocean VOC uptake and emissions and their biogeochemical cycling.

3. Methane emissions from boreal and tropical forest ecosystems derived from in-situ measurements

Methane is a climatologically important greenhouse gas, which plays a key role in regulating water vapour in the stratosphere and hydroxyl radicals in the troposphere. Recent findings that vegetation emits methane have stimulated efforts to ascertain the impact of this source on the global budget. In this work, we present the results of high frequency (ca. 1 minute^{-1}) methane measurements conducted in the boreal forests of Finland and the tropical forests of Suriname, in April-May, 2005 and October 2005 respectively. The measurements were performed using a gas chromatograph - flame ionization detector (GC-FID). The average of the median mixing ratios during a typical diel cycle were 1.83 μmol mol^{-1} and 1.74 μmol mol^{-1} for the boreal forest ecosystem and tropical forest ecosystem respectively, with remarkable similarity in the time series of both the boreal and tropical diel profiles. Night time methane emission flux of the boreal forest ecosystem, calculated from the increase of methane during the night and measured nocturnal boundary layer heights yields a flux of (3.62 ± 0.87) x 10^{11} molecules cm^{-2} s^{-1}(or 45.5 ± 11 Tg CH_4 yr^{-1} for global boreal forest area). By using a source apportionment method based on land use type in the footprint area, a first order emission flux of ~ 6.7 Tg CH_4 yr^{-1} is estimated for the boreal vegetation. These results highlight the importance of the boreal and tropical forest ecosystems for the global budget of methane. The results are also

discussed in the context of recent work reporting high methane mixing ratios over tropical forests using space borne near infra-red spectroscopy measurements.

3.1 Introduction

Methane is the most abundant hydrocarbon (circa 1.8 μmol mol^{-1}) in the atmosphere. It has significant implications for climate warming and atmospheric chemistry, as it plays a key role in regulating stratospheric water vapour and tropospheric hydroxyl radicals (Khalil, 2000). Atmospheric methane mixing ratios have nearly tripled since pre-industrial times (Prather et al. 2001; IPCC 2001), and while it is generally agreed that approximately 600 Tg CH_4 yr^{-1}(1 Tg = 10^{12} g) is released to the atmosphere globally, estimates of some of the individual source and sink terms within the global budget are rather uncertain (Lelieveld et al., 1998). For example, the range of the emission estimates for wetlands, the single largest natural methane source, is 92-232 Tg CH_4 yr^{-1} with a best guess estimate of 145 Tg CH_4 yr^{-1} (Wuebbles et al., 2002; Matthews et al., 2000; Prather et al., 2001). With such uncertainties in the existing global budget of methane, the discovery that terrestrial plants emit methane under aerobic conditions (Keppler et al., 2006) and reports of enhanced methane emissions from Siberian thaw lakes (Walter et al., 2006), have reinvigorated efforts to better constrain sources and sinks. The global estimate of a 62-236 Tg CH_4 yr^{-1} vegetation source by Keppler et al. (2006), was based on an extrapolation of incubation chamber measurements using the metric of net primary productivity (NPP) for various ecosystems, and subsequent studies (Houweling et al., 2006; Ferreti et al., 2006; Kirschbaum et al., 2006; Parsons et al., 2006), have presented revised upper limit estimates in the range of 60-176 Tg CH_4 yr^{-1}, based on

alternative up-scaling approaches. However, as the underlying production mechanism is still unknown, any extrapolation to the global scale is highly speculative. Reanalysis of methane measurements conducted in Venezuela (Crutzen et al., 2006; Sanhueza et al., 2006) concluded that tropical savannah vegetation also emits methane. Using space borne near infra-red remote sensing by the scanning imaging absorption spectrometer for atmospheric chartography (SCHIAMACHY), Frankenberg et al. (2005) observed almost 40 nmol mol^{-1} higher mixing ratios of methane over tropical rainforests compared to values predicted by a global 3D transport model (TM3) for the period October – November, 2003. Space borne measurements provide greater spatial coverage compared to local in situ measurements at surface sites, which are closer to sources and sinks. On the other hand, the column averaging employed in volume mixing ratio (VMR) retrievals of space borne measurements, has potential offsets and biases (Bergamaschi et al., 2007; Frankenberg et al., 2006), rendering remote sensing measurements less precise and less accurate than in-situ field measurements. A combination of in-situ and satellite retrieved methane measurements from forested regions therefore appears to be an ideal approach to assess the methane vegetative emission. However, such in-situ data (i.e. real time diel profiles of methane) from the boreal and tropical forests are surprisingly sparse, even though boreal and tropical forests collectively represent almost 76 percent of all forested land and hence have a large potential impact on the global methane budget.

In this study, we present the results from a high frequency gas

chromatograph equipped with a flame ionization detector (GC-FID). Measurements were taken approximately every minute within a boreal forest ecosystem in Finland and a tropical forest ecosystem in Suriname in April-May, 2005 and October 2005 respectively. We discuss trends in the diel profiles, calculate the nighttime ecosystem flux for the boreal forest ecosystem and speculate on the implications of these results.

3.2 Experimental

3.2.1 Site description: Boreal forest

Measurements were conducted from 16 April to 1 May 2005, as part of the BACCI / QUEST III campaign near (< 100m) the SMEAR II measurement station (Station for Measuring Forest Ecosystem-Atmosphere Relations) in Hyytiäla, southern Finland (61°51' N, 24°17' E, 170 m a.s.l.). About 600 m to the south west of the measurement station, there is an oblong lake (circa 2 km long). Figure 3.1 (a). shows a picture of the boreal forest vegetation in the vicinity of the measurement tower. In addition to measurements of routine meteorological parameters such as wind direction, wind speed etc., the SMEAR II station also conducts tower based measurements of gases such as CO_2 and O_3 throughout the year, providing a comprehensive suite of supporting measurements as detailed in Hari and Kulmala (2005) and Vesala et al. (1998). A detailed distribution of the different land use categories in a 1600 km^2 area around the SMEAR II station has been described recently in Haapanala et al.

Figures 3.1 (a) and 3.1 (b): View of boreal forest vegetation in Hyytiäla (61°51´N, 24° 17´E, 170 m a.s.l) (above) and view of tropical forest vegetation in Brownsberg (4° 56´N, 55°10´ W, 514 m a.s.l) (below).

(2006) using data derived from satellite photographs and forest inventories of the National Land Survey of Finland. The 1600 km^2 area around the SMEAR II station has spruce dominated forest (*Picea abies*; 25.5 %), pine dominated forest (*Pinus sylvestris*; 22.7 %), mixed forest (European aspen : *Populus tremula* and Birch : *Betula pendula* and *pubescens*; 20.9 %), deciduous forest (2 %), agriculture (10.2%), wetlands (0.7 %) and water bodies (13 %). The Scots pine forest was planted in 1964 and in 2004 the canopy height was around 14 m (Rinne et al., 1999; Hari and Kulmala, 2005).

Figure 3.2 shows the wind rose plot for the period of our study in

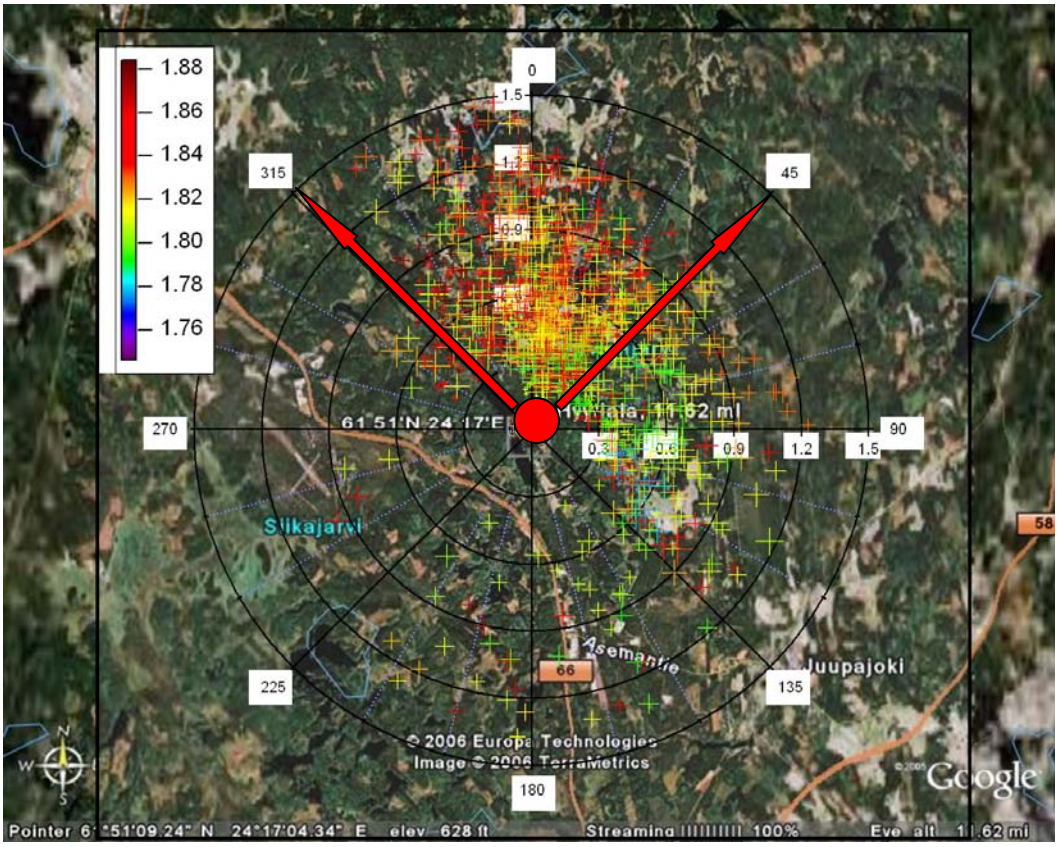

Figure 3.2: Wind rose plot showing methane (coloured markers and scale), wind speed (radii) and wind direction (angle) in Hyytiäla during the campaign.

Hyytiäla. During the campaign the wind blew mostly from the 0°-135° and 315°-360° wind sectors. Wind speeds were generally less than 1 m s^{-1}, although occasionally they reached speeds of up to 1.5 m s^{-1}. Our study was conducted in April-May, which marks the transition from winter to spring as the ground begins to thaw and the temperature increases marking the onset of photosynthetic activity (Suni et al., 2003). The minimum and maximum temperatures during the period of our study were around -5°C (typically at circa 06:00 local time (LT)) and 11°C (typically at circa 14:00 LT), with no well defined increasing trend, from the first to the last day of the study.

The annual mean temperature at the site is 3°C. The warmest month is July with a mean temperature of 16°C and the coldest is February with mean temperature of –8°C. Detailed long term climatic data for the site is available in Drebs et al. (2002).

3.2.2 Site description: Tropical forest

High frequency methane measurements were also conducted within the nature reserve of Brownsberg (4°56' N, 55°10'W, 512 m a.s.l.), Suriname from 5 - 14 October, 2005, as part of the Guyana Atmosphere-Biosphere exchange and Radical Intensive Experiment with the Learjet (GABRIEL) campaign. Brownsberg is situated around 120 km inland and is topographically elevated with respect to the Brokopondo lake (circa 40 km long), which lies south east of the measuring site. Figure 3.1 (b) gives a view of the vegetation from Brownsberg where the canopy height was typically around 40 m. Rainforest vegetation is too diverse to be classified in terms specific plant types, however, based on the United States Geological Survey (USGS) world vegetation maps, the main general vegetation types in the area are lowland evergreen broad leaf trees, semi-evergreen moist broadleaf trees and some schlerophyllus dry forest trees. Upwind from the site is 300 – 400 km of pristine rainforest before the coast of French Guyana. During October, Suriname experiences the long dry season, in which steady south easterly winds advect clean marine air westwards over the rainforest. Typically, the range of temperatures experienced during this period is between 20°C – 32°C.

3.2.3 Sampling procedure and measurements

Ambient forest air was sampled within the canopy, at heights of 8.5 m and 35 m for the boreal and the tropical forests respectively. Employing the same sampling procedure for both sites, ambient air was drawn rapidly (circa 6 L min^{-1}; inlet residence time < 12 seconds) and continuously through 0.64 cm diameter and 25m long shrouded Teflon tubing using an external pump (Rietschle Thomas, Memmingen GmbH, Memmingen). From this main flow of ~ 6 L min^{-1}, 1.2 L min^{-1} was drawn continuously by an internal pump within the methane measurement device. The instrument used was a commercial gas chromatograph equipped with a flame ionization detector (GC-FID) (Model 55C Hydrocarbon Analyzer, Thermo Electron Corporation, Massachusetts, USA). Nitrogen was used as carrier gas while hydrogen and zero air were used as fuel for the FID detector. Central to the instrument's operation is an eight port, two position, rotary valve which is used to introduce the gas sample into the analyzer and to control the flow of gases through the chromatographic column. The operational temperature of this column is 65°C. After separation from other airborne components within the column, the methane peak is measured by the FID and the signal area is converted into a mixing ratio by comparison with the signal produced by a calibration gas (3.96 μmol mol^{-1} methane standard procured from Westfalen AG, Germany; stated accuracy 2 %). The detection limit of the instrument is 20 nmol mol^{-1} methane and the measurement range is 0-20 μmol mol^{-1} methane, over which the detector responds linearly. One measurement was taken approxi-

mately every 70 seconds (frequency of measurements = 0.014 Hz).

The accuracy and precision errors are each, ± 2 % of the measured value. However, for the data presented here, the overall uncertainty has been determined as 2.58 %, comprising of the 2% accuracy error (a systematic error which is the same for all measurements) and a reduced precision error of 0.58 % for each data point due to the 15 minute time averaging employed in preparing the box and whisker plots (Figures 3.3 and 3.4).

In order to check for instrumental drifts, all the basic instrumental operational parameters such as the oven temperature, column temperature and support gas pressures were monitored continuously, in addition to regular in-field calibrations performed at the start, middle and end of the measurement campaigns.

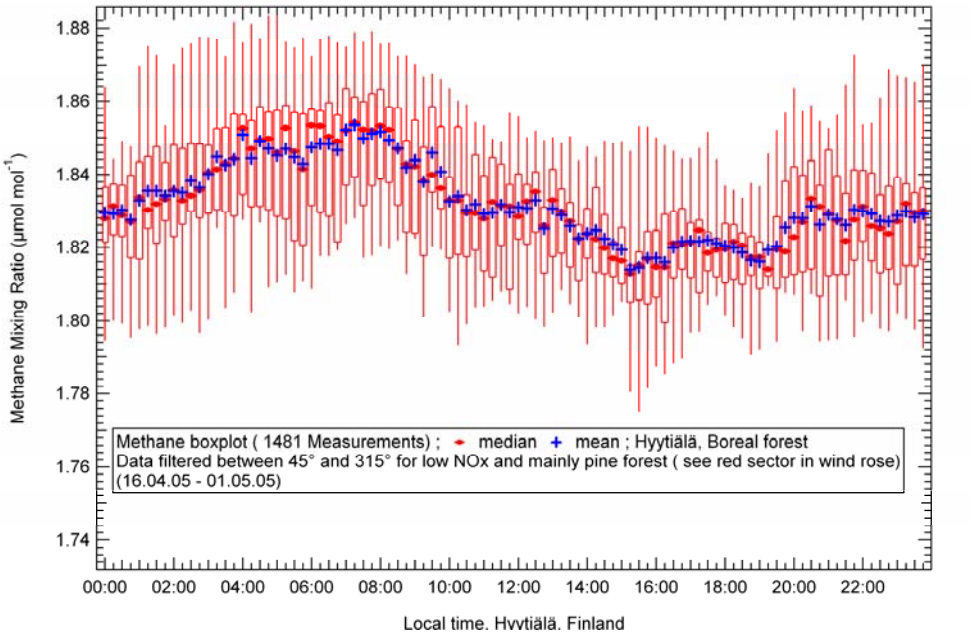

Figure 3.3: Box and whisker plot for diel cycle of filtered methane data (315° - 45° wind sector) from Hyytiäla (61°51´N, 24° 17´E, 170 m a.s.l), Finland during the BACCI / QUEST III Campaign.

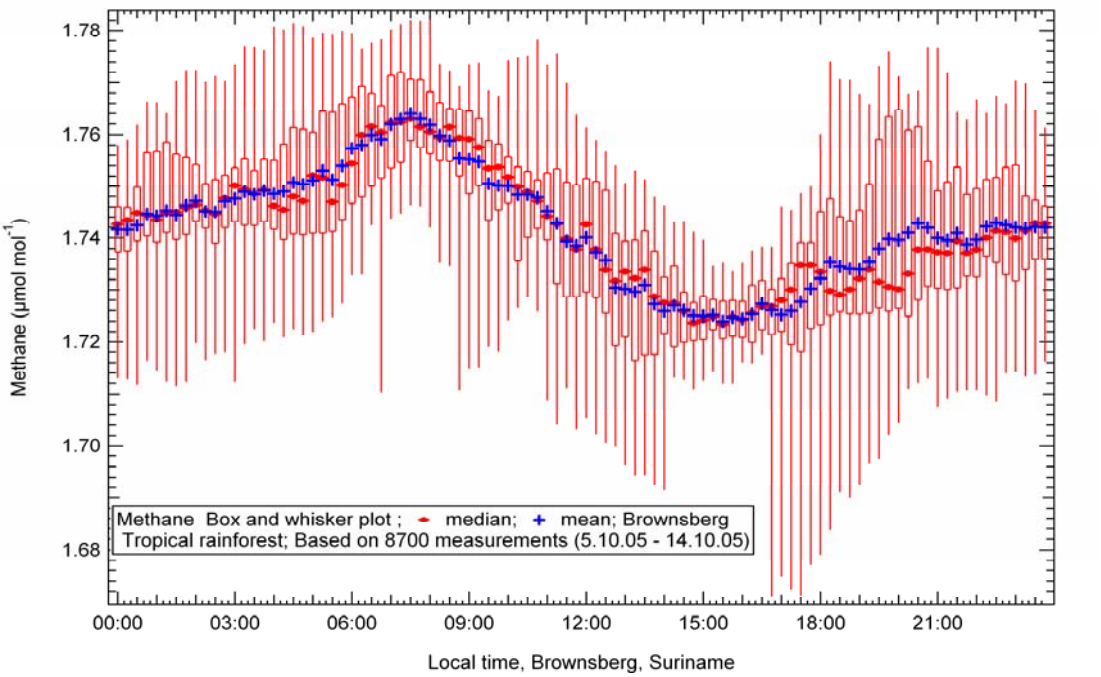

Figure 3.4: Box and whisker plot for diel cycle of methane data from Brownsberg (4° 56´N, 55°10´ W, 514 m a.s.l), Suriname during the GABRIEL campaign.

At the SMEAR II station, carbon dioxide was measured using an infrared light absorption analyser (URAS 4 CO_2, Hartmann & Braun, Frankfurt am Main, Germany) while the wind speed and wind direction were measured with an ultrasonic anemometer (Ultrasonic anemometer 2D, Adolf Thies GmbH, Göttingen, Germany).

3.3 Results

3.3.1 Boreal forest: Trends in methane mixing ratios and diel cycle

Methane mixing ratios were highest when the winds were blowing from the north, which has extensive forest cover and low population (Hari and Kulmala et al., 2005). In order to minimise

influences from anthropogenic emissions (from the city of Tampere south east of the site), and from wetlands (primarily south west of the site, Haapanala et al., 2006), the methane data was filtered to include data only from the 315°-45° wind sector. A box and whisker diel plot of the filtered data for the entire campaign is shown in Figure 3.3. As per convention, the box encloses all values from the 25-75 percentile while the whiskers encompass all values in the 5-95 percentile range. It can be seen that the median and mean values compare closely most of the time, indicating that no sharp bursts of methane emissions were detected. The plot also shows a distinct diel variation in the mixing ratios of methane, with lowest median values of around 1.81 μmol mol^{-1} occurring typically between 15:00 -16:00 LT and the highest median mixing ratios of the day (~ 1.85 μmol mol^{-1}) occurring at around 06:00 LT. Variability in the methane mixing ratios during the campaign was seen to be least for the measurements between 16:00 and 18:00 LT and higher during the early morning hours. Also evident is a steady increase in the median methane mixing ratios from around 20:00 LT in the evening (just after sunset) till 06:00 LT in the morning (just before sunrise). The average of the median mixing ratios during a typical diel cycle was 1.83 μmol mol^{-1}.

3.3.2 Tropical forest: Trends in methane mixing ratios and diel cycle

Figure 3.4 shows a box and whisker plot derived from the continuous 8700 high frequency (70 seconds) measurements conducted in Brownsberg from 5 - 14 October, 2005. The median mixing ratios of

methane again show a clear diel variation. The median mixing ratios were highest (~ 1.76 μmol mol^{-1}) from 06:30 to 08:00 LT in the morning, and lowest (~ 1.72 μmol mol^{-1}) from 14:30 to 16:00 LT in the afternoon. Variability is comparatively higher between 16:30 and 19:00 LT. Median and mean values again differ only slightly, except between 19:30 to 20:30 LT, when the difference is almost 10 nmol mol^{-1}. Remarkably, the median methane mixing ratios show a distinct increase from 19:45 LT in the evening till around 05:45 LT in the morning. The average of the median mixing ratios during a typical diel cycle at Brownsberg was 1.74 μmol mol^{-1}.

3.3.3 Determining the night time methane flux for the boreal forest ecosystem

In order to calculate the nighttime methane flux for the boreal forest using median mixing ratios in the box and whisker diel profile (Fig. 3.3), it is necessary to measure the nocturnal boundary layer (NBL) growth. Additionally, to establish whether the NBL is well mixed, it is also important to assess whether there is any significant gradient in the vertical profile of methane. In Section 3.3.4 we describe how the boundary layer heights were deduced while Section 3.3.5 explains how vertical gradients were assessed. Finally, Section 3.3.6 details the flux calculation methodology.

3.3.4 Determining the boundary layer height

Balloon soundings with temperature and humidity sensors were

launched (approximately thrice a day) during the campaign to determine the height of the boundary layer. As the height of the boundary layer scales directly with the calculated flux (see Section 3.3.3), and is therefore an important step of the flux calculation methodology, we have illustrated how the NBLs were deduced using typical examples in Figures 3.5 (a) and 3.5 (b). Figure 3.5 (a) shows the vertical profiles of potential temperature and relative humidity measured on 23 April at 19:45 LT while Figure 3.5 (b) shows how the boundary layer heights were established from the turning points of the potential temperature vertical profiles at 19:45 LT on 24 April, and 05:45 LT on 25 April, 2005. Table 3.1 lists the boundary layer height values that were measured in the evening (~ 20:00 LT) and the morning (~06:00 LT), on consecutive days from 24 - 28 April. From these values the average evening time (~20:00 LT) boundary layer height was established as 80 m while the average morning time (~06:00 LT) boundary layer height was established as 180 m. A gradual growth of this magnitude is in keeping with current understanding of nocturnal boundary layer dynamics (Stull, 1988).

Table 3.1: Boundary layer heights at Hyytiäla (61°51’ N, 24°17’ E, 170 m, a.s.l.).

Date	Time (L T)	B.L.Height (m)
24 April	19:45	80
25 April	05:45	160
25 April	19:30	70
26 April	05:35	190
27 April	20:00	90
28 April	05:50	210

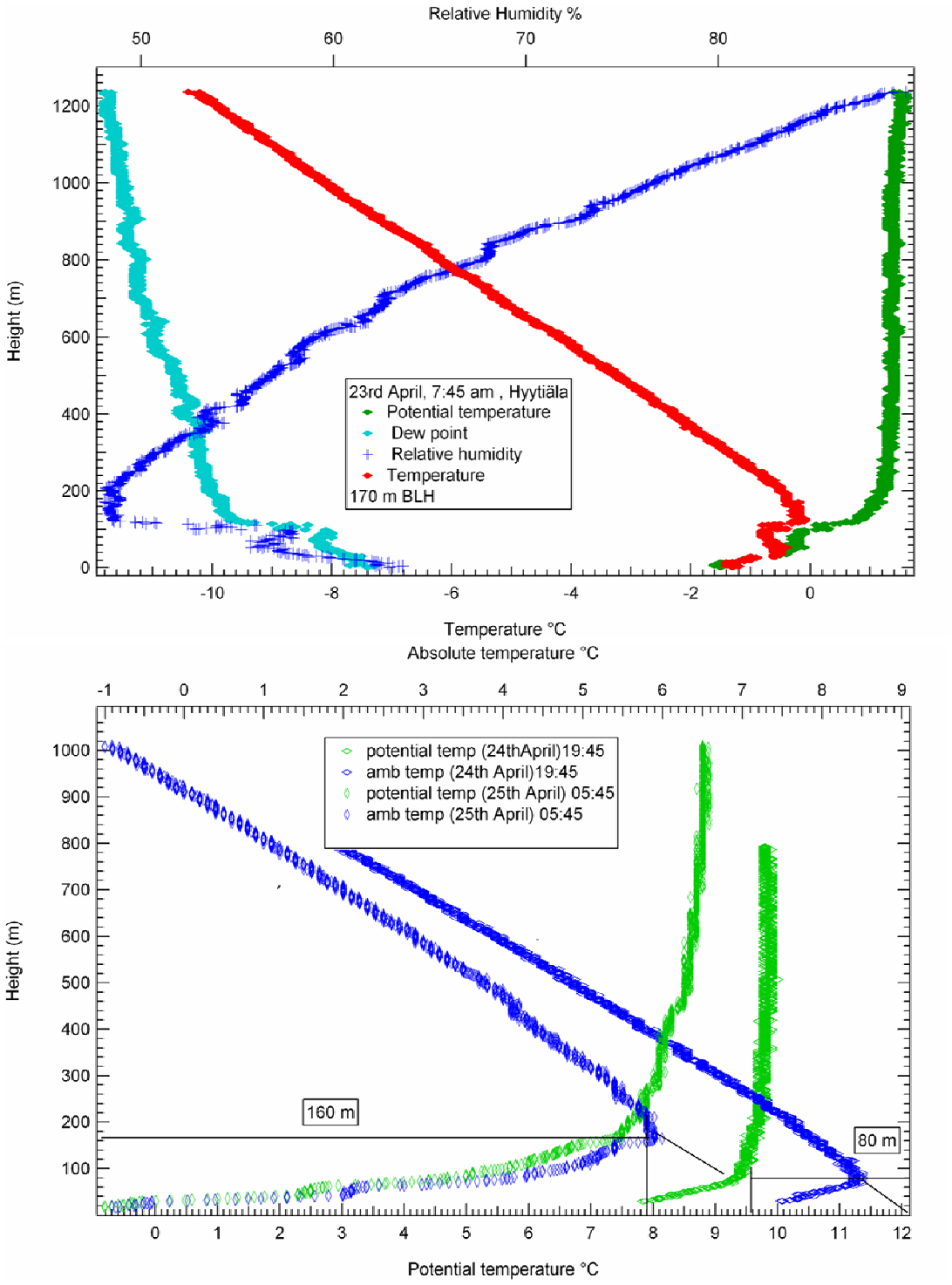

Figures 3.5 (a) and 3.5 (b): Typical example for determination of boundary layer height at Hyytiäla (61°51´N, 24° 17´E, 170 m a.s.l) using several physical parameters (above) and potential temperature profile (below).

3.3.5 Assessing vertical gradients

Vertical gradients within the nocturnal boundary layer (NBL) were assessed using vertical profiles of carbon dioxide made at multiple heights from the SMEAR II measurement tower (heights: 4.2 m, 8.4 m, 16.8 m, 33.6 m, 50.4 m, 67.4 m, 74 m) at the start (17 and 18 April), middle (20 and 21 April) and end (30 April and 1 May) of the study period (16 April to 1 May). Like methane, carbon dioxide is

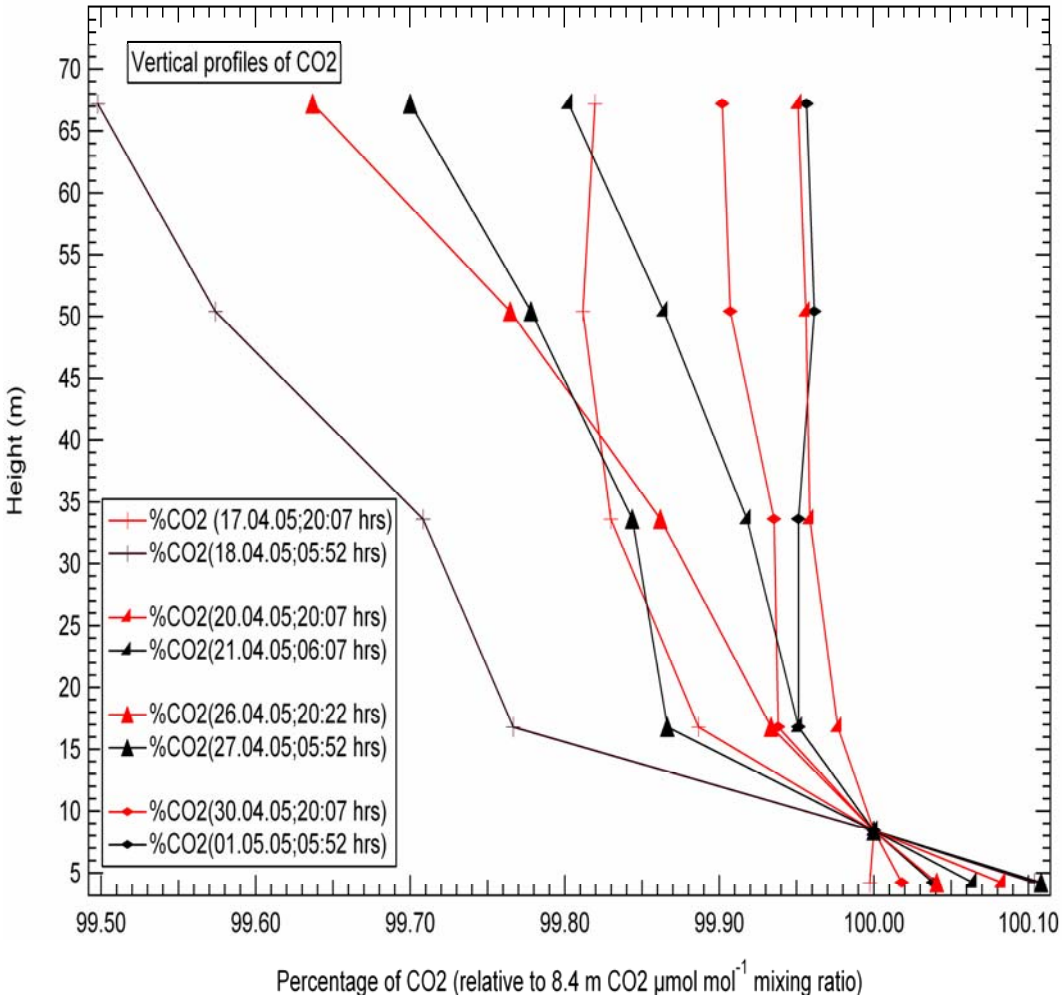

Figure 3.6: Assessing vertical gradients in the NBL at Hyytiäla (61°51´N, 24° 17´E, 170 m a.s.l) using CO_2 profiles.

lifetime (on the order of several years). Thus within the NBL, the vertical gradients of both methane and carbon dioxide will be driven by physical parameters rather than chemical reactions with other species. Figure 6 shows the carbon dioxide vertical profiles in the evening, when the NBL starts to grow (~20:00 LT) and in the morning (~06:00 LT), when it has attained its maximum height. In order to examine gradients with respect to the methane sampling height of 8.5 m, the values in Figure 3.6 are represented as a percentage of the carbon dioxide mixing ratio at the 8.5 m level. It can also be seen in Figure 3.6, that the difference between the highest point and the 8.5 m level is typically less than 0.3 % and in no case more than 0.5 %. This shows that the NBL was well mixed and that mixing ratios measured at the 8.5 m level can be taken to be representative of the entire mixed NBL, for both carbon dioxide and methane.

3.3.6 Flux calculation

Consider a box of cross section area A cm² and height 80 m at 20:00 LT which grows to a height of 180 m at 06:00 LT. Then using the mass balance approach, the total number of methane molecules in the box at 06:00 LT ($N_{06:00}$) can be expressed as the contribution of the initial number of methane molecules in the box at 20:00 LT ($N_{20:00}$), the increase due to the emission flux (F_{CH4}), assumed to be constant from 20:00 - 06:00 LT, and the contribution of methane molecules due to mixing of residual air from above ($N_{Residual\ Layer}$), as the box grows from 80m at 20:00 LT to 180 m at 06:00 LT.

Parameterizing the above as an equation we get,

$$N_{06:00} = N_{20:00} + F_{CH4} \, x \, A \, x \, (36000) + N_{Residual\ Layer} \quad (3.1)$$

Where,

$N_{06:00}$ = CH_4 [t=06:00] x C.F. x A x 18000;

$N_{20:00}$ = CH_4 [t=20:00] x C.F. x A x 8000;

$N_{Residual\ Layer}$ = CH_4 [avg. b/w 16:00 LT and 19:00 LT] x C.F. x A x 10000;

C.F. is the factor used for converting nmol mol^{-1} to molecules cm^{-3} = 2.69 x 10^{10};

and from Figure 3.3,

CH_4 [t=06:00] = median mixing ratio at 06:00 LT = 1850 nmol mol^{-1}

CH_4 [t=20:00] = median mixing ratio at 20:00 LT = 1820 nmol mol^{-1}

and CH_4 [avg. b/w 16:00 and 19:00], the average of median mixing ratios between 16:00 LT and 19:00 LT (assumed to be the residual layer mixing ratio) = 1819 nmol mol^{-1}

Using appropriate values in equation (1), we derive a net night time ecosystem emission flux of 3.62 x 10^{11} CH_4 molecules cm^{-2} s^{-1}.

3.4 Discussion

3.4.1 Boreal forest data

Previous works on methane emissions from boreal forest ecosystems have been mainly based in Canada and the United States (Simpson et al., 1999, Simpson et al., 1997). At Hyytiäla, a background forest site comprising of more than 80% vegetation in 1600 km^2 of surrounding area (Haapanala et al., 2006), research has

been mainly focused on aerosol and emissions of reactive biogenic compounds such as terpenes and oxygenated volatile organic compounds (Kulmala et al., 2004; Tunved et al., 2006; Yassaa and Williams, 2007).

To our knowledge, this is the first time that such high resolution methane diel profiles have been reported from a boreal forest ecosystem, showing night time emission and hence accumulation of methane within the NBL. The atmospheric lifetime of methane is around 8.9 years and so the diel variation at Hyytiäla cannot be explained by the reaction of methane with hydroxyl radicals during daytime. Rather, the diel profile of methane is driven by the dynamics of the boundary layer coupled with biogenic emissions or uptake. After sunset, the ground starts to cool radiatively, causing the growth of a stable nocturnal boundary layer (NBL). Thus there is a decoupling (inhibited gas exchange) of the surface boundary layer from the free troposphere (Stull, 1988). Although during the night the nocturnal boundary layer deepens, mixing ratios of methane rise through the night clearly indicating an emission. After sunrise, the ground starts to get warmer and the surface heat flux causes the boundary layer to grow until it reaches its maximum height in the afternoon. The volume of this daytime well mixed layer is greater than the volume of the well mixed NBL, and the dilution effect of air from above overwhelms the emissions during the day, leading to a daytime decrease in the volume mixing ratio of methane (see Figure 3.3). When compared with three month averaged mixing ratios for April-June, 2003 of circa 1.75 μmol mol^{-1} methane over Hyytiäla

(Figure 5 in Bergamaschi et al., 2007) based on SCHIAMACHY measurements, the value of 1.83 μmol mol^{-1} presented here for 2005 is almost 80 nmol mol^{-1} higher. The flux of circa 4 mg methane m^{-2} day^{-1} (1.74 x 10^{11} molecules cm^{-2} s^{-1}) reported in the same work is also considerably smaller in comparison to our night time flux of 3.62 x 10^{11} molecules cm^{-2} s^{-1}. One explanation for this difference could be that source strengths could have increased (or sinks decreased) in 2005 compared to 2003. Alternatively, it might be that potential offsets and biases in the SCHIAMACHY (Frankenberg et al., 2006; Bergamaschi et al., 2007) retrieval scheme cause it to underestimate methane over Hyytiäla.

Boreal forests have been reported previously as net sinks of methane, although the uptake of methane by soils has not been well characterized (Tyler 1991; Steudler et al., 1989). Simpson et al. (1997) reported a net emission flux of 0.8 - 1.05 x 10^{11} molecules cm^{-2} s^{-1} (mixing ratio circa 1.82 – 1.90 μmol mol^{-1}) from a boreal forest in Saskatchewan during springtime (April-September, 1994) using micrometeorological tower measurements. Reports of the boreal forest as a net sink for methane are almost exclusively based on data from chamber measurements (Savage et al., 1997; Schiller and Hastie et al, 1996; Whalen et al., 1992). Simpson et al. (1999) first raised concerns that the apparent discrepancy is most probably because chamber measurements are conducted close to the surface and are influenced strongly by the soil, which is known to uptake methane. Further, Simpson et al. (1997) reported that micrometeorological measurements conducted only at the base of the tower indicated the

forest to be a sink while overall, the forest was found to be a net source of methane.

As detailed in Khalil (2000) and references therein, methane emissions can vary considerably based on seasonality, land use changes and environmental parameters such as soil temperature and water table levels. Nevertheless, bottom up estimates using in-situ field measurements, are useful to get an idea about the possible contribution of particular ecosystem types to the global budget. Extrapolating the net night time methane emission flux of 3.62 x 10^{11} molecules cm^{-2} s^{-1} derived in this work, to the global boreal forest area of 1.5 x 10^{17} cm^2 (Tunved et al., 2006), we estimate an annual boreal forest ecosystem flux of 45.5 Tg CH_4 yr^{-1}. This is around 7.5 % of the estimated global 600 Tg CH_4 yr^{-1} released into the atmosphere. It should be noted however, that this flux calculation methodology is rather sensitive to the NBL estimates. Based on the NBL height variability observed at Hyytiäla (see Table 3.1), this introduces an uncertainty of up to ± 25 % for the calculated flux.

Is it possible to use the derived net ecosystem flux, which is a composite of lake, wetland and vegetation sources, for a "tentative" estimate of the contribution of boreal vegetation to the global methane budget? Average fluxes compiled by Bartlett and Harriss (1993) for broad ecosystem types show that values for the boreal wetlands are between 3.71 - 4.1 x 10^{12} molecules cm^{-2} s^{-1}(or 87-96 ng m^{-2} s^{-1}). The average methane emission flux, from southern boreal lakes (located between 60°57', 24°27' and 61°22', 25°15') for the growing seasons of April-September (years 1998-2002), is 2.15 x 10^{12}

molecules cm^{-2} s^{-1}(Bergstrom et al., 2006). Thus a wetland flux of 4.1 x 10^{12} molecules cm^{-2} s^{-1} and lake emission flux of 2.15 x 10^{12} molecules cm^{-2} s^{-1} can be considered as generous estimates for wetland and lake emissions in Hyytiäla (61°51' N, 24°17' E) during April-May. Knowing that wetlands and water bodies make up 0.7% and 13 % of the 1600 km^2 footprint area around the measurement site (Section 2.1) a conservative estimate of the boreal vegetation can be calculated as follows:

Wetland flux + *Lake flux* + *Vegetation flux* = *Net ecosystem flux* (3.2)

That is,

0.7 % of 4.18 x 10^{12} molecules cm^{-2} s^{-1} + 13 % of 2.15 x 10^{12} molecules cm^{-2} s^{-1} + Vegetation flux = 3.62 x 10^{11} molecules cm^{-2} s^{-1}

Solving the above yields a boreal vegetation flux of 5.32 x 10^{10} molecules cm^{-2} s^{-1}. Upscaling for the global boreal forest area of 1.5 x 10^{17} cm^2 (Tunved et al., 2006), the contribution of boreal vegetation to the total methane budget is estimated to be circa 6.7 Tg CH_4 yr^{-1}. It should be noted that this is a lower limit estimate because the sink term due to the boreal forest soil has been neglected in Equation 2, and according to Keppler et al.(2006) plants emit 2-5 fold more methane during the day, so that the net ecosystem flux might actually be higher if day time emissions could be included. The estimate of 6.7 Tg CH_4 yr^{-1} derived here is higher than the range of 1.1- 4.1 Tg CH_4 yr^{-1} reported by Keppler et al. (2006) for boreal vegetation emissions, based on the upscaling metric of net primary productivity (NPP). Using the metrics of leaf mass index and photosynthesis rates for different biomes, Kirschbaum et al. (2006) upscaled the results of

Keppler et al. (2006) and reported boreal vegetation emission estimates of 2.8 Tg yr^{-1} and 0.6 Tg yr^{-1}, respectively. Remarkably, emulating the Kirschbaum et al. (2006) approach of biome leaf mass for upscaling, Parsons et al. (2006) revaluated the results of Keppler et al. (2006) and proposed an estimate of 3.6 Tg CH_4 yr^{-1} for boreal vegetation. This shows that even estimates based on the same upscaling approach can yield somewhat different results, although all are comparable to the value we derive here. Our results from the field indicate that boreal vegetation contributes at least circa 1 % of the total methane budget, while the boreal ecosystem contributes almost 7.5%.

3.4.2 Tropical forest data

Analogous to the boreal methane profile, the diel profile from Brownsberg (Figure 3.4) is also characterized by an increase in the median methane mixing ratios during nighttime. Carmo et al. (2006) and Crutzen et al. (2006) have reported similar profiles from upland amazon forests and tropical savannah grasslands, respectively. Frankenberg et al. (2005) observed enhanced mixing ratios of methane over tropical rainforests and called for in-situ measurements to validate their measurements. It is interesting to note that compared to the SCHIAMACHY measurements of 1.76 µmol mol^{-1} methane, and the global chemistry transport model (TM3) value of 1.72 µmol mol^{-1} for the same season in 2003 over Suriname, the average of all our in situ measurements in 2005 is 1.74 µmol mol^{-1}. If we assume that the sources and sinks in 2003 and 2005 were not significantly

different, then the in-situ measurements would seem to suggest that the enhanced emissions over the Suriname rainforest are probably not as strong as first reported in Frankenberg et al. (2005). The latter argument is supported by the work of Bergamaschi et al. (2007) that extended the original analysis by Frankenberg et al (2006), and reported that SCHIAMACHY CH_4 retrievals may have some bias (up to ~30 nmol mol^{-1}) that depends on latitude and season.

Krejci et al. (2005) have estimated the NBL over the rainforest in Suriname to be less than 250 m. Brownsberg is situated on a hill (512 a.s.l.) and the presence of the nearby Brokopondo lake (also called Prof. Dr. Bloomstein lake) may potentially impact our methane measurements. So while the measurements at Brownsberg (512 m a.s.l.), resemble tower type measurements with respect to the surrounding rainforest, overall the situation presents a less than ideal site for flux measurements. Still for the sake of discussion, if we assume that methane was well mixed within the NBL and that the NBL height over the rain forest was 100 m at ~ 19:45 LT and 200 m at ~ 05:45 LT, then applying the method described in Section 3.3.3, we "tentatively" estimate a night time emission flux of 3.77 x 10^{11} molecules cm^{-2} s^{-1}. It is interesting to note that this flux value, falls within the flux range of 0.96 - 9.1 x 10^{11} molecules cm^{-2} s^{-1}(or 4-38 Tg yr^{-1}), reported by Carmo et al. (2006) from the upland forest area (1.5 x 10^6 km^2) of the Amazon region.

3.5 Conclusion

The boreal forest ecosystem as a whole is a significant source of methane (~ 45.5 ± 11 Tg CH_4 yr^{-1}) while boreal vegetation appears to contribute modestly (~1 % of the total global budget). With regard to the source apportionment for deriving the boreal vegetation flux, uncertainties in the flux values of individual sources such as wetlands and lakes render more uncertainty to the derived vegetation flux. Nevertheless, the approach is useful for making a first order field estimate of the potential contribution of boreal vegetation to the ecosystem flux and the derived estimate (~ 7 Tg yr^{-1}) appears to be well within the uncertainties of the existing emission sources (e.g. wetlands) from boreal ecosystems. High temporal resolution measurements, from the boreal forest and tropical forest ecosystems, made over longer time periods are needed to assess methane emissions from these regions more accurately, because based on the short term data presented in this work, it appears that boreal forest ecosystem emissions may be currently underestimated while tropical forest ecosystem emissions may be slightly over estimated. Collectively, the nighttime emissions from boreal and tropical forest ecosystems indicate a global source contribution of circa 100 Tg CH_4 yr^{-1}, which is almost 16.7 % of the global budget of circa 600 Tg CH_4 yr^{-1}. Until the mechanism of methane production from plants under aerobic conditions, is better understood, examining net ecosystem fluxes under in-situ natural conditions, would help in constraining the contribution due to the new vegetation source and assessing whether

their magnitude is of the order of uncertainties in the existing sources or higher.

Furthermore, C-13 isotope measurements can help to apportion the methane sources in a better manner and thus a combined approach of in-situ measurements at suitable remote and homogeneous sites, remote sensing retrievals and isotope studies would help to reduce the uncertainties in the global methane budget much more effectively.

4. The Comparative Reactivity Method – A new tool to measure total OH Reactivity in ambient air

OH radicals play a vital role in maintaining the oxidizing capacity of the atmosphere. To understand variations in OH radicals both source and sink terms must be understood. Currently the overall sink term, or the total atmospheric reactivity to OH, is poorly constrained. Here, we present a new on-line method to directly measure the total OH reactivity (i.e total loss rate of OH radicals) in a sampled air mass. In this method, a reactive molecule (X), not normally present in air, is passed through a glass flow reactor and its concentration is monitored with a suitable detector. OH radicals are then introduced in the glass flow reactor at a constant rate to react with X, first in the presence of zero air and then in the presence of ambient air containing VOCs and other OH reactive species. Comparing the amount of X exiting the reactor with and without the ambient air allows the air reactivity to be determined. In our existing set up, X is pyrrole and the detector used is a proton transfer reaction mass spectrometer. The present dynamic range for ambient air reactivity is ~ 4 s^{-1} to 300 s^{-1}. The system has been tested and calibrated with different single and mixed hydrocarbon standards showing excellent linearity and accountability with the reactivity of the standards. Field tests in the tropical rainforest of Suriname (93 s^{-1}) and the urban atmosphere of Mainz (19.5 s^{-1}) Germany, show the promise of the new method and indicate that that a significant fraction

of OH reactive species in the tropical forests is likely missed by current measurements. Suggestions for improvements to the technique and future applications are presented.

4.1 Introduction

Every year, approximately 1.3 billion tonnes of natural and anthropogenic gases are emitted into the troposphere. Photochemical reactions, initiated by the hydroxyl radical (OH), oxidize many of these emitted primary atmospheric pollutants such as carbon monoxide (CO), sulphur dioxide (SO_2), nitrogen oxides (NO_x = NO and NO_2) and VOCs (Volatile Organic Compounds) into forms, which are more readily removed from the atmosphere by deposition or formation of aerosol. Ultimately, if a carbon compound remains in the gas phase it will be oxidised to CO_2 and water by the OH radical, which is therefore vital for maintaining the self cleansing capacity of the atmosphere (Heard and Pilling, 2003; Lelieveld et al., 2004). In order to ascertain how well we understand these OH initiated photochemical processes, measured ambient OH radical concentrations from field studies are often compared with OH radical concentrations predicted by photochemical models (e.g. Poppe et al., 1994; Hofzumahaus et al., 1996; Carslaw et al., 2002; Holland et al., 2003; Martinez et al., 2003; Olson et al., 2004; Ren et al., 2005; Ren et al., 2006; Smith et al., 2006).

However, the accuracy of photochemical models depends to a large extent on how well the OH sources, OH sinks and associated chemical mechanisms are represented. For example, if the model predicts significantly higher OH concentrations than the measured OH concentrations, it could be due to an overestimation of the OH sources and / or an underestimation of the OH sinks. Currently, the source term is better understood and more readily quantified than the

sink. While the source involves a limited number of reactants and rate coefficients that can be determined using available instruments, the sink is dependent on a multitude of species, all of which compete for the available OH. An accurate sink term can constrain models and help in clarifying the possible reasons for discrepancies between models and measurements. Furthermore, by a comparison analysis with simultaneous measurements of VOCs and the other OH-reactive species, it also helps to constrain the VOC budget.

Atmospheric OH is produced primarily by the photolysis of O_3 with solar UV ($\lambda \leq 320$ nm) followed by reaction of the excited oxygen atoms (O^1D) with water vapour,

$$O_3 + h\nu \rightarrow O_2 + O(^1D) \quad (4.1)$$

$$O(^1D) + H_2O \rightarrow 2OH \quad (4.2)$$

The reactions of OH radicals with VOCs in the atmosphere can be summarized by the following four generalized reactions. In the first step, OH attacks a saturated hydrocarbon in the presence of O_2,

$$RH + OH + O_2 \rightarrow RO_2 + H_2O \quad (4.3)$$

to produce water and an alkyl peroxy radical, where R = any organic moiety.

Next, the alkyl peroxy radical may react with NO when present,

$$RO_2 + NO \rightarrow RO + NO_2 \quad (4.4)$$

to produce an alkoxy radical that reacts with O_2,

$$RO + O_2 \rightarrow \text{carbonyls} + HO_2 \quad (4.5)$$

This step produces carbonyls and HO_2. Alternatively, the alkyl

peroxy radicals, RO_2 and HO_2, may also react with each other,

$$RO_2 + R'O_2 \rightarrow \text{peroxides, alcohols, carbonyls} + O_2 \qquad (4.6)$$

resulting in the production of peroxides, alcohols and carbonyls, which may dissolve into the liquid phase and precipitate out of the atmosphere or further react with OH. Both R and R´ can be any organic moiety.

Reaction (4.3) represents the main sink term of OH radicals in the atmosphere, namely reaction with the generic hydrocarbon RH. Often, the overall sink term is estimated by calculating OH loss frequencies (products of concentration and rate coefficient) for all individually measured species and summing them. Thus, the OH reaction frequency (also termed OH reactivity) of a chemical is given by

$$\text{OH Reaction Frequency of Reactant X } (s^{-1}) = k_{X+OH}\,[X] \qquad (4.7)$$

where k_{X+OH} is the rate coefficient for the reaction of X with OH

However, it is not certain whether all relevant OH reactive species are measured by the suite of measurement techniques deployed in current field studies. Roberts et al. (1998) and Maris et al. (2003) determined the total carbon budget of ambient VOCs, but while this information is useful for understanding what fraction of the carbon budget remains unidentified during VOC measurements, it lacks the critical information about how reactive the missing carbon might be for chemical reactions in the atmosphere (e.g. 10 ppbC of isoprene is not equivalent to 10 ppbC of methane for OH reactivity).

Lewis et al. (2000) identified more than 500 reactive VOCs in

urban air using an improved method of peak deconvolution for double-column (orthogonal) gas chromatography and concluded that a large number of VOCs, particularly with more than 6 carbon atoms and especially aromatics, are missed in the more commonly employed single column gas chromatography measurements. More recently, Goldstein et al. (2004) and Holzinger et al. (2005) reported the presence of unknown reactive biogenic compounds (up to 30 times the emission of total monoterpenes observed in the forest canopy on a molar basis), from a pine forest in California. Direct OH reactivity measurement techniques circumvent the daunting task of measuring all the OH reactive species individually, in order to obtain the total OH reactivity (sink) and can even serve as a diagnostic tool for missing reactivity due to possibly unmeasured reactive species (Di Carlo et al., 2004). Additionally, OH production rates can also be estimated by simultaneous measurements of total OH reactivity and OH concentrations, assuming the steady state of OH using

$$\frac{d\,OH}{d\,t} = P_{OH} - k\,[OH] = 0 \tag{4.8}$$

where P_{OH} and k represent the OH production rate and the measured first-order decay rate of OH radicals, respectively. Information about the lifetime of OH is also easily obtained by taking the reciprocal of the measured OH reactivity.

In the last decade, new instruments capable of directly measuring the OH reactivity of ambient air have been developed (Kovacs and Brune, 2001; Sadanaga et al., 2004b). With some variations, all of them employ laser induced fluorescence (LIF) to

monitor the loss rate (decay) of OH radicals in a flow reactor in the presence of ambient air. While these measurement systems have provided new insights on the OH reactivity budget, their cost and large size are deterrents to their widespread deployment for field studies. Thus other techniques capable of measuring the total OH reactivity of ambient air that are more economical and portable than the existing LIF based method, would be a valuable addition to current atmospheric measurements.

In this study, we present a new method for direct online measurements of the total OH reactivity of ambient air. This method can be easily integrated with commonly employed in-situ analytical techniques such as gas chromatography and chemical ionization mass spectrometry at modest additional costs. Presented below is a detailed description of the general concept, the glass flow reactor design, the method validation and calibration, choice of reagent (in this case pyrrole; C_4H_5N) and the detector system employed (in this case a proton transfer reaction mass spectrometer). First field results from the tropical rainforest in Suriname and the urban atmosphere of Mainz, Germany, are shown and potential interferences from NO and relative humidity are investigated. Finally an outlook for future applications of the new method is given.

4.2 Methodology

4.2.1 Concept of Comparative Reactivity Method (CRM)

Figure 4.1 illustrates the general concept. A reactive molecule (X), not normally present in air, is introduced into a glass flow reactor and its concentration C1 is monitored with a suitable detector, in the air exiting the reactor. After some time when C1 is well determined, OH radicals (OH < [X]) are introduced into the reactor at a constant rate to react with X. This causes C1, the monitored concentration of X, to decrease to C2, as X reacts with the OH radicals. The decrease in the monitored concentration of X (from C1 to C2) also gives the concentration of the OH radicals, as all the OH is titrated away by X. Next, an air sample containing OH reactive species is introduced into the flow reactor. The various species present in ambient air then compete with X for the available OH radicals, so that the concentration of X in the air exiting the reactor increases to C3. Comparing the amount of X exiting the reactor without (C2) and with the ambient air (C3) allows the introduced air sample's OH reactivity to be determined in a quantitative manner, provided the system is suitably calibrated. Some general criteria that the reagent molecule X must satisfy are

1) it reacts with OH at a suitable rate so as to compete with reactive species in ambient air;
2) the rate coefficient for reaction with OH should be well measured / established;
3) must be volatile (to make into a good bottled standard);

4) it must have the necessary physical and chemical properties for easy and accurate detection (without interferences) using a suitable detector (e.g. proton affinity of X should be greater than water to be detectable by a proton transfer reaction mass spectrometer (PTR-MS)
5) it should not be present in ambient air (under normal circumstances) as this can complicate the analysis. In the present version of the CRM developed in Mainz, the reagent molecule X is pyrrole (C_4H_5N) and the detector is a PTR-MS.

4.2.2 Determining OH Reactivity: Derivation of the basic equation for CRM

Based on the method of relative rates, an expression may be derived for the total OH reactivity of species present in the introduced air sample (denoted by R_{air}) in terms of the measured [X] signals C1, C2 and C3 (shown in Figure 4.1).

Let the amount of X available for reaction with OH be C1 and k_{OH+X} be the rate coefficient for the reaction of X with OH. Then, considering the two processes determining the OH loss in the set up, namely, 1) reaction with X (rate is $R_x = k_{OH+X}$ C1) and 2) reaction with all the OH reactive species present in the introduced air (rate is R_{air}), the loss of OH radicals due to reaction with X alone, when both processes act simultaneously, is the experimentally measured [X] signal (C1– C3), expressed as:

$$(C1 - C3) = \frac{R_X}{R_X + R_{air}} \quad (C1 - C2) \tag{4.9}$$

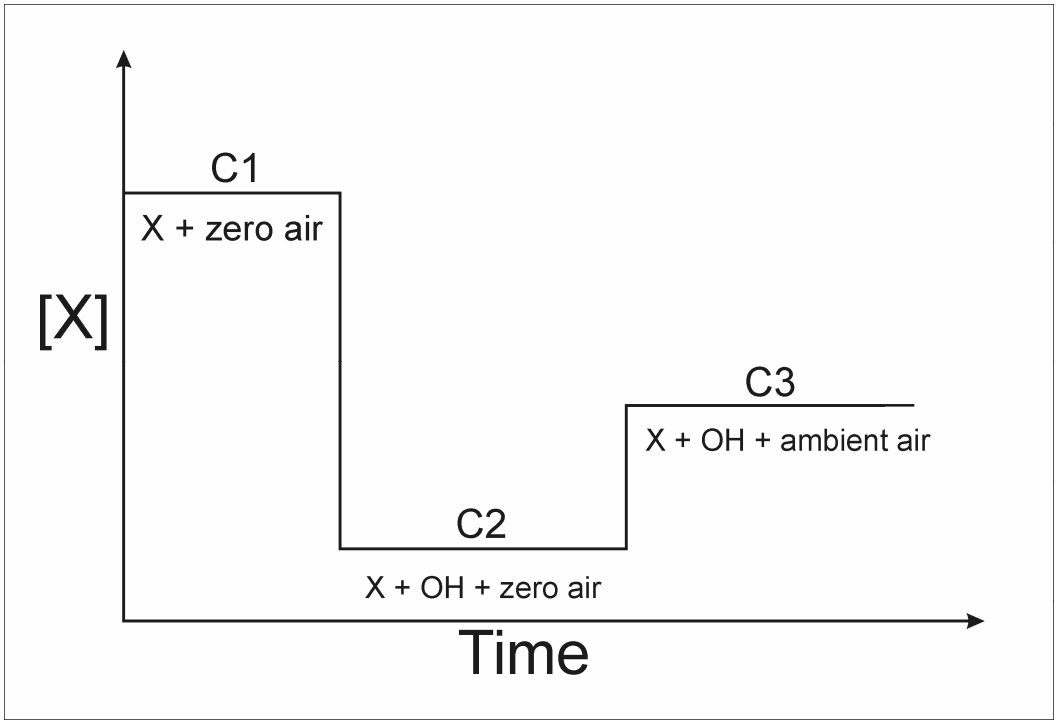

Figure 4.1: Schematic illustrating concept of the Comparative Reactivity Method.

where the experimentally measured [X] signal (C1 - C2) is the concentration of OH radicals available for reaction with [X] and the ambient air .

Re-arranging (9), to derive the expression for R_{air}, we get

$$R_{air} = \frac{(C3 - C2)}{(C1 - C3)} \quad R_X \tag{4.10}$$

Substituting $R_x = k_{OH+X}$ C1, in (10), we arrive at the basic equation of the Comparative Reactivity Method,

$$R_{air} = \frac{(C3 - C2)}{(C1 - C3)} \quad k_{OH+X} \; C1 \tag{4.11}$$

C1, C2 and C3 have the units of molecules cm^{-3} and k_{OH+X} has the unit of cm^3 $molecule^{-1}$ s^{-1}, so that the unit for R_{air} is s^{-1}. It should be noted that Equation 4.11 assumes that mixing within the reactor does

not favour reaction of X with OH compared with the reaction of ambient air with OH or vice versa.

4.3. Experimental

The set up consists of a small glass flow reactor (where pyrrole and ambient air/standards mix and react with OH radicals), a PTR-MS which detects pyrrole in the air exiting the reactor and a set of mass flow controllers along with two gas bottles (nitrogen and zero air).

4.3.1 Glass flow reactor

Figure 4.2 shows a schematic of the glass reactor along with its inlets and outlets labelled as arms A, B, C, D and E. The length and volume of the glass reactor are approximately 14 cm and 94 cm^3, respectively. The typical flow rate inside the reactor is approximately 260 ml $minute^{-1}$.

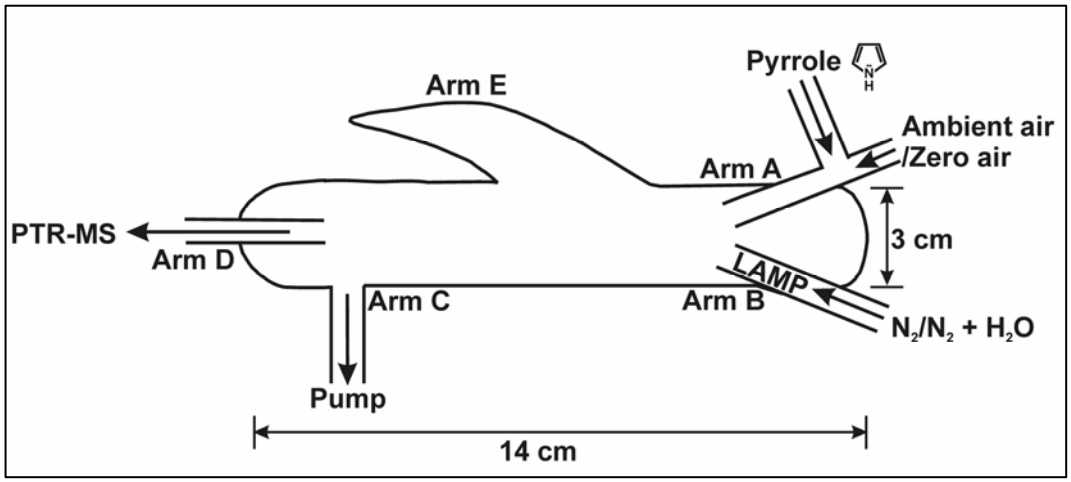

Figure 4.2: Schematic of the glass reactor used in the Mainz CRM instrument.

Gas phase pyrrole (Westfalen A.G., stated uncertainty 5 %; 10 μmol mol^{-1}) is mixed with zero air (Synthetic air, Westfalen A.G., 99.999 % purity, < 0.5 μmol mol^{-1} THC) and introduced through inlet A at a constant flow. Its concentration is monitored in the air exiting the reactor (outlet D) with a PTR-MS. Inlet B consists of a pen ray spectral mercury vapour lamp (L.O.T Oriel GmbH & Co. KG), over which humidified nitrogen / nitrogen (Westfalen A.G., 99.9999 % purity) is passed at a constant flow rate. The humidification is accomplished by bubbling gaseous nitrogen through water, which is maintained at room temperature (298 K). When the lamp is switched on, OH radicals are produced due to photolysis of the water vapour (at λ = 184.9 nm) present in the humidified nitrogen. The lamp is 5 cm long and the maximum time the OH radicals spend in arm B before they emerge into the glass flow reactor , is 0.6 seconds. This method of producing OH radicals has been used extensively in gas phase kinetic studies, including calibration of OH measurement instruments, and for more details the reader is referred to Heard and Pilling (2003) and references therein.

The tapered arm E is a Wood´s horn which minimizes reflection of the mercury lamp down the reactor and hence photochemical reactions along the length of the glass reactor. Outlet C is connected to an exhaust pump (Model NO22AV.18, KNF Neuberger, Germany) that draws out the excess air from the main flow. The total incoming flow rate (A + B) is circa 260 ml min^{-1}, slightly more (~ 5 ml min^{-1}) than the combined flow through the exhaust pump (arm C) and the PTR-MS. To prevent an over-pressure

from building up within the reactor, and to ensure that the pressure in the reactor is always atmospheric pressure (760 Torr), one of the lines linked to arm A (with a T-shaped Teflon joint) is kept open-ended at all times. The pressure and temperature of the glass flow reactor air are also monitored using a digital pressure manometer (Model 13 AN, Greisinger Elektronik, Germany) and a temperature probe connected to the line exiting arm C. A total of four mass flow controllers (MKS Instruments, Deutschland GmbH) are used to maintain constant flows in arm A (one each for pyrrole and zero air), arm B (one for nitrogen) and arm C (for the exhaust pump). All the gas carrier lines leading into and from the reactor are plumbed using short (< 1m) 1/4 inch (outer diameter (o.d.)) and 1/8 inch (o.d.) Teflon tubing.

To sample ambient air for reactivity, the zero air is switched off and an equivalent amount of ambient air is pumped in, using a Teflon VOC sampling pump (Laboport N86-KN18) connected to the same tubing, which introduces zero air and pyrrole into the set up (at arm A). This causes dilution of the ambient air within the reactor, and the dilution factor has to be taken into account while determining the total OH reactivity of the introduced ambient air. It is worth mentioning that the ambient air is not subject to any gas chromatography column, preconcentration step or laser excitation and its reactivity is directly converted into a pyrrole signal (the modulation C3 - C2 in Fig. 4.1), so that any potential losses of VOCs and/or associated artefacts are minimised. Typical pyrrole and OH radical mixing ratios in the set up are ~100 nmol mol^{-1} (~ 2.69 x 10^{12} molecules cm^{-3}) and up to 80 nmol mol^{-1} (~ 2.15 x 10^{12} molecules cm^{-3}), respectively.

4.3.2 PTR-MS: The Detector

A proton transfer reaction mass spectrometer (PTR-MS) is used to monitor the mixing ratio of pyrrole in the air exiting the flow reactor through arm D. In the last decade, extensive VOC measurements have been conducted using proton transfer reaction mass spectrometers (Lindinger et al. 1998a; de Gouw and Warneke, 2007).Within the instrument, organic species with a proton affinity greater than water are chemically ionised by proton transfer with H_3O^+ ions and the products are detected using a quadrupole mass spectrometer (Lindinger et al., 1998b). The entire inlet system of the PTR-MS including switching valves is made of Teflon. Details about the operation of the PTR-MS used here, including its mass identifications, its sensitivity and detection limits for masses other than pyrrole (C_4H_5N) are given elsewhere (Williams et al. 2001, Salisbury et al., 2003; Sinha et al., 2007a). Pyrrole is detectable by the PTR-MS since its proton affinity (209.2 kcal mol^{-1}) is higher than that of water (165.2 kcal mol^{-1}) and the signal is observed without fragmentation at mass 68 ($C_4H_5NH^+$) in the PTR-MS. There are no known species in ambient air that could interfere at mass 68 within the PTR-MS, and experience from field campaigns has shown this mass to be rather stable. It is advantageous that mass 68 is an even mass (pyrrole has a nitrogen atom), since most organic compounds detectable by PTR-MS (e.g. methanol, acetone, acetaldehyde and isoprene) are detected after protonation at odd masses. Pyrrole is not normally present in ambient air, and has only been observed in emission plumes from specific energy production processes such as

coal gasification and shale and coal-based oil production (Sickles et al., 1977).

Calibrations performed with custom prepared pyrrole standards from Westfalen A.G. show that the protonated ion of pyrrole (m/z = 68) does not fragment within the instrument and high mixing ratios of up to circa 250 nmol mol^{-1} do not significantly decrease the signal of the H_3O^+ reagent ions. Furthermore, no significant humidity effect has been observed at the pyrrole signal (mass 68). The linearity of the pyrrole signal is excellent (r = 0.99 between the investigated range of 0.5 to 250 nmol mol^{-1}) and the total uncertainty in the measured pyrrole signal is estimated to be 11 %. This includes a 5 % accuracy error inherent in the pyrrole gas standard and a 2 σ precision error of 6 %, while measuring pyrrole at 25 nmol mol^{-1}(the typical baseline value, C2). As a detector for the CRM technique, the PTR-MS offers the added advantage of tracking humidity changes in the air exiting the flow reactor (more details in Section 4.4.2.3), by monitoring masses 37 (cluster ion $H_3O^+ \cdot H_2O$) and 55 (cluster ion $H_3O^+ \cdot (H_2O)_2$), which can be used as proxies for water vapour in the air sampled by the PTR-MS. Further details of this approach are available in Ammann et al. (2006).

4.4 Results

4.4.1 Calibrations and method validation

Several tests with single and mixed hydrocarbon standards were performed to ascertain whether the comparative reactivity method can reliably quantify samples of known reactivity. Figure 4.3 shows an

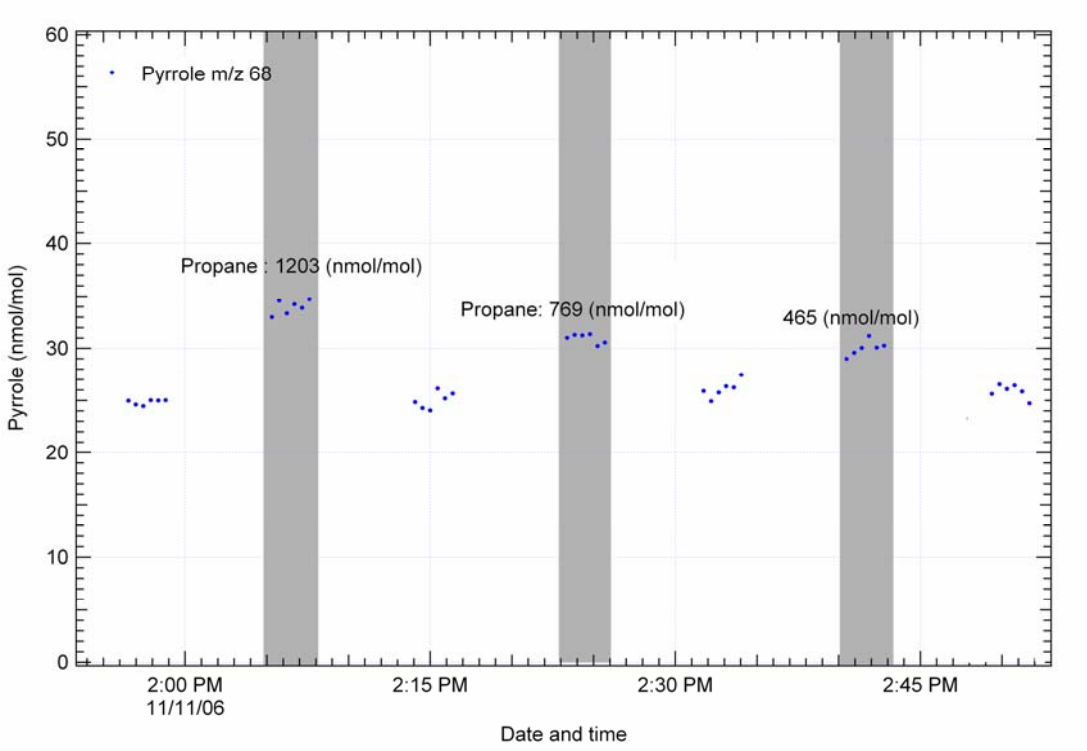

Figure 4.3: Example plot showing raw reactivity data and modulations with propane.

example plot of the measured reactivity data versus the reactivity introduced using a standard. A propane gas standard (Westfalen A.G.; 33 μmol mol^{-1}; stated uncertainty 4 %) was introduced at different concentrations through the same line that is used to introduce ambient air into the flow reactor. The PTR-MS is blind to propane since the proton affinity of propane is less than that of water. The occasions when propane was introduced are indicated by shaded areas. As can be seen in Figure 4.3, the baseline value (corresponding to C2 in Figure 1) of pyrrole is ~ 25 nmol mol^{-1} and after every modulation (increase in signal corresponding to C3 in Figure 1) with propane concentrations of 1203 nmol mol^{-1}, 769 nmol $mol^{-1}$and 465 nmol mol^{-1}, respectively, the pyrrole signal reproducibly returns to its baseline value (from C3 to C2), within the instrumental precision error of ~6

%. This shows that the modulation (from C2 to C3) occurs due to the competition between propane and pyrrole for the available OH radicals. The rate coefficient for the reaction of propane with OH is $(1.1 \pm 0.2) \times 10^{-12}$ cm^3 $molecule^{-1}$ s^{-1} (http://kinetics.nist.gov/kinetics/index.jsp, version 7.0, release version 1.4). Using equation (7), the reactivity due to the propane amounts shown in Figure 4.3, are calculated to be ~ 35.3 s^{-1}, 22.5 s^{-1} and 13.6 s^{-1}, respectively. The breaks in the data plot in Figure 4.3 correspond to periods where the instrumental background was measured. The background signal is collected by passing the sampled air over a Pt catalyst kept at 350 °C to oxidize all the organics. This enables correction for the noise at the measured masses and results in more accurate quantification.

Figure 4.4 shows the reactivity measured with the CRM technique (vertical axis) plotted against the reactivity introduced into the flow reactor (horizontal axis) due to several standards in different experiments. In addition to propane, a 19 component hydrocarbon mixture was used as a reactivity standard. The 19 component hydrocarbon mixture is a commercial gas standard (Apel-Riemer Environmental Inc.) and contains numerous compounds spanning four orders of magnitude in OH reaction rates. These are methanol, acetone, acetaldehyde, hexanal, trans-2-hexenal, methyl ethyl ketone, methyl vinyl ketone, acetonitrile, isoprene, alpha pinene, toluene, benzene, 1,3-dimethyl benzene, 2-methyl furan, 2-pentanone, 1,3,5-trimethyl benzene, 1,2,4,5- tetramethyl benzene, cis-2-butene dimethyl sulphide and dimethyl disulphide. Akin to propane, the reactivity due to the standards is calculated using equation (4.7) and

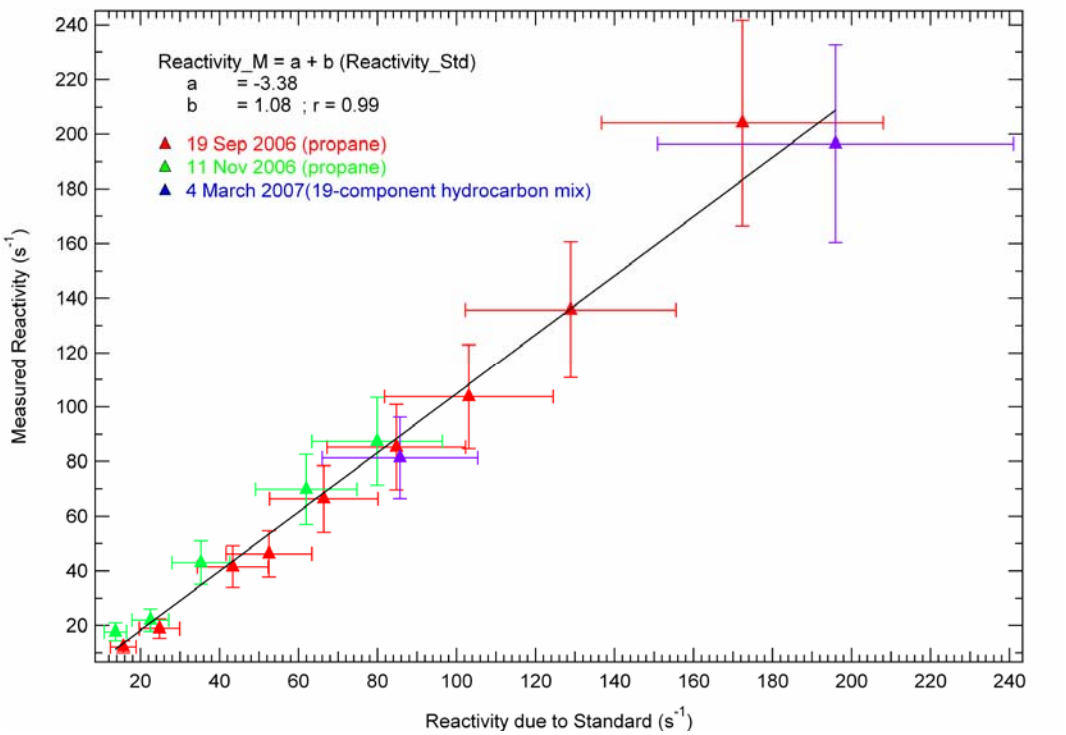

Figure 4.4: Method validation and calibration using several standards on different occasions (good reproducibility) .

using rate coefficients taken from the latest IUPAC recommendations on gas kinetic data evaluation for atmospheric chemistry (Atkinson et al., 2006)

For 1,2,4,5- tetra methyl benzene, no data was available and so its OH rate coefficient was assumed to be 1 x 10^{-11} cm^3 $molecule^{-1}$ s^{-1}(similar to rate coefficients of ~ 1.3 x 10^{-11} cm^3 $molecule^{-1}$ $s^{-1}$for 1,3-dimethyl benzene and 1,4-dimethyl benzene and 3 x 10^{-11} cm^3 $molecule^{-1}$ s^{-1} for 1,3,5-trimethyl benzene). For the 19-component hydrocarbon standard's data shown in Figure 4.4, the hydrocarbon concentrations introduced were ~7 nmol mol^{-1} and 16 nmol mol^{-1}, which are notably higher than the general abundance levels of these VOCs in the atmosphere. The horizontal error bars in Figure 4.4

represent the total uncertainty in the reactivity of the standards, which includes the uncertainties in the VOC +OH-rate coefficient (typically ~ 15-20 %), the accuracy of the standard (~ 5 %) and the flow fluctuations (~ 10 %). The measured reactivity (plotted on the vertical axis in Figure 4.4) is obtained by interpolating the measured baseline (corresponding to C2 in Figure 4.1) and applying equation (4.11) to the measured pyrrole signals C1, C2 and C3.

The vertical error bars (18.38 %) in Figure 4.4 represent the total uncertainty in the measured OH reactivity and include the uncertainty in the pyrrole + OH rate coefficient (1.20 ± 0.16) x 10^{-10} cm^3 $molecule^{-1}$ s^{-1}, flow fluctuations of the mass flow controllers (~ 10 %), uncertainty in the pyrrole standard (5%) and instrumental precision error (~ 6 %). Overall, it can be seen from Figure 4.4 that the CRM measurements show excellent linearity (r = 0.99) and good accountability (slope of measured reactivity versus reactivity due to standard = 1.08) for the reactivity range of circa 3 s^{-1} to 196 s^{-1} due to propane as well as the 19-component hydrocarbon standard. This means that the dynamic range for the reactivity of ambient air (typically diluted in the flow reactor by a factor 1.4 – 2) would be ~ 4.5 to 300 s^{-1}. The intercept of the line in Figure 4.4 is negative (a = -3.3) which indicates that at low reactivity ranges of < 3 s^{-1} the method may lack sufficient sensitivity.

4.4.2 Investigation of possible interferences

Three main potential interferences have been identified while operating the comparative reactivity method in its present

configuration. These are: photolysis of pyrrole; recycling of OH at high NO due to the NO+ HO_2 reaction; and drastic changes in the relative humidity within the set-up when ambient air is sampled. A detailed discussion of each is presented in the following sub-sections.

4.4.2.1 Photolysis of pyrrole

The pen ray mercury lamp (L.O.T Oriel GmbH & Co. KG) used for producing OH radicals by photolysis of water vapour at 184.9 nm, also has emission lines at 253.6 nm, 312.5 nm, 365 nm and 435.8 nm. Pyrrole is reported to absorb at some of these wavelengths (Bavia et al., 1976; Cronin et al., 2004). Thus photolysis of pyrrole can potentially complicate the reactivity assessment. Figure 4.5 shows a plot characterizing the lamp induced photolysis of pyrrole for different initial amounts of introduced pyrrole (C0 on the horizontal axis in Figure 4.5) within the CRM flow reactor. Switching on the lamp inside the set-up without bubbling the nitrogen through water (so that no OH radicals are generated) gives the decrease in pyrrole (from C0 to C1) due to photolysis alone.

In every session of CRM measurements, the C1 value is obtained experimentally and so the initial amount of pyrrole (corresponding to C1 in Figure 4.1), which is available for reaction with OH, is known accurately. This is valid provided that the photodissociation quantum yield of pyrrole at ~ 760 torr is not significantly influenced by addition of water vapour. As shown, photolysis of pyrrole in the set-up can be a significant interference if it remains unaccounted (up to 25 % in Figure 4.5). However,

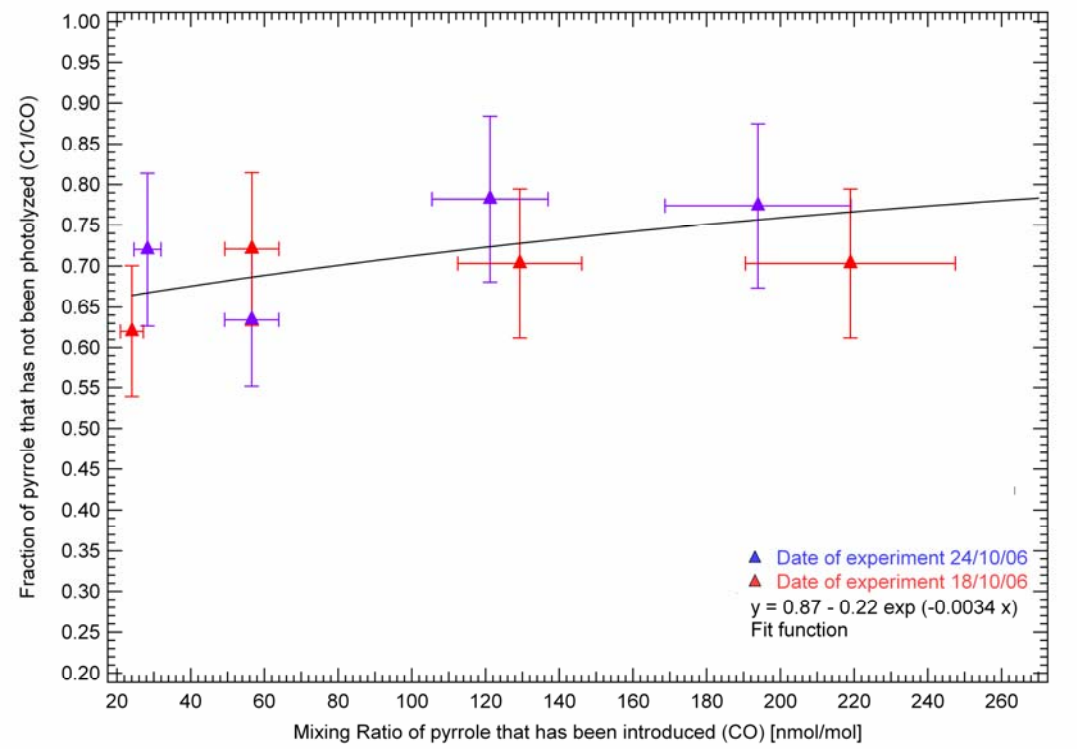

Figures 4.5: Plot quantifying loss of pyrrole in the CRM flow reactor by photolysis.

measuring and hence knowing its contribution to the observed decrease in the pyrrole signal, when the lamp is switched on in the presence of moist N_2 for OH production ensures that this interference is adequately quantified and hence has negligible influence on the measurements.

4.4.2.2 Recycling of OH due to HO_2 + NO

The pen- ray mercury lamp produces OH radicals by the photolysis of water vapour at atmospheric pressure in the following manner

$$H_2O \xrightarrow{184.9nm} OH + H \qquad (4.12)$$

While the above step is performed only in a flow of N_2, zero air

containing oxygen (O_2) enters the flow reactor through arm A (see Figure 4.2), so that HO_2 is also rapidly produced within the flow reactor by the following reaction:

$$H + O_2 + M \longrightarrow HO_2 + M \qquad (4.13)$$

If NO is then present in the sampled ambient air, it can recycle OH radicals:

$$NO + HO_2 \xrightarrow{k = 8.8 x 10^{-12}} OH + NO_2 \qquad (4.14)$$

Figure 4.6 shows the suppression in the pyrrole signal (vertical axis) for different amounts of added NO (horizontal axis) while sampling air containing propane (~ 16.5 s^{-1} of reactivity; 558 nmol mol^{-1} propane). Note that even at such high values of propane in the

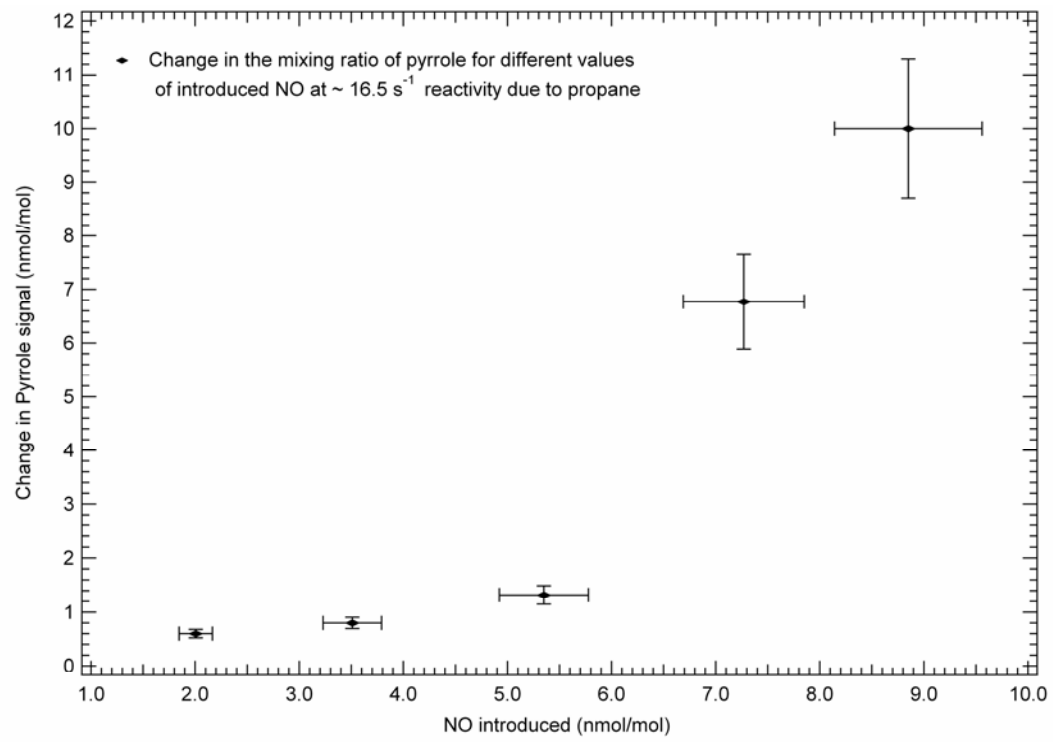

Figure 4.6: Results of the NO sensitivity study to determine its impact on the CRM measurements.

introduced air sample, the pyrrole signal is not affected significantly (that is, by more than the instrumental precision error of ~1 nmol mol^{-1} for pyrrole at ~ 25 nmol mol^{-1}) for added NO concentrations of up to3.5 nmol mol^{-1}. Above 5 nmol mol^{-1} of NO, however, the suppression in the pyrrole signal due to reaction with the recycled OH seems to be non-linear and causes significant interference in the CRM measurements, most likely by causing the measurements to underestimate the actual reactivity.

4.4.2.3 Humidity difference between zero air and ambient air

If the zero air used in lieu of ambient air to determine the pyrrole baseline signal (corresponding to C2 in Figure 4.1) differs substantially in humidity from that of the sampled ambient air, then the amount of OH radicals generated within the flow reactor might change, causing artefacts in the measured C2 and C3 pyrrole signals. When the zero air is drier than the ambient air entering the flow reactor, more OH radicals may be produced while sampling/ modulating with ambient air due to photolysis of the 'extra' water vapour present in the sampled ambient air. As a result, there can be a suppression of the measured pyrrole signal (C3) causing the measurements to underestimate the actual reactivity. Conversely, if the zero air is wetter than the sampled ambient air, less OH radicals may be available for reaction with pyrrole during the sampling of ambient air, leading to an enhancement of the measured pyrrole signal

(C3) and resulting in measurements that may overestimate the actual OH reactivity.

To ascertain how significant this interference might be, the zero air flowing into the set-up was humidified to different degrees by mixing varying amounts of wet and dry zero air prior to its introduction into the flow reactor through arm A (see Figure 4.2). Then, the variation in the pyrrole baseline (signal C2) was monitored for different degrees of humidified zero air. The humidity of the flow reactor air is tracked using mass 55 (cluster ion H_3O^+ $(H_2O)_2$), with the PTR-MS, similar to the approach of Ammann et al. (2006). Figure 4.7 shows the results, with the increase in the pyrrole signal (vertical axis) plotted against the corresponding decrease in humidity (horizontal axis). It is evident that repeating the experiment on different occasions which involved reassembling the whole set up and slightly different flows (see data for 14 August, 2005 and 26 October, 2006 in Figure 4.7) produces a consistent trend line.

The data in the top left hand corner of Figure 4.7 were obtained under the extreme condition of measuring the change in the pyrrole signal (C2) while using saturated zero air (~ 90 %) and dry zero air, taken directly from the bottle. Figure 6 also shows that for changes in mass 55 (humidity tracer) of up to ~ 20000 counts per second (cps) the change in the pyrrole signal is < 1nmol mol^{-1}, which is within the precision error of the PTR-MS. Therefore, while conducting ambient air reactivity measurements, the diluting zero air is humidified to lie within the 20000 cps range of the mass 55 signal observed for ambient air. So, while drastic changes in humidity can cause a

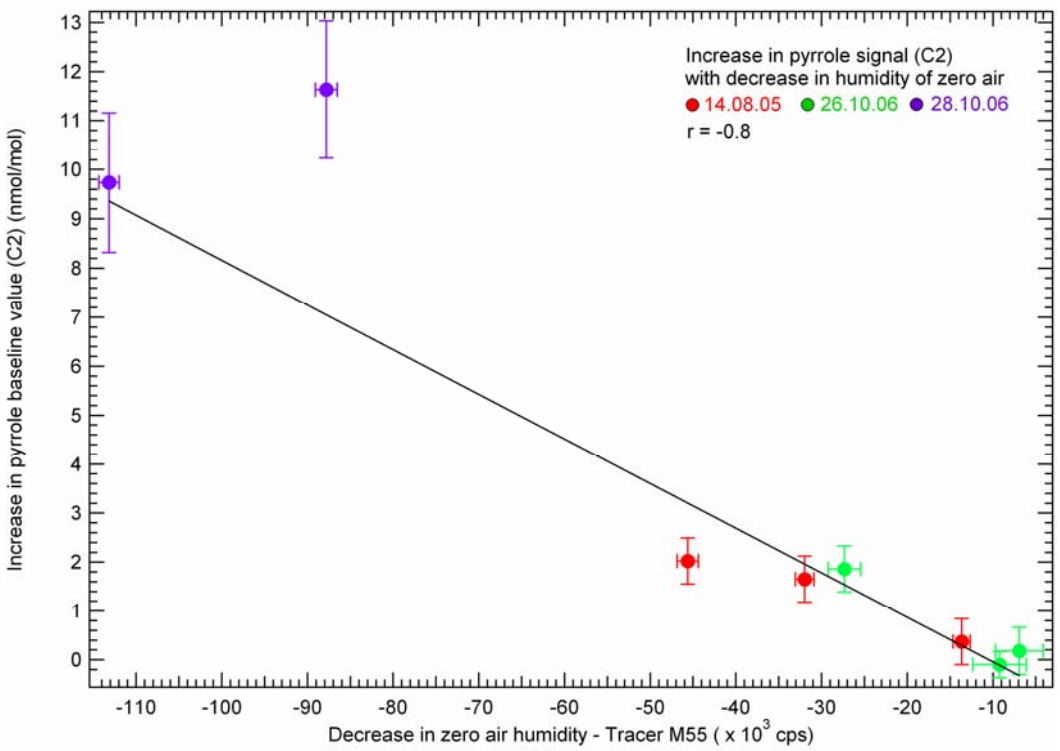

Figure 4.7: Changes in the measured pyrrole signal due to changes in relative humidity within the flow reactor.

significant interference, care is taken to match the mixing gases to the ambient humidity and thereby significant interferences are avoided.

4.4.4 Field deployment and first CRM results of ambient air OH reactivity

To test the capability and performance of the technique under markedly different ambient conditions, measurements were conducted first in the urban atmosphere of Mainz, Germany, and then in the tropical rainforest air of Suriname in August and October 2005, respectively.

4.4.4.1 Total OH Reactivity of Mainz air: Urban environment

Figure 4.8 shows the diel OH reactivity profile for Mainz air, measured with the CRM technique from 18 - 20 August 2005. Ambient air was sampled outside our laboratory (49°59'N, 8°14'E) at the Max Planck Institute for Chemistry in Mainz, circa 8 m above the ground. Just outside the laboratory there is an undergrowth of bushes and plants. The sampled ambient air was introduced directly into the CRM flow reactor using ~ 12 m long, 1/2 inch (o.d.) Teflon tubing, using a VOC sampling pump (Laboport N86-KN18). The inlet residence time for the ambient air was < 20 s and the measurement frequency was 0.025 Hz. During the measurements, NO in Mainz air was typically less than 1.5 nmol mol^{-1}(Landesamt für Umwelt,

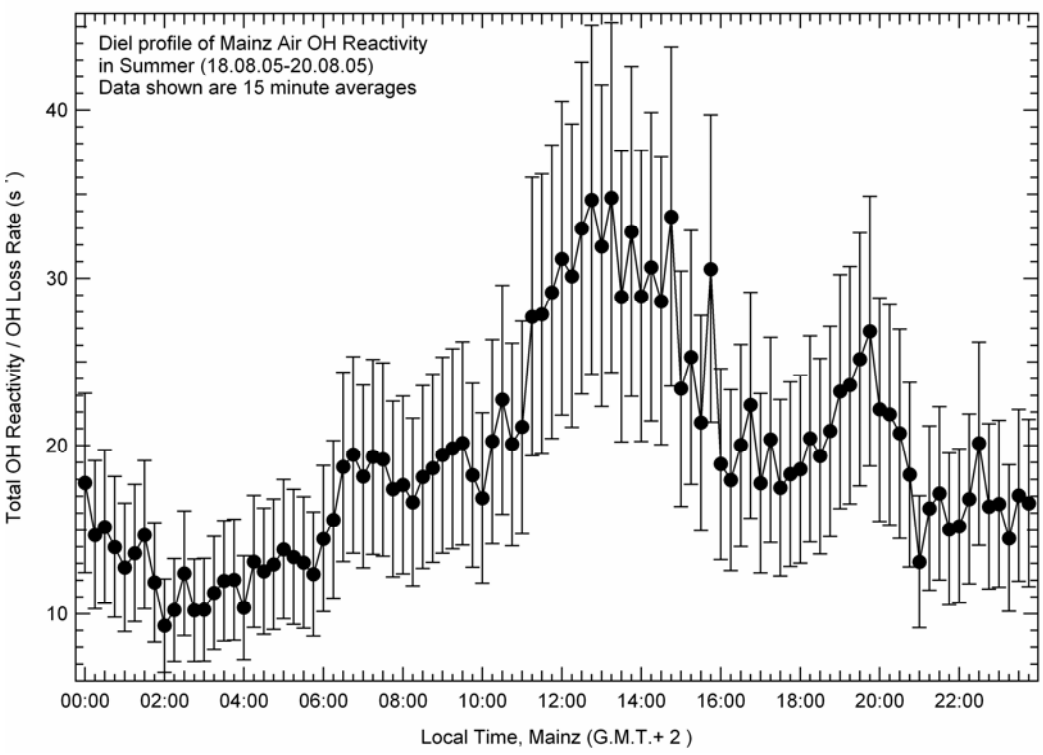

Figure 4.8: Diel mean profile (black circles) of the total OH Reactivity of Mainz (urban site) air measured during summer (August 2005) with the CRM instrument.

Wasserwirtschaft und Gewerbeausicht Rheinland-Pfalz). The average value of the total OH reactivity of Mainz air was ~ 19.5 s^{-1}. OH reactivity was observed to be highest during the afternoon (13:00 L.T.), reaching peak values of ~ 35 ± 10 s^{-1}, while lowest values (~ 9 ± 3 s^{-1}) were observed early in the morning between 2:00 to 4:00 L.T.

4.4.4.2 Total OH Reactivity of Suriname rainforest air: Forest environment

Figure 4.9 shows OH reactivity measurements of rainforest air at the peak of diel emissions. The measurements were taken in the nature reserve of Brownsberg (4°56' N, 55°10'W, 512 m a.s.l.) in Suriname, within the canopy (35 m) height. Details about the sampling methodology along with the site description are given elsewhere (Sinha et al., 2007b; Williams et al., 2007). Ambient forest air reactivity was measured for almost 2 hours on 6 October 2005 before the PTR-MS broke down. Earlier, from 2 to 5 October 2005, the PTR-MS was used to measure ambient air directly (without reactivity measurements) to determine diel emission profiles for VOCs such as acetone (mass 59), acetaldehyde (mass 45), isoprene (mass 69) and the isoprene oxidation products, methyl vinyl ketone and methacrolein (detected collectively at mass 71). The calculated diel reactivity profile derived from the ambient air PTR-MS measurements of these species is shown on the right vertical axis of Figure 4.9. The CRM reactivity measurements shown in Figure 4.9 were taken when forest air seemed to have maximum OH reactivity, as they coincide with the peak of diel forest emissions. The average of

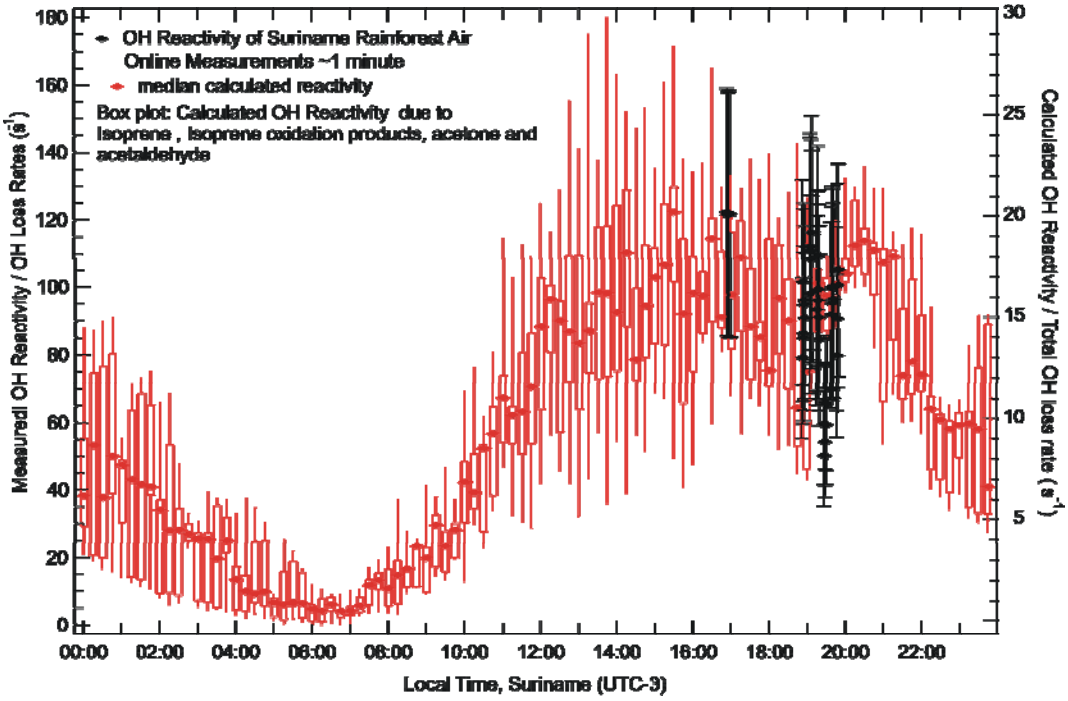

Figure 4.9: Total OH reactivity measurements (black markers) of rainforest air in Brownsberg, Suriname along with diel median profile of calculated OH reactivity (red markers) due to isoprene, mvk, methacrolein , acetone and acetaldehyde), obtained during the dry season in October 2005

all the OH reactivity measurements (~ 2 hours of data) was circa 93 s^{-1}, with a peak OH reactivity of approximately 122 ± 36 s^{-1}.

4.5. Discussion

The results shown here demonstrate that a new and promising online technique capable of directly measuring the total OH reactivity of ambient air has been developed. Using pyrrole and a PTR-MS, as the reagent molecule and detector, respectively, the dynamic range of the technique in its existing configuration is ~ 4.5 s^{-1} to 300 s^{-1} for ambient air. The overall uncertainty of the measurements is typically ± 25 %. At lower ambient air reactivity ranges (< circa 5 s^{-1}), the

uncertainty can be up to 40 %. This is sensitive enough to constrain the OH reactivity (OH sink) and test for missing OH reactants during field campaigns (when OH reactivity > 5 s^{-1}). The technique performs quite well with propane and mixed hydrocarbon standards and accounts for the introduced reactivity within the measurement uncertainty (slope of the calibration line = 1.08).

While major potential interferences have been investigated in Section 4.4.3, other minor interferences have also been considered. Ambient air VOCs which absorb in the UV region may undergo photolysis within the set up. However, the fact that the calibration line due to the 19 component hydrocarbon standard (containing VOCs such as acetaldehyde, hexanal and aromatics and methyl vinyl ketone, which absorb UV light and are introduced at concentrations of 7 to 17 nmol mol^{-1}), falls on the same trend line as that of propane (see Figure 4.3), suggests that this is not a sizeable effect. To test for secondary chemistry along the flow reactor reaction length and sensitivity to slight change of flows (~ 20 ml $minute^{-1}$) the PTR-MS probe (inlet D of the flow reactor; Figure 4.2) was placed at different points along the length of the flow reactor. However, no noticeable change in the measured pyrrole signal was observed. This simple test is also applied in the field, while sampling ambient air to investigate the influence of secondary chemistry within the flow reactor. It is also worth mentioning that the lifetime of OH radicals within the flow reactor set up is always < 4 ms.

Ozone is also produced within the flow reactor by photolysis of O_2 due to the 184.9 nm lamp emission line. Moreover the ratio of

O_3/OH in our flow reactor set up is similar to that found in ambient air (10^3). However, the ozone (produced at μmol mol^{-1} level) hardly affects the pyrrole signal since the pyrrole + O_3 reaction rate ($k_{O3 + pyrrole}$ = 1.57 x 10^{-17} cm^3 $molecule^{-1}$ s^{-1} (Atkinson et al., 1984) is several orders of magnitude slower than the reaction rate with OH radicals. When terpenes and sesquiterpenes are present in ambient air, they can react with O_3 within the flow reactor and recycle OH (Paulson et al., 1999; Hasson et al., 2003). Also, some RO_2 reactions with HO_2 may also generate OH (Hasson et al., 2004), again potentially affecting the reactivity measurement. However, the recycled OH due to ozonolysis of these reactive alkenes and the Hasson reactions within the flow reactor is negligible compared to the high OH radical concentrations (~ 2.15 x 10^{12} molecules cm^{-3}) generated in-situ by photolysis of water vapour. For the same reason, the CRM method may actually perform better under such ambient air conditions (of highly reactive terpenes in ambient air) than the LIF based method. This is because the regenerated OH radicals may mask the actual OH decay rate within the LIF instrument's flow reactor and cause an underestimation of the actual measured decay rate and OH reactivity.

In the future, we will conduct calibration tests using single component standards such as formaldehyde (which absorbs UV radiation) and a reactive terpene/ sesquiterpene, as well. Other reactor designs that allow only the OH to enter the reactor (and not the light) will also be tested. The NO sensitivity studies have shown that in the existing configuration of CRM, high NO in sampled air causes interference. We found significant interference at NO> 5 nmol mol^{-1}

for propane at~16.5 s^{-1} reactivity, but while sampling ambient air, the interference may become significant even at lower NO concentrations. In this respect, it would be useful and interesting to compare the CRM technique with the LIF based reactivity measurement technique to test for systematic offsets between the two analytical approaches. Under our experimental conditions, it is likely that the NO interference will cause the measurements to underestimate the actual reactivity. Thus, low NO_x environments such as tropical forests (NO< 20 pmol mol^{-1}, e.g. Brownsberg) and pristine marine environments appear to be ideal sites for the deployment of the existing CRM instrument.

Further modifications to improve the sensitivity, precision and automation of the instrument and to minimize / remove interferences can proceed now that the first validation is complete. For example, a mercury pen-lamp equipped with an interference filter (Acton) to transmit only the 184.9 nm line, would significantly reduce photolysis related interferences. OH sources that are not HO_2 sources exist and may help in improving the current system (e.g. photolysis of H_2O_2 (small cross section only), F + H_2O, photolysis of N_2O followed by the reaction of O^1D with water). The existing sampling strategy for introducing ambient air into the flow reactor, which uses a VOC sampling Teflon pump (Laboport N86-KN18), could also be modified so that the ambient air enters the set-up directly without going through a pump. This would help to minimize the loss of sticky reactive VOCs, which may contribute significantly to OH reactivity. While we have used the reagent and detector system of pyrrole and a

PTR-MS, respectively, in principle it should be possible to apply the Comparative Reactivity Concept to other suitable reagent molecules (e.g. labeled isotopes of isoprene) and detectors (e.g. fast response GC-MS systems). Other reagent molecules, which have a slower reaction rate than that of pyrrole with OH may also afford better sensitivity at lower ranges of ambient air OH reactivity.

The instrument has been successfully deployed in the field to measure the total OH reactivity of ambient air in the contrasting environments of Mainz (urban), Germany and Brownsberg (rainforest air), Suriname. The measurements indicated that at the peak of diel emissions, Suriname forest air was 3.5 times more reactive than the urban air of Mainz (122 s^{-1} compared to 35 s^{-1}; Figure 4.7). The total OH reactivity measurements for Mainz air lie well within the range of total OH reactivity measurements reported in literature for urban air sites. Table 4.1 presents a summary of ambient air OH reactivity measurements from urban and forest sites. Kovacs et al. (2003) have

Table 4.1: Summary of ambient air OH reactivity measurements.

Site	Ave / Med^{+} (s^{-1})	Max (s^{-1})	Reference
Nashville,TN, U.S.A.	11	25	Kovacs et al. (2003)
New York City, U.S.A.	19	50	Ren et al. (2003)
Tokyo, Japan	40	85	Sadanaga et al. (2005)
M.C.M.A, Mexico	33	200	Shirley et al. (2005)
Pine forest, U.S.A.	-	13	Di Carlo et al. (2004)
Mainz, Germany	19	35	This work
Rainforest, Suriname	93§	122§	This work

+ = average was used when median was not available; § = measurement period was at peak of diel emissions

reported ambient air OH reactivity values of 11 - 19 s^{-1} at Nashville, TN, USA. In the same campaign, a comparison of the measured OH reactivity and the calculated reactivity due to the measured reactants (70 VOCs), showed that on average, the measured OH reactivity was 1.45 times higher (Martinez et al., 2003). Using laser induced fluorescence based techniques, maximum OH reactivity values of 50 s^{-1}in New York City (Figure 4.8 in Ren et al., 2003), 85 s^{-1} in suburban Tokyo (Sadanaga et al., 2004a; Sadanaga et al., 2005; Yoshino et al., 2006), and 200 s^{-1} in Mexico city (Figure 4.9 in Shirley et al., 2006) have been observed.

To our knowledge, the ambient air OH reactivity measurements from Brownsberg are the first total OH reactivity measurements from a tropical rainforest site, an ecosystem that is known for strong biogenic emissions (Karl et al., 2004; Goldstein and Galbally, 2007). Di Carlo et al. (2004) observed missing OH reactivity in a mixed transition forest consisting of northern hardwood, aspen and white pine in north Michigan. Our limited OH reactivity measurements from Brownsberg also indicate that a significant fraction of important OH reactive compounds are likely missed in conventional measurements at forest sites (see Figure 9), since isoprene, isoprene oxidation products, acetone and acetaldehyde make up only ~ 30 % of the measured sink). In future studies, it will be interesting to measure a more comprehensive suite of VOCs and other OH-reactive species such as NO_2 and SO_2, together with direct OH reactivity measurements to better understand the budget of OH sinks. Rate constants for the reaction of OH with almost all measured ambient

VOCs are known. By summing up the calculated reactivity due to all the measured VOCs (i.e. summation of VOC concentration times its rate coefficient) and comparing it with the direct OH reactivity measurement, one can additionally examine the reactive carbon budget and assess the importance of the missing VOC reactants.

4.6. Conclusion

This study has shown that the Comparative Reactivity Method (CRM) is a sound and feasible concept that can be applied for direct measurements of the total OH reactivity of ambient air. Applying the CRM concept to the reagent and detector system of pyrrole and a PTR-MS, respectively, a new online measurement technique with a dynamic range of ~ 4.5 to 300 s^{-1} for ambient air and accuracy of ± 25 % has been developed. Sensitivity studies (involving changing parameters) have been carried out, and high NO (> 5 nmol mol^{-1}) in ambient air has been identified as the major interference. Therefore low NO_x environments such as remote forest sites and marine environments are ideal for deploying the new instrument, and improvements in the existing set up are needed for conducting measurements in strongly NO_x polluted environments. Moderately polluted Mainz air measurements (NO ≤ 1.5 nmol mol^{-1}) are consistent with OH reactivity measurements reported previously for urban air. Our measurements from the tropical rainforest (for which no other data exists) indicate that a significant fraction of OH reactive species is likely missed in current measurements. Further OH reactivity measurements, combining comprehensive measurements of

VOCs and other OH reactive species are needed to clarify whether sinks are currently underestimated in forest environments and to constrain the budget of reactive VOCs.

Finally, several measurement groups routinely employ proton transfer reaction mass spectrometers and gas chromatography detectors for measuring VOCs in ambient air during field campaigns. It would be relatively easy and economical to integrate a flow reactor and employ the CRM based technique proposed in this study with these detectors for direct quantification of the OH sink, using either pyrrole or another suitable molecule. One of the future objectives will also be to compare the newly developed CRM based instrument with the existing more comprehensive laser induced fluorescence (LIF) based reactivity measurement technique, to test for systematic offsets between the two analytical approaches. Hopefully, this study will stimulate further efforts in the application of the Comparative Reactivity Method for ambient air OH reactivity measurements.

5. Summary, Conclusions and Outlook

Air-sea fluxes of VOCs from a Norwegian fjord following a phytoplankton bloom in a mesocosm experiment

This study has shown that photosynthetically active radiation (PAR) and ocean biology can strongly influence the emissions and / or uptake of acetone, acetaldehyde and isoprene and methanol from the ocean to the atmosphere. For example, it was observed that under conditions of high biological activity and a PAR of ~ 450 μmol photons m^{-2} s^{-1}, the ocean acted as a net source of acetone. However, if either of these criteria (namely light and prolific biology) was not fulfilled then the ocean acted as a net sink of acetone. This new insight into the biogeochemical cycling of acetone at the ocean-air interface has helped to explain discrepancies from earlier works such as Jacob et al. (2002) who reported the ocean to be a net acetone source (27 Tg yr^{-1}) and Marandino et al. (2005) who reported the ocean to be a net sink of acetone (- 48 Tg yr^{-1}, negative sign implying it is a sink). For methanol, the ocean acted as a net sink throughout the study period, in agreement with previous studies, with the night time uptake showing a strong correlation with phytoplankton abundance (r = 0.86). If plankton take up methanol directly or indirectly, it could help explain why ocean waters have a constant undersaturation with respect to methanol. During this study, the ocean acted as a net source for isoprene and acetaldehyde, with the emissions correlating with light ($r_{avcorr,\ isoprene}$ = 0.49 ; $r_{avcorr,\ acetaldehyde}$ = 0.70) and phytoplankton abundance. Such a result is significant because it can help in resolving discrepancies between measured and

modeled acetaldehyde concentrations by considering an additional biological source for acetaldehyde in the marine boundary layer. Current photochemical models consider acetaldehyde in the marine boundary layer to be almost exclusively formed by the oxidation of ethane and other hydrocarbons. High inter - VOC correlations between the day time emission fluxes of acetone and acetaldehyde (r_{av} = 0.96), acetaldehyde and isoprene (r_{av} = 0.88) and acetone and isoprene (r_{av} = 0.85), will be useful for modeling the air-sea emission fluxes of these VOCs. The net flux of dimethyl sulphide (DMS) was always from the sea to the overlying air, which is consistent with earlier works that have reported that the ocean is a net source of DMS. As the air-sea flux of each trace gas depends differently on light and biological activity, extremely large variations in such fluxes can be expected as a consequence of the range of solar and biological conditions over the global oceans. Therefore, specifically parameterized models constrained by measurements from locations that represent the varied geographical areas of the global ocean will provide more accurate estimates of the oceanic contribution to the global budgets of these volatile organic compounds.

In future, possible methanol uptake at night by phytoplankton species must be investigated in detail. To further improve our understanding of the biogeochemical cycling of VOCs at the sea-air interface, future mesocosm experiments should monitor both aqueous and gas phase concentrations and the mesocosm air should be actively circulated with a fan to ensure thorough mixing in the gas phase. Also, a more exhaustive suite of biological parameters, measured at a

higher frequency than in this study may yield valuable insights for biological production and / or consumption of VOCs in the seawater. Evidently, the mesocosm approach is a new and novel technique particularly suited for clarifying the vast uncertainties that exist in the field of oceanic VOC uptake and emissions and their biogeochemical cycling.

Methane emissions from boreal and tropical forest ecosystems derived from in-situ measurements

This study has highlighted the importance of the boreal and tropical forest ecosystems for the global methane budget. Night time methane emission flux of the boreal forest ecosystem, calculated from the increase of methane during the night and measured nocturnal boundary layer heights yielded a flux of (3.62 ± 0.87) x 10^{11} molecules cm^{-2} s^{-1}(or 45.5 ± 11 Tg CH4 $yr^{-1}$for global boreal forest area). This is circa 7.5 % of the annual global methane budget of ~ 600 Tg yr^{-1}. A remarkably similar increase in night time methane mixing ratios was observed for the tropical forest ecosystem as well, but lack of information about the nocturnal boundary layer growth hindered the calculation of the methane flux, from the tropical forest ecosystem. The average of the median mixing ratios during a typical diel cycle were 1.83 μmol mol^{-1} and 1.74 μmol mol^{-1} for the boreal forest ecosystem and tropical forest ecosystem respectively, with remarkable similarity in the time series of both the boreal and tropical diel profiles. Such similarity in methane profiles at widely different forest vegetations and climates is quite remarkable and future investigations should examine whether such behaviour is true for

other forest sites as well. Until the mechanism of methane production from plants under aerobic conditions, is better understood, examining net ecosystem fluxes under in-situ natural conditions, would help in constraining the contribution due to the suggested new vegetation source and assessing whether their magnitude is within the uncertainties of the existing sources or significantly higher. Based on our first order approach to ascertain the range of methane emissions from boreal vegetation in the spring season, it appears that the boreal vegetation contributes only modestly to the global budget (~1 %). This contribution is well within the uncertainties of the existing emission sources (e.g. wetlands) from boreal ecosystems.

High temporal resolution measurements, from the boreal forest and tropical forest ecosystems, made over longer time periods are needed to assess methane emissions from these regions more accurately. Based on the short term data presented in this work, it appears that boreal forest ecosystem emissions may be currently underestimated while tropical forest ecosystem emissions may be slightly over estimated. Furthermore, ^{13}C isotope measurements can help to apportion the methane sources in a better manner and thus a combined approach of in-situ measurements at suitable remote and homogeneous sites, remote sensing retrieval studies and isotope studies would help to reduce the uncertainties in the global methane budget much more effectively.

The Comparative Reactivity Method – A new tool to measure the total OH Reactivity of ambient air

In this study, a new technique capable of directly measuring the total OH reactivity of ambient air has been developed and deployed for measurements in an urban and forest site. The new technique is based on a novel approach called the Comparative Reactivity Method (CRM). In this method, a reactive molecule (X), not normally present in air, is passed through a glass reactor and its concentration is monitored with a suitable detector. OH radicals are then introduced in the flow reactor at a constant rate to react with X, first in the presence of zero air and then in the presence of ambient air containing VOCs and other OH reactive species. Comparing the amount of X exiting the reactor with and without the ambient air allows the air reactivity to be determined. Applying the CRM concept to the reagent and detector system of pyrrole and a PTR-MS, the new measurement technique has a dynamic range of ~ 4.5 to 300 s^{-1} for ambient air and an accuracy of ± 25 %. The technique was validated, calibrated and tested for interferences. Sensitivity studies (involving changing parameters) identified high NO in ambient air (greater than 5 nmol mol^{-1}) as the major interference. Consequently, low NO_x environments such as remote forest sites and marine environments are deemed ideal for deploying the new instrument, and improvements in the existing set up will be necessary for conducting measurements in polluted NO_x (> 5 nmol mol^{-1}) environments.

The measurements of the OH reactivity of Mainz air are consistent with OH reactivity measurements reported previously from

other urban sites. Using the technique in a tropical rainforest site in Suriname, measurements indicated that a significant fraction of OH reactive species were unknown. Further OH reactivity measurements, combining comprehensive measurements of VOCs and other OH reactive species are needed to clarify whether sinks are currently underestimated in forest environments. Such studies will also help in constraining the budget of reactive VOCs.

The newly developed technique is preferable to the only other existing technique currently used for measuring OH reactivity of ambient air directly, which is based on the laser induced fluorescence (LIF) system. Firstly it can be applied to any detector, can be easily adapted to suit reactive and unreactive environments, and it is both smaller and less expensive than the LIF system. Several measurement groups routinely employ proton transfer reaction mass spectrometers (PTR-MS) and gas chromatography detectors for measuring VOCs in ambient air during field campaigns. It would be feasible and economical to integrate a glass reactor, as described here, and employ the CRM based technique proposed in this study with these detectors, for direct quantification of the OH sink using either pyrrole or another suitable molecule. Thus, this new technique is a valuable addition to the current suite of atmospheric measurement techniques.

One of the future objectives will also be to compare the newly developed CRM based instrument with the existing less mobile / more expensive, laser induced fluorescence (LIF) based reactivity measurement technique, to test for systematic offsets between the two analytical approaches. Hopefully, this study will stimulate further

efforts in the application of the Comparative Reactivity Method for ambient air OH reactivity measurements.

In conclusion, it can be said that all these studies have helped in improving the current understanding of VOC emissions and uptake from the ocean and forest ecosystems. Additionally, a promising new technique to directly measure the total OH reactivity of ambient air has been developed, validated and field deployed, enhancing the suite of existing atmospheric measurement techniques.

Bibliography

Ammann, C., Brunner, A., Spirig, C., and Neftel, A., Technical note: Water vapour concentration and flux measurements with PTR-MS: Atmos. Chem. Phys., 6, 4643-4651, 2006.

Andreae, M.: Ocean-Atmosphere Interactions in the global biogeochemical sulphur cycle, Mar. Chem., 30 (1-3), 1-29, 1990.

Apel, E., Hills, A., Lueb, R., Zindel, S., Eisele, S. and Riemer, D.: A fast-GC/MS system to measure C-2 to C-4 carbonyls and methanol aboard aircraft, J. Geophys. Res.-Atmos., 108 (D20), 8794-8811, 2003.

Atkinson, R., Aschmann, S. M., Winer, A. M., and Carter, W. P. L., Rate Constants for the Gas-Phase Reactions of OH Radicals and O3 with Pyrrole at 295+/-1k and Atmospheric-Pressure: Atmos. Environ., 18, 2105-2107, 1984.

Atkinson, R.; Baulch, D. L.; Cox, R. A.; Crowley, J.; Hampson, R. F., Jr.; Kerr, J. A.; Rossi, M. J.; Troe, J., "Summary of Evaluated Kinetic and Photochemical Data for Atmospheric Chemistry", IUPAC Subcommittee on Gas Kinetic Data Evaluation for Atmospheric Chemistry, available at http://www.iupac-kinetic.ch.cam.ac.uk/index.html, web version 2006.

Bartlett, K., Harriss, R., Review and assessment of methane emissions from wetlands. Chemosphere 26, 261– 320, 1993.

Barlow, R.G., Cummings, D.G. and Gibb, S.W.: Improved resolution of mono- and divinyl chlorophylls a and b and zeaxanthin and

lutein in phytoplankton extracts using reverse phase C-8 HPLC, Mar. Ecol. Prog., Ser. 161, 303-307, 1997.

Bavia, M., Bertinelli, F., Taliani, C., and Zauli, C., Electronic-Spectrum of Pyrrole in Vapor and Crystal: Mol. Phys., 31, 479-489, 1976.

Bergamaschi, P., Frankenberg, C., Meirink, J. F.,Krol, M., Dentener, F., Wagner, T., Platt, U., 2007. Satellite chartography of atmospheric methane from SCIAMACHY on board ENVISAT:2. Evaluation based on inverse model simulations, J. Geophys. Res., 112, D02304, doi:10.1029/2006JD007268.

Bergstrom, I., Makelab, S., Kankaalab, P., Kortelainen, P., Methane efflux from littoral vegetation stands of southern boreal lakes: An upscaled regional estimate, Atmospheric Environment, doi: 10.1016/j.atmosenv.2006.08.014, 2006.

Bonsang, B., Polle, C. and Lambert, G.: Evidence for Marine production of isoprene, Geophys. Res. Lett., 19 (11), 1129-1132, 1992.

Brasseur, G.P., Orlando, J.J., Tyndall, G.S., Atmospheric chemistry and global change, Oxford University Press, Inc., 1999.

Broadgate, W., Liss, P. and Penkett, S.: Seasonal emissions of isoprene and other reactive hydrocarbon gases from the ocean, Geophys. Res. Lett., 24 (21), 2675-2678, 1997.

Broadgate, W., Malin, G., Kupper, F., Thompson, A. and Liss, P.: Isoprene and other non-methane hydrocarbons from seaweeds: a source of reactive hydrocarbons to the atmosphere, Mar. Chem., 88 (1-2), 61-73, 2004.

Carslaw, N., Creasey, D. J., Heard, D. E., Jacobs, P. J., Lee, J. D., Lewis, A. C., McQuaid, J. B., Pilling, M. J., Bauguitte, S., Penkett, S. A., Monks, P. S., and Salisbury, G., Eastern Atlantic Spring Experiment 1997 (EASE97) - 2. Comparisons of model concentrations of OH, HO2, and RO2 with measurements: J. Geophys. Res.-Atmos., 107, 2002.

Carmo, J. B., Keller, M., Dias, J.D., Camargo, P.B., and Crill P., A source of methane from upland forests in the Brazilian Amazon, Geophys. Res. Lett., 33, L04809, doi:10.1029/2005GL025436, 2006.

Carpenter, L. J., Lewis, A.C., Hopkins, J. R., Read, K. A., Longley, I. D. and Gallagher, M. W.: Uptake of methanol to the North Atlantic Ocean surface, Global Biogeochem. Cycles, 18, GB4027, doi: 10.1029/2004GB002294, 2004.

Colomb, A., Williams, J., Crowley, J., Gros, V., Hofmann, R., Salisbury, G., Kluepfel, T., Kormann, R., Stickler, A., Forster, C. and Lelieveld J.: Airborne measurements of trace organic species in the upper troposphere over Europe: the impact of deep convection, Environ.Chem., 3, 244–259, doi:10.1071/EN06020, 2006.

Cronin, B., Nix, M. G. D., Qadiri, R. H., and Ashfold, M. N. R., High resolution photofragment translational spectroscopy studies of the near ultraviolet photolysis of pyrrole: Phys. Chem. Chem. Phys., 6, 5031-5041, 2004.

Crutzen, P. J., Sanhueza, E., and Brenninkmeijer, C. A. M., Methane production from mixed tropical savanna and forest vegetation

in Venezuela, Atmos. Chem. Phys. Discuss., 6, 3093 – 3097, http://www.atmos-chem-phys-discuss.net/6/3093/2006/, 2006.

Dacey, J. and Wakeham, S.: Oceanic dimethyl sulfide - production during zooplankton grazing on phytoplankton, Science, 233 (4770), 1314-1316, 1986.Derenbach, J.: Zur Homogenisation des Phytoplanktons für die Chlorophyllbestimmung, Kieler Meeresforschungen, XXV (1), 166-171, 1969.

de Gouw, J., and Warneke, C., Measurements of volatile organic compounds in the earths atmosphere using proton-transfer-reaction mass spectrometry: Mass Spectrom. Rev., 26, 223-257, 2007.

de Laat, A., de Gouw, J., Lelieveld, J. and Hansel, A.: Model analysis of trace gas measurements and pollution impact during INDOEX, J. Geophys. Res.-Atmos., 106 (D22), 28469-28480, 2001.

Di Carlo, P., Brune, W. H., Martinez, M., Harder, H., Lesher, R., Ren, X. R., Thornberry, T., Carroll, M. A., Young, V., Shepson, P. B., Riemer, D., Apel, E., and Campbell, C., Missing OH reactivity in a forest: Evidence for unknown reactive biogenic VOCs: Science, 304, 722-725, 2004.

Drebs, A., Nordlund, A., Karlsson, P., Helminen, J., and Rissanen, P., Climatological statistics of Finland 1971–2000, Finnish Meteorological Institute, Helsinki, 99 pp, ISBN 951-697-568-2, 2002.

Engel, A., Zondervan, I., Aerts, K., Beaufort, L., Benthien, A., Chou, L., Delille, B., Gattuso, J., Hailay, J., Heemann, C., Hoffmann,

L., Jacquet, S., Nejstgaard, J., Pizay, M., Rochelle-Newall, E., Schneider, U.,Terbrueggen, A. and Riebessell, U. : Testing the direct effect of CO2 concentration on a bloom of the coccolithophoroid Emiliania huxleyi in mesocosm experiments, Limnol. Oceanogr., 50 (2), 493-507, 2005.

Ferretti, D. F., Miller, J. B., White, J. W. C., Lassey, K. R., Lowe, D. C., and Etheridge, D. M., Stable isotopes provide revised global limits of aerobic methane emissions from plants, Atmos. Chem. Phys., 7, 237–241, 2006.

Field, C., Behrenfeld, M., Randerson, J. and Falkowski, P.: Primary production of the biosphere: Integrating terrestrial and oceanic components, Science, 281 (5374), 237-240, 1998.

Frankenberg, C., Meirink, J. F., van Weele, M., Platt, U., and Wagner, T., Assessing methane emissions from global space-borne observations, Science, 308, 1010–1014, 2005.

Frankenberg, C., Meirink, J. F., Bergamaschi, P., Goede, A. P. H. , Heimann, M., Korner, S., Platt, U., van Weele, M., and Wagner, T., Satellite chartography of atmospheric methane from SCIAMACHY on board ENVISAT: Analysis of the years 2003 and 2004, J. Geophys. Res., 111, D07303, doi:10.1029/2005JD006235, 2006.

Gabric, A., Whetton, P. and Cropp, R.: Dimethylsulphide production in the subantarctic southern ocean under enhanced greenhouse conditions, Tellus B, 53 (3), 273-287, 2001.

Galbally, I. and Kirstine, W.: The production of methanol by flowering plants and the global cycle of methanol, J Atmos

Chem, 43 (3), 195-229, 2002.

Glueckauf, E. In Compendium of Meteorology; Malone, T. F., Ed.; American Meteorological Society: Boston, pp 3–10, 1951

Goldstein, A. H., McKay, M., Kurpius, M. R., Schade, G. W., Lee, A., Holzinger, R., and Rasmussen, R. A., Forest thinning experiment confirms ozone deposition to forest canopy is dominated by reaction with biogenic VOCs: Geophys. Res. Lett., 31, 2004.

Goldstein, A. H., and Galbally, I. E., Known and unexplored organic constituents in the earth's atmosphere: Environ. Sci. Technol., 41, 1514-1521, 2007.

Guenther, A., Hewitt, C., Erickson, D., Fall, R., Geron, C., Graedel, T., Harley, P., Klinger, L., Lerdau, M., Mckay, W., Pierce, T., Scholes, B., Steinbrecher, R., Tallamraju, R., Taylor, J. and Zimmerman, P.: A global-model of natural volatile organic-compound emissions, J. Geophys. Res.-Atmos., 100 (D5), 8873-8892, 1995.

Haapanala, S., Rinne, J., Hakola, H., Hellen, H., Laakso, L., Lihavainen, H., Janson, R.,and Kulmala M., Boundary layer concentrations and landscape scale emissions of volatile organic compounds in early spring, Atmos. Chem. Phys. Discuss., 6, 10567–10589, 2006.

Haagen-Smit, A., Chemistry and Physiology of Los Angeles Smog, J. Ind. Eng. Chem. 44, 1342, 1952.

Hari, P. and Kulmala, M., Station for measuring ecosystem-

atmosphere relations (SMEAR II), Boreal Environ. Res., 5, 315–322, 2005.

Hasson, A. S., Chung, M. Y., Kuwata, K. T., Converse, A. D., Krohn, D., and Paulson, S. E., Reaction of Criegee intermediates with water vapor - An additional source of OH radicals in alkene ozonolysis? J. Phys. Chem. A, 107, 6176-6182, 2003.

Hasson, A. S., Tyndall, G. S., and Orlando, J. J., A product yield study of the reaction of HO2 radicals with ethyl peroxy (C2H5O2), acetyl peroxy (CH3C(O)O-2), and acetonyl peroxy (CH3C(O)CH2O2) radicals: J. Phys. Chem. A, 108, 5979-5989, 2004.

Heard, D. E., and Pilling, M. J., Measurement of OH and HO2 in the troposphere: Chem. Rev., 103, 5163-5198, 2003.

Heikes, B., Chang, W., Pilson, M., Swift, E., Singh, H., Guenther, A., Jacob, D., Field, B., Fall, R., Riemer, D. and Brand, L.: Atmospheric methanol budget and ocean implication, Global Biogeochem. Cycles, 16 (4), 1133-1146, 2002.

Hofzumahaus, A., Aschmutat, U., Hessling, M., Holland, F., and Ehhalt, D. H., The measurement of tropospheric OH radicals by laser-induced fluorescence spectroscopy during the POPCORN field campaign: Geophys. Res. Lett., 23, 2541-2544, 1996.

Holland, F., Hofzumahaus, A., Schafer, R., Kraus, A., and Patz, H. W., Measurements of OH and HO2 radical concentrations and photolysis frequencies during BERLIOZ: J. Geophys. Res.-Atmos., 108, 2003.

Holzinger, R., Lee, A., Paw, K. T., and Goldstein, A. H., Observations of oxidation products above a forest imply biogenic emissions of very reactive compounds: Atmos. Chem. Phys., 5, 67-75, 2005.

Houweling, S., Rockmann, T., Aben, I., Keppler, F., Krol, M., Meirink, J. F., Dlugokencky, E. J., and Frankenberg , C., Atmospheric constraints on global emissions of methane from plants, Geophys. Res. Lett., 33, L15821, doi:10.1029/2006GL026162, 2006.

Huebert, B., Blomquist, B., Hare, J., Fairall, C., Johnson, J. and Bates, T.: Measurement of the sea-air DMS flux and transfer velocity using eddy correlation, Geophys. Res. Lett., 31 (23), doi: 10.1029/2004GL021567, L23113, 2004.

Jacob, D., Field, B., Jin, E., Bey, I., Li, Q., Logan, J., Yantosca, R. and Singh, H.: Atmospheric budget of acetone, J. Geophys. Res.-Atmos., 107 (D10), 4100-4117, 2002.

Jacob, D., Field, B., Li, Q., Blake, D., de Gouw, J., Warneke, C., Hansel, A., Wisthaler, A., Singh, H. and Guenther, A.: Global budget of methanol: Constraints from atmospheric observations, J. Geophys. Res.-Atmos., 110 (D8), 590-595, 2005.

Karl, T., Potosnak, M., Guenther, A., Clark, D., Walker, J., Herrick, J. D., and Geron, C., Exchange processes of volatile organic compounds above a tropical rain forest: Implications for modeling tropospheric chemistry above dense vegetation: J. Geophys. Res.-Atmos., 109, 2004.

Karl, T., Harley, P., Guenther, A., Rasmussen, R., Baker, B., Jardine, K. and Nemitz, E.: The bi-directional exchange of oxygenated VOCs between a loblolly pine (Pinus taeda) plantation and the atmosphere, Atmos. Chem. Phys., 5, 3015-3031, 2005.

Keppler, F., Hamilton, J. T. G., Brass, M., and Roeckmann, T., Methane emissions from terrestrial plants under aerobic conditions, Nature, 439, 187–191, 2006.

Kesselmeier, J., and Staudt, M., Biogenic volatile organic compounds (VOC): An overview on emission, physiology and ecology: J. Atmos. Chem., 33, 23-88, 1999.

Kettle, A. and Andreae, M.: Flux of dimethylsulfide from the oceans: A comparison of updated data seas and flux models, J. Geophys. Res.-Atmos., 105 (D22), 26793-26808, 2000.

Khalil, M.A.K.: Atmospheric methane: an introduction. In: Khalil, M. (Ed.), Atmospheric Methane: Its Role in the Global Environment. p.p. 1-8, Springer-Verlag, New York, NY, 2000.

Kiene, R. P.: Microbial sources and sinks for methylated sulfur compounds in the marine environment, in *Microbial growth on C1 Compounds*. 15-33, Kelly, D. P. and Murrell, J. C. (eds.),Intercept Ltd., London, 1993

Kirschbaum, M. U. F., Bruhn, D., Etheridge, D. M., Evans, J. R., Farquhar, G. D., Gifford, R. M., Paul, K. I., and Winters, A. J., A comment on the quantitative significance of aerobic methane release by plants, Functional Plant Biology, 33, 521–530, 2006.

Kovacs, T. A., and Brune, W. H., Total OH loss rate measurement: J. Atmos. Chem., 39, 105-122, 2001.

Kovacs, T. A., Brune, W. H., Harder, H., Martinez, M., Simpas, J. B., Frost, G. J., Williams, E., Jobson, T., Stroud, C., Young, V., Fried, A., and Wert, B., Direct measurements of urban OH reactivity during Nashville SOS in summer 1999: J. Environ. Monit., 5, 68-74, 2003.

Krejci, R., Strom, J., de Reus, M., Williams, J., Fischer, H., Andreae, M.O., and Hansson, H.C., Spatial and temporal distribution of atmospheric aerosols in the lowermost troposphere over the Amazonian tropical rainforest, Atmos. Chem. Phys., 5, 1527–1543, 2005.

Kulmala, M., Suni, T., Lehtinen K. E. J., Dal Maso, M., Boy, M., Reissell, A., Rannik, U¨ ., Aalto, P., Keronen, P., Hakola, H., Back, J., Hoffmann, T., Vesala, T., and Hari, P., A new feedback mechanism linking forests, aerosols, and climate, Atmos. Chem. Phys., 4, 557–562, 2004.

Lelieveld, J., Crutzen, P., Dentener, F., Changing concentration, lifetime and climate forcing of atmospheric methane, Tellus, 50B, 128–150, 1998.

Lelieveld, J., Dentener, F. J., Peters, W., and Krol, M. C., On the role of hydroxyl radicals in the self-cleansing capacity of the troposphere: Atmos. Chem. Phys., 4, 2337-2344, 2004.

Levy, H., Normal atmosphere: large radical and formaldehyde concentrations predicted, Science, 173, 141–143 1971.

Lewis, A. C., Carslaw, N., Marriott, P. J., Kinghorn, R. M., Morrison, P., Lee, A. L., Bartle, K. D., and Pilling, M. J., A larger pool of ozone-forming carbon compounds in urban atmospheres:

Nature, 405, 778-781, 2000.

Lewis, A., Hopkins, J., Carpenter, L., Stanton, J., Read, K. and Pilling, M.: Sources and sinks of acetone, methanol, and acetaldehyde in North Atlantic marine air, Atmos. Chem. Phys., 5, 1963-1974, 2005.

Lindinger, W., Hansel, A., and Jordan, A., On-line monitoring of volatile organic compounds at pptv levels by means of proton-transfer-reaction mass spectrometry (PTR-MS) - Medical applications, food control and environmental research: Int. J. Mass Spectrom., 173, 191-241, 1998a.

Lindinger, W., Hansel, A., and Jordan, A., Proton-transfer-reaction mass spectrometry (PTR-MS): on-line monitoring of volatile organic compounds at pptv levels: Chem. Soc. Rev., 27, 347-354, 1998b.

Liss, P. and Mervilat, L.: Air-sea gas exchange rates: Introduction and synthesis, in *The Role of Air-Sea Exchange in Geochemical Cycling*. Buat-Menard, P. and Reidel, D. (eds.),Norwell, Mass., 1986

Mao, H., Talbot, R., Nielsen, C. and Sive, B.: Controls on methanol and acetone in marine and continental atmospheres, Geophys. Res. Lett., 33 (2), L02803-L02807, 2006.

Marandino, C., De Bruyn, W., Miller, S., Prather, M. and Saltzman, E.: Oceanic uptake and the global atmospheric acetone budget, Geophys. Res. Lett., 32 (15), doi: 10.1029/2005GL023285, L15806, 2005.

Marie, D., Brussaard, C. P. D., Partensky, F. and Vaulot, D.:

Enumeration of phytoplankton, bacteria and viruses in marine samples. In Robinson J.P., Darzynkiewicz, Z., Dean, P.N., Orfao, A., Rabinovitch, P., Tanke, H., Wheeless, L. (eds.), *Current protocols in cytometry*.John Wiley & Sons, Chichester, pp. 11.11.1-11.11.15, 1999a.

Marie, D., Brussard, C., Thyrhaug, R.,Bratbak, G., Vaulot, D.: Enumeration of marine viruses in culture and natural samples by flow cytometry, Appl.Environ. Microb., 65, 45-52, 1999b.

Maris, C., Chung, M. Y., Lueb, R., Krischke, U., Meller, R., Fox, M. J., and Paulson, S. E., Development of instrumentation for simultaneous analysis of total non-methane organic carbon and volatile organic compounds in ambient air: Atmos. Environ., 37, S149-S158, 2003.

Martinez, M., Harder, H., Kovacs, T. A., et al., OH and HO2 concentrations, sources, and loss rates during the Southern Oxidants Study in Nashville, Tennessee, summer 1999: J. Geophys. Res.-Atmos., 108, 2003.

Matthews, E., Wetlands. In: Khalil, M. (Ed.), Atmospheric Methane: Its Role in the Global Environment. Springer-Verlag, New York, NY, pp. 202– 233, 2000.

Matsunaga, S., Mochida, M., Saito, T. and Kawamura, K.: In situ

measurement of isoprene in the marine air and surface seawater from the western North Pacific, Atmos. Environ., 36 (39-40), 6051-6057, 2002.

McKeen, S., Gierczak, T., Burkholder, J., Wennberg, P., Hanisco, T., Keim, E., Gao, R., Liu, S., Ravishankara, A. and Fahey, D.: The photochemistry of acetone in the upper troposphere: A source of odd-hydrogen radicals, Geophys. Res. Lett., 24 (24), 3177-3180, 1997.

Milne, P., Riemer, D., Zika, R. and Brand, L.: Measurement of vertical-distribution of isoprene in surface seawater, its chemical fate, and its emission from several phytoplankton monocultures, Mar. Chem., 48 (3-4), 237-244, 1995.

Nguyen, B., Gaudry, A., Bonsang, B. and Lambert, G.: Re-evaluation of role of dimethyl sulfide in sulfur budget, Nature, 275 (5681), 637-639, 1978.

Nguyen B.C., Belviso S., Mihalopoulos N., Gostan J., Nival P.: Dimethylsulfide production during natural phytoplankton blooms, Marine Chemistry, 24, 133-141, 1988.

Northway, M., de Gouw, J., Fahey, D., Gao, R., Warneke, C., Roberts, J. and Flocke, F.: Evaluation of the role of heterogeneous oxidation of alkenes in the detection of atmospheric acetaldehyde, Atmos. Environ., 38 (35), 6017-6028, 2004.

Olivier, J. G. J., Bouwman, A. F., Vandermass, C. W. M. and Berdowski, J. J. M.: Emission database for global atmospheric research (EDGAR), Environ. Monit. Assess., 31 (1-2), 93-106,

1994.

Olson, J. R., Crawford, J. H., Chen, G., et al., Testing fast photochemical theory during TRACE-P based on measurements of OH, HO2, and CH2O: J. Geophys. Res.-Atmos., 109, 2004.

Palmer, P. and Shaw, S.: Quantifying global marine isoprene fluxes using MODIS chlorophyll observations, Geophys. Res. Lett., 32 (9), L09805-L09810, 2005.

Parsons, A. J., Newton, P.C.D., Clark, H. and Kelliher F. M., Scaling methane emissions from vegetation, Trends in Ecology and Evolution, doi:10.1016/ j.tree.2006.05.017, 2006.

Paulson, S. E., Chung, M. Y., and Hasson, A. S., OH radical formation from the gas-phase reaction of ozone with terminal alkenes and the relationship between structure and mechanism: J. Phys. Chem. A, 103, 8125-8138, 1999.

Poppe, D., Zimmermann, J., Bauer, R., et al., Comparison Of Measured Oh Concentrations With Model-Calculations: J. Geophys. Res.-Atmos., 99, 16633-16642, 1994.

Prather, M., Ehhalt, D., Dentener, F., Derwent, R., Dlugokencky, E., Holland, E., Isaksen, I., Katima, J., Kirchhoff, V., Matson, P., Midgley, P., and Wang, M.: Atmospheric chemistry and greenhouse gases, Chapter 4, in: Climate Change 2001, The scientific basis: Contribution of working group I to the Third assessment report of the Intergovernmental Panel on Climate, edited by: Houghton, J. T., Ding, Y., Griggs, Y., Noguer, M., v.d. Linden, P. J., Dai, X., Maskell, K.,and Johnson, C. A., pp.

881, Cambridge University Press, Cambridge, United Kingdom and New York, NY, US, 2001.

Ren, X. R., Brune, W. H., Cantrell, C. A., Edwards, G. D., Shirley, T., Metcalf, A. R., and Lesher, R. L., Hydroxyl and peroxy radical chemistry in a rural area of Central Pennsylvania: Observations and model comparisons: J. Atmos. Chem., 52, 231-257, 2005.

Ren, X. R., Brune, W. H., Oliger, A., Metcalf, A. R., Simpas, J. B., Shirley, T., Schwab, J. J., Bai, C. H., Roychowdhury, U., Li, Y. Q., Cai, C. X., Demerjian, K. L., He, Y., Zhou, X. L., Gao, H. L., and Hou, J., OH, HO2, and OH reactivity during the PMTACS-NY Whiteface Mountain 2002 campaign: Observations and model comparison: J. Geophys. Res.-Atmos., 111, 2006.

Ren, X. R., Harder, H., Martinez, M., Lesher, R. L., Oliger, A., Shirley, T., Adams, J., Simpas, J. B., and Brune, W. H., HOx concentrations and OH reactivity observations in New York City during PMTACS-NY2001: Atmos. Environ., 37, 3627-3637, 2003.

Rinne, J., Hakola, H., and Laurila, T., Vertical fluxes of monoterpenes above a Scots pine stand in the boreal vegetation zone, Phys. Chem. Earth (B), 24, 711–715, 1999.

Roberts, J. M., Bertman, S. B., Jobson, T., Niki, H., and Tanner, R., Measurement of total nonmethane organic carbon (C-y): Development and application at Chebogue Point, Nova Scotia, during the 1993 North Atlantic Regional Experiment

campaign: J. Geophys. Res.-Atmos., 103, 13581-13592, 1998.

Sadanaga, Y., Yoshino, A., Kato, S., and Kajii, Y., Measurements of OH reactivity and photochemical ozone production in the urban atmosphere: Environ. Sci. Technol., 39, 8847-8852, 2005.

Sadanaga, Y., Yoshino, A., Kato, S., Yoshioka, A., Watanabe, K., Miyakawa, Y., Hayashi, I., Ichikawa, M., Matsumoto, J., Nishiyama, A., Akiyama, N., Kanaya, Y., and Kajii, Y., The importance of NO2 and volatile organic compounds in the urban air from the viewpoint of the OH reactivity: Geophys. Res. Lett., 31, 2004a.

Sadanaga, Y., Yoshino, A., Watanabe, K., Yoshioka, A., Wakazono, Y., Kanaya, Y., and Kajii, Y., Development of a measurement system of OH reactivity in the atmosphere by using a laser-induced pump and probe technique: Rev. Sci. Instrum., 75, 2648-2655, 2004b.

Salisbury, G., Williams, J., Holzinger, R., Gros, V., Mihalopoulos, N., Vrekoussis, M., Sarda-Esteve, R., Berresheim, H., von Kuhlmann, R., Lawrence, M. and Lelieveld, J.: Ground-based PTR-MS measurements of reactive organic compounds during the MINOS campaign in Crete, July-August 2001, Atmos. Chem. Phys., 3, 925-940, 2003.

Sanhueza, E., and Donoso, L., Methane emission from tropical savanna *Trachypogon sp.* grasses, Atmos. Chem. Phys., 6, 5315–5319, 2006.

Savage, K., Moore, T.R., Crill, P.M., Methane and carbon dioxide exchanges between the atmosphere and northern boreal forest

soils. Journal of Geophysical Research, 102, 29 279-29 288, 1997.

Schiller, C.L., Hastie, D.R., Nitrous oxide and methane fluxes from perturbed and unperturbed boreal forest sites in northern Ontario. Journal of Geophysical Research, 101(D17), 22 767-22 774, 1996.

Sciare, J., Mihalopoulos, N. and Dentener, F.: Interannual variability of atmospheric dimethylsulfide in the southern Indian Ocean, J. Geophys. Res.-Atmos., 105 (D21), 26369-26377, 2000.

Shaw, S., Chisholm, S. and Prinn, R.: Isoprene production by Prochlorococcus, a marine cyanobacterium, and other phytoplankton, Mar. Chem., 80 (4), 227-245, 2003.

Shirley, T. R., Brune, W. H., Ren, X., Mao, J., Lesher, R., Cardenas, B., Volkamer, R., Molina, L. T., Molina, M. J., Lamb, B., Velasco, E., Jobson, T., and Alexander, M., Atmospheric oxidation in the Mexico City Metropolitan Area (MCMA) during April 2003: Atmos. Chem. Phys., 6, 2753-2765, 2006.

Sickles, J.E., Eaton, W.C., Ripperton, L.A. and Wright, R.S., US Environmental Protection Agency, EPA-60017-77-104, 1977.

Simpson, I.J., Edwards, G.C., Thurtell, G.W., den Hartog, G., Neumann, H.H., Staebler, R.M., Micrometeorological measurements of methane and nitrous oxide exchange above a boreal aspen stand. Journal of Geophysical Research, 102(D24), 29 331-29 341, 1997.

Simpson, I.J., Edwards, G.C., Thurtell, G.W., Variations in methane and nitrous oxide mixing ratios at the southern boundary of a

Canadian boreal forest, Atmospheric Environment, 33, 1141-1150, 1999.

Singh, H., Chen, Y., Staudt, A., Jacob, D., Blake, D., Heikes, B. and Snow, J.: Evidence from the Pacific troposphere for large global sources of oxygenated organic compounds, Nature, 410 (6832), 1078-1081, 2001.

Singh, H., Chen, Y., Tabazadeh, A., Fukui, Y., Bey, I., Yantosca, R., Jacob, D., Arnold, F., Wohlfrom, K., Atlas, E., Flocke, F., Blake, D., Blake, N., Heikes, B., Snow, J., Talbot, R., Gregory, G., Sachse, G., Vay, S. and Kondo, Y.: Distribution and fate of selected oxygenated organic species in the troposphere and lower stratosphere over the Atlantic, J. Geophys. Res.-Atmos., 105 (D3), 3795-3805, 2000.

Singh, H., Ohara, D., Herlth, D., Sachse, W., Blake, D., Bradshaw, J., Kanakidou, M. and Crutzen, P.: Acetone in the atmosphere - Distribution, Sources and Sinks, J. Geophys. Res.-Atmos., 99 (D1), 1805-1819, 1994.

Singh, H., Salas, L., Chatfield, R., Czech, E., Fried, A., Walega, J., Evans, M., Field, B., Jacob, D., Blake, D., Heikes, B., Talbot, R., Sachse, G., Crawford, J., Avery, M., Sandholm, S. and Fuelberg, H.: Analysis of the atmospheric distribution, sources, and sinks of oxygenated volatile organic chemicals based on measurements over the Pacific during TRACE-P, J. Geophys. Res.-Atmos., 109 (D15), D15S07-D15S20, 2004.

Singh, H., Tabazadeh, A., Evans, M., Field, B., Jacob, D., Sachse, G., Crawford, J., Shetter, R. and Brune, W.: Oxygenated volatile

organic chemicals in the oceans: Inferences and implications based on atmospheric observations and air-sea exchange models, Geophys. Res. Lett., 30 (16), 1862-1867, 2003.

Sinha, V., Williams, J., Meyerhofer, M., Riebesell, U., Paulino, A. I., and Larsen, A., Air-sea fluxes of methanol, acetone, acetaldehyde, isoprene and DMS from a Norwegian fjord following a phytoplankton bloom in a mesocosm experiment: Atmos. Chem. Phys., 7, 739-755, 2007a.

Sinha, V., Williams, J., Crutzen P., Lelieveld J., Methane emissions from boreal and tropical forest ecosystems derived from in-situ measurements: To be submitted to Atmos. Chem. Phys.Discuss., 2007b.

Smith, S. C., Lee, J. D., Bloss, W. J., Johnson, G. P., Ingham, T., and Heard, D. E., Concentrations of OH and HO2 radicals during NAMBLEX: measurements and steady state analysis: Atmos. Chem. Phys., 6, 1435-1453, 2006.

Steudler, P.A., Bowden, R.D., Mellico, J.M., and Aber, J.D., Influence of nitrogen uptake in temperate forest soils, Nature, 341, 314-316, 1989.

Stull, R.B., An introduction to boundary layer meteorology, Kluwer Academic Publishers, Dordrecht, Netherlands, 1988.

Suni, T., Berninger, F., Vesala, T., Markkanen, T., Hari, P., Mäkelä, A., Ilvesniemi, H., Hänninen, H., Nikinmaa, E., Huttula, T., Laurila, T., Aurela, M., Grelle, A., Lindroth, A., Arneth, A., Shibistova, O., and Lloyd, J., Air temperature triggers the recovery of evergreen boreal forest photosynthesis in spring.

Global Change Biology, 9, 1410-1426, 2003.

Tie, X., Guenther, A. and Holland, E.: Biogenic methanol and its impacts on tropospheric oxidants, Geophys. Res. Lett., 30 (17), 1881-1885, 2003.

Tunved, P., Hansson, H.-C., Kerminen, V.M., Strom, J., Dal Maso, M., Lihavainen, H., Viisanen, Y., Aalto, P. P., Komppula, M., and Kulmala, M., High Natural Aerosol Loading over Boreal Forests, Science, 312, 261–263, 2006.

Tyler, S.C., The global methane budget, in: Microbial production and consumption of greenhouse gases : methane, nitrogen oxides and halomethanes, edited by J.E. Rogers and W.B. Whitman, 298 p.p., Am. Soc. for Microbiol, Washington D.C., 1991.

Vesala, T., Haataja, J., Aalto, P., et al., Long-term field measurements of atmosphere-surface interactions in boreal forest combining forest ecology, micrometeorology, aerosol physics and atmospheric chemistry, Trends in Heat Mass Mom Transf, 4, 17—35, 1998.

Walter, K. M., Zimov, S. A., Chanton, J. P., Verbyla, D. , Chapin, F. S., Methane bubbling from Siberian thaw lakes as a positive feedback to climate warming, Nature, 443, 71-75, 2006.

Warneke, P., Chemistry of the natural atmosphere, Academic Press, 2000.

Whalen, S.C., Reeburgh, W.S., Barber, V.A., Oxidation of methane in boreal forest soils: a comparison of seven measures, Biogeochemistry 16(3), 181-211, 1992.

Williams, J.: Organic trace gases: An overview, Environ.Chem., 1

125-136, 2004a.

Williams, P. and Egge, J.: The management and behaviour of the mesocosms, Estuar Coast Shelf S., 46, 3-14, 1998.

Williams, J., Holzinger, R., Gros, V., Xu, X., Atlas, E. and Wallace, D.: Measurements of organic species in air and seawater from the tropical Atlantic, Geophys. Res. Lett., 31 (23), doi: 10.1029/2004GL020012, L23S06, 2004b.

Williams, J., Poschl, U., Crutzen, P., Hansel, A., Holzinger, R., Warneke, C., Lindinger, W. and Lelieveld, J.: An atmospheric chemistry interpretation of mass scans obtained from a proton transfer mass spectrometer flown over the tropical rainforest of Surinam, J Atmos Chem, 38 (2), 133-166, 2001.

Williams, J., Yassaa, N., Bartenbach, S., and Lelieveld, J., Mirror image hydrocarbons from Tropical and Boreal forests: Atmos. Chem. Phys., 7, 973-980, 2007.

Wuebbles, D.J., Hayhoe, K., Atmospheric methane and global change, Earth-Science Reviews, 57, 177–210, 2002.

Yassaa, N., Williams, J., Enantiomeric monoterpene emissions from natural and damaged Scots pine in a boreal coniferous forest measured using solid-phase microextraction and gas chromatography/mass spectrometry, Journal of Chromatography A, 1141, 138–144, 2007.

Yoshino, A., Sadanaga, Y., Watanabe, K., Kato, S., Miyakawa, Y., Matsumoto, J., and Kajii, Y., Measurement of total OH reactivity by laser-induced pump and probe technique - comprehensive observations in the urban atmosphere of Tokyo:

Atmos. Environ., 40, 7869-7881, 2006.

Zhou, X. and Mopper, K.: Carbonyl-compounds in the lower marine troposphere over the Caribbean sea and Bahamas, J. Geophys. Res.- Oceans, 98 (C2), 2385-2392, 1993.

Zhou, X. and Mopper, K.: Photochemical production of low-molecular-weight carbonyl compounds in seawater and surface microlayer and their air-sea exchange, Mar. Chem., 56 (3-4), 201-213, 1997.

Abbreviations

A	Surface Area
BACCI	Biosphere Atmosphere Cloud Climate Interaction
B.D.L	Below Detection Limit
C.F.	factor for converting nmol mol^{-1} to molecules cm^{-3} = 2.69×10^{10}
Chl a	Chlorophyll a
CRM	Comparative Reactivity Method
DMS	Dimethyl Sulphide
DOM	Dissolved Organic Matter
E	Emission from seawater to atmosphere
F_{CH4}	Methane flux
F_{voc}	flux of the VOC
FID	Flame Ionization Detector
GABRIEL	Guyana Atmosphere-Biosphere Exchange and Radical Intensive Experiment with the Learjet
GC	Gas Chromatography
GC-FID	Gas Chromatograph - Flame Ionization Detector
GF/F	Glass Fibre Filters
HPLC	High Performance Liquid Chromatography
IUPAC	International Union of Pure and Applied Chemistry
IPCC	Intergovernmental Panel of Climate Change
k	first-order decay rate of OH radicals
LIF	Laser Induced Fluorescence
LT	Local Time

MVK	Methyl vinyl ketone
$m_{in,voc}$	VOC mixing ratios in the inflowing ambient marine air
$m_{out,voc}$	VOC mixing ratios in the mesocosm air
M_{voc}	molecular weight of the VOC
n	Number of measurements
$N_{06:00}$	Number of Methane Molecules at 6:00
$N_{20:00}$	Number of Methane Molecules at 20:00
$N_{Residual\ Layer}$	Number of Methane Molecules in the residual layer
NBL	Nightime Boundary Layer
NPP	Net Primary Productivity
OVOC	Oxygenated Volatile Organic Compounds
OH	Hydroxyl radical
PAN	Peroxy Acetyl Nitrate
PAR	Photosynthetically Active Radiation
PeECE	Pelagic Ecosystem CO_2 Enrichment study
P_{OH}	OH production rate
PTR-MS	Proton Transfer Reaction Mass Spectrometer
Q	flow rate of the ambient air into the mesocosm
QUEST III	Quantification of Aerosol Nucleation in the European Boundary Layer
$r_{avcorr,}$	average Pearson linear correlation coefficient in the duplicate mesocosms
$r_{avcorr,\ isoprene}$	average Pearson linear correlation coefficient for isoprene in the duplicate mesocosms
$r_{avcorr,\ acetaldehyde}$	average Pearson linear correlation coefficient for acetaldehyde in the duplicate mesocosms

$r_{avcorr, dms}$	average Pearson linear correlation coefficient for DMS in the duplicate mesocosms
r_{av}	Pearson Correlation Coefficient
R_{air}	OH decay rate of the OH reactive species present in the introduced air
R_X	Reaction rate of X with OH
SCHIAMACHY	Scanning Imaging Absorption Spectrometer for Atmospheric Chartography
SMEAR II	Station for Measuring Forest Ecosystem- Atmosphere Relations
TM3	global 3D chemistry Transport Model
U	Uptake from atmosphere to seawater
USGS	United States Geological Survey
V_m	Molar gas volume
VMR	Volume mixing ratio
VOCs	Volatile Organic Compounds
σ	Standard deviation

List of Tables

List of Figures

Curriculum vitae

Vinayak Sinha

born on 10.06.1977 in Chingola, Zambia

Areas of Research Interest

Analytical chemistry, Proton transfer reaction mass spectrometry, Atmospheric methane emissions, Emissions and uptake of oxygenated volatile organic compounds in the marine boundary layer

Academic Qualifications

Doctoral Scholar : Max Planck Institute for Chemistry in Mainz.

2004-present

M.Tech: Modern Methods of Chemical Analysis(CGPA

2002-2004 9.11/10) Indian Institute of Technology, New Delhi- (INDIA)

Title of M.Tech Thesis: Structural elucidation of asphaltenes through degradation and analytical studies.

M.Sc.: ***Chemistry (90%)***

2000-2002 Sri Sathya Sai Institute of Higher Learning, Prashantinilayam, Anantpur, AP (INDIA)

B.Sc.(Hons): ***Chemistry (summa cum laude)***

1997-2000 Sri Sathya Sai Institute of Higher Learning, Prashantinilayam, Anantpur, AP (INDIA)

Class XII (HSC): ***Central Board of Secondary Education(CBSE), New Delhi.(71%)***

1996 St. Michael's High School, Patna, Bihar.

Class X (SSC): ***Indian School Certificate Examination(ICSE), New Delhi.(91%)***

1994 Don Bosco Academy, Patna, Bihar.

Computer Skills:

Fortran 77 , GW Basic and working knowledge of C++, Igor Pro

Industrial Summer Training and Workshops:

- Six Weeks Vocational Industrial Summer Training at Indian Oil R&D Centre, Sector-13, Faridabad.(A Government of India Undertaking) from June 1st till July 25th,2003.
- 1st French - German summer school on Aerosol, Heterogeneous Chemistry and Climate in Ile d'Oleron, France, September 19th to October 1st , 2004.
- Autumn school on measurement techniques in Atmospheric Chemistry, organized by the University of Utrecht and the Max Planck Institute for Chemistry, Mainz in Oberwesel, Germany, 7th till 13th October, 2006.

Awards and Citations

- Awarded the ***Petrotech-CII Fellowship*** by Petrotech Society & Confederation of Indian Industries at 5th International Petroleum Conference and Exhibition (9-12 January,2003), New Delhi.
- Awarded the ***Dr Adivi Reddy Gold Medal*** for distinction as University Topper in BSc Chemistry Honours Course at Sri Sathya Sai Institute of Higher Learning, Prashantinilayam.

- Qualified ***National Eligibility Test (NET' 2001)*** in ***Chemical Sciences*** conducted by Council of Scientific and Industrial Research ***(CSIR)*** INDIA**.**
- Qualified ***Graduate Aptitude Test in Engineering (GATE' 2002)*** in ***Chemistry*** with ***89.46*** percentile.

Major Field Campaigns:

- Hohenpeissenberg OH intercomparison and Photochemistry Experiment (HOHPEX 2004) held near the Ammergauer Alps in Germany - July, 2004.
- Biosphere Atmosphere Cloud Climate Interaction (BACCI-2005) Campaign held in Hyytiäla, Finland – April-May, 2005.
- Pelagic Ecosystem CO_2 Enrichment Study (PeECE-III) Campaign held in the Norwegian fyords, Bergen, Norway – May-June, 2005.
- Guyanas Atmosphere- Biosphere. exchange and Radicals Intensive Experiment with the Learjet (GABRIEL) Campaign : Ground based measurements in the tropical rainforest, Brownsberg, Suriname – October, 2005.
- Organics over the ocean modifying particles in both hemispheres (OOMPH): A ship campaign aboard the French research ship Marion Dufrense- Leg 2 from Puenta Arenas, Chile to Reunion islands – February–March, 2007.

Publications:

Sinha, V., Williams, J., Meyerhofer, M., Riebesell, U., Paulino, A. I., and Larsen, A., Air-sea fluxes of methanol, acetone, acetaldehyde, isoprene and DMS from a Norwegian fjord

following a phytoplankton bloom in a mesocosm experiment: Atmos. Chem. Phys., 7, 739-755, 2007.

Sinha, V., Byravan, S., and Mashelkar, R. A., Issues in Indian Science: Science, 309, 557-558, 2005.

Sinha, V., Williams, J., Crutzen P., Lelieveld J., Methane emissions from boreal and tropical forest ecosystems derived from in-situ measurements: To be submitted to Atmos. Chem. Phys., 2007.

Sinha, V., Williams, J., Crowley, J., Lelieveld J., The Comparative Reactivity Method – A new tool to measure the total OH Reactivity of ambient air : To be submitted to Environ. Sci. Technol., 2007.

Conference contributions

Sinha, V., Williams, J., Crutzen P., Lelieveld J., Methane emissions from boreal and tropical forest ecosystems derived from in-situ measurements: Poster presentation at the American Geophysical Union (AGU) General Assembly Fall Meeting, San Francisco, U.S.A., December, 2006.

Sinha, V., Williams, J., Meyerhofer, M., Riebesell, U., Paulino, A. I., and Larsen, A., Air-sea fluxes of methanol, acetone, acetaldehyde, isoprene and DMS from a Norwegian fjord following a phytoplankton bloom in a mesocosm experiment: Poster presentation at the American Geophysical Union (AGU) General Assembly Fall Meeting, San Francisco, December, 2006.

Sinha, V., Williams, J., Crowley, J., Lelieveld J., The Comparative Reactivity Method – A new tool to measure the total OH

Reactivity of ambient air : Poster presentation at the European Geophysical Union (EGU) General Assembly Meeting, Vienna, Austria, April, 2007.

Awarded the ***Petrotech-CII Fellowship at the 5th International Petroleum Conference and Exhibition (9-12 January,2003)*** held at New Delhi, India.